Legacy Mercury in Alviso Slough, South San Francisco Bay, California: Concentration, Speciation and Mobility

Open-File Report 2007-1240

U.S. Department of the Interior
U.S. Geological Survey

Cover:

Top—Data Collection at Alviso Slough. Photo by M. Marvin-DiPasquale.
Bottom Left—Aerial Photo with Alviso Slough emphasized in blue, modified from GoogleEarth™ image.
Bottom Right—Sediment core sample. Photo by M. Cox.

Legacy Mercury in Alviso Slough, South San Francisco Bay, California: Concentration, Speciation and Mobility

By Mark Marvin-DiPasquale and Marisa H. Cox

Open-File Report 2007-1240

U.S. Department of the Interior
U.S. Geological Survey

U.S. Department of the Interior
DIRK KEMPTHORNE, Secretary

U.S. Geological Survey
Mark D. Myers, Director

U.S. Geological Survey, Reston, Virginia 2007

For product and ordering information:
World Wide Web: http://www.usgs.gov/pubprod
Telephone: 1-888-ASK-USGS

Suggested citation:
Marvin-DiPasquale, M., Cox, M.H., 2007, Legacy Mercury in Alviso Slough, South San Francisco Bay, California: Concentration, Speciation and Mobility: Menlo Park, CA , U.S. Geological Survey, Open-File Report number 2007-1240, 98p

Contents

Figures

Tables

Conversion Factors

SI to Inch/Pound

Multiply	By	To obtain
	Length	
centimeter (cm)	0.3937	inch (in.)
meter (m)	3.281	foot (ft)
kilometer (km)	0.6214	mile (mi)
	Area	
square meter (m^2)	0.0002471	acre
square kilometer (km^2)	247.1	acre
square centimeter (cm^2)	0.001076	square foot (ft^2)
square meter (m^2)	10.76	square foot (ft^2)
square centimeter (cm^2)	0.1550	square inch (ft^2)
square kilometer (km^2)	0.3861	square mile (mi^2)
	Volume	
cubic centimeter (cm^3)	0.06102	cubic inch (in^3)
cubic meter (m^3)	35.31	cubic foot (ft^3)
cubic kilometer (km^3)	0.2399	cubic mile (mi^3)
kilometer per hour (km/h)	0.6214	mile per hour (mi/h)
	Mass	
gram (g)	0.03527	ounce (oz)
kilogram (kg)	2.205	pound (lb)

Temperature in degrees Celsius (°C) may be converted to degrees Fahrenheit (°F) as follows:
°F=(1.8×°C)+32
Vertical and horizontal coordinate information is referenced to the World Geodetic System of 1984(WGS 84).

Legacy Mercury in Alviso Slough, South San Francisco Bay, California: Concentration, Speciation and Mobility

By Mark Marvin-DiPasquale and Marisa H. Cox

Abstract

Mercury (Hg) is a significant contaminant in the waters, sediment and biota of San Francisco Bay, largely resulting from extensive historic regional mining activities. Alviso Slough represents one of the most mercury contaminated waterways entering south San Francisco Bay, as it is associated with the drainage of the New Almaden mercury mining district. Wetland habitat restoration of former salt manufacturing ponds adjacent to Alviso Slough is currently being planned. One management scenario being considered is a levee breach between Alviso Slough and Pond A8, which will allow reconnection of the salt pond with the tidal slough. This action is projected to increase the tidal prism within Alviso Slough and result in some degree of sediment remobilization as the main channel deepens and widens. The focus of the current study is to assess: a) the current mercury species composition and concentration in sediments within the Alviso Slough main channel and its associated fringing marsh plain, b) how much of each mercury species will be mobilized as a result of projected channel deepening and widening, and c) potential changes in inorganic 'reactive' mercury bioavailability (for conversion to toxic methylmercury) associated with the mobilized sediment fraction. The current report details the field sampling approach and all laboratory analyses conducted, as well as provides the complete dataset associated with this project including a) a quantitative assessment of mercury speciation (total mercury, reactive mercury and methylmercury), b) estimates of the quantity of sediment and mercury mobilized based on 20-foot and 40-foot levee wall notch scenarios, and c) results from a sediment scour experiment examining the changes in the reactive mercury pool under four treatment conditions (high / low salinity and oxic / anoxic water). Ancillary sediment data also collected and reported herein include bulk density, organic content, magnetic susceptibility, percent dry weight, grain size, pH, oxidation-reduction potential, core photography, and detailed lithographic descriptions.

Introduction

Mercury (Hg) is a legacy contaminant, mined historically from the California Coast Ranges and transported to the Sierra Nevada for use in gold extraction during the Gold Rush era of the mid- to late 1800's (Alpers and others, 2005). Mercury enters San Francisco Bay (SFB) from runoff associated with the hundreds of abandoned mercury and gold mining sites located around the Bay watershed, as well as from the contemporary urban landscape (CRWQCB, 2006). One of the most prolific mercury-producing mining areas in North America, located in the hills south of San Jose, California, is the New Almaden Mining District, which generated over 3.7×10^7 kg of mercury between 1845 and 1975 (Cargill and others, 1980). The watershed draining the New Almaden Mining District includes the Guadalupe River, which ultimately flows into Alviso Slough and South SFB (**Figure 1**), all of which exhibit elevated levels of mercury in surface sediments along this drainage flow path (Conaway and others, 2003; Thomas and others, 2002). Estimates of mercury transported annually from the New Almaden region to South SFB can range from a few kilograms to hundreds of kilograms per year, depending largely on the inter-annual variation in rainfall, as most of the mercury is associated with sediments that are mobilized during episodic high flow events (McKee and others, 2005; Thomas and others, 2002).

In 2003, the State of California and the U.S. Government purchased over 16,000 acres of corporately owned salt production ponds from the Cargill Salt Company. The majority of these ponds (15,000 acres) are located in South SFB, with the balance (1,400 acres) located along the Napa River in the North SFB (Life_Science!, 2003). With a primary goal being wetlands restoration, this represents the largest single land purchase of its kind in U.S. history. More information on the South Bay Salt Pond Restoration Project can be found at URL: *http://www.southbayrestoration.org*.

Avian research throughout SFB indicates that elevated mercury levels are found in fish and invertebrate eating bird populations in South SFB region in general, and in populations associated with the South Bay salt ponds (Ackerman and others, 2007; Ackerman and others, (in press)). Methylmercury (MeHg) is the organic form of mercury that is largely produced in anoxic sediments from inorganic divalent mercury (Hg(II)) by bacteria (Compeau and Bartha, 1985). It is a known neurotoxin and is of environmental concern due to its propensity to bioaccumulate in aquatic food webs (Wiener and others, 2003). Previous research has indicated that wetland environments appear to be particularly efficient areas for the microbial MeHg production (Lacerda and Fitzgerald, 2001; Zillioux and others, 1993). A recent national study of 20 U.S. watersheds concluded that wetland spatial density was the leading determinant of MeHg productions within a study basin (Krabbenhoft and others, 1999), and that MeHg concentration in water was correlated with mercury levels in fish (Brumbaugh and others, 2001). These findings, coupled with the potential for substantial wetland restoration throughout SFB, has raised concerns that increased wetland density may lead to an increase in local MeHg production and bioaccumulation (Davis and others, 2003), although direct mechanistic evidence of this linkage is lacking.

As part of the salt production process, and apart from specific bay water intake points, salt ponds are effectively isolated hydrologically from the adjacent estuary and from tidal influence. A number of management strategies are currently being considered with respect to the existing salt ponds, including 1) maintaining them as managed high salinity ponds for birds, 2) converting them to fully tidal wetlands by removing existing levees or breaching levees, or 3) converting them to partially muted tidal wetlands by installing tide control structures through existing levees (i.e. a levee notch) (PWA and others, 2006). The long-term plan for Pond A8 is conversion to fully tidal wetlands by levee breaching or removal. However, the pond's location in the heart of the Guadalupe River discharge to the Bay makes mercury contamination a particular concern. Therefore, controlling the degree of tidal exchange and observing the effects of the pond/slough interaction is the currently preferred course of action. Therefore, the third strategy is currently being considered for Pond A8, which is adjacent to Alviso Slough and part of the Alviso salt pond complex in South SFB. Recent hydrodynamic modeling and geomorphic analysis conducted by Philip Williams and Associates, Ltd. (PWA), indicates that some deepening and widening of the current Alviso Sough channel will occur due to the increased tidal energy associated with an engineered levee notch (EDAW and others, 2007). The extent of sediment scouring will increase as a function of the size of the levee notch. Two notch scenarios were considered, which consist of either a 20-foot (6.1 meter) or 40-foot (12.2 meter) wide armored notch in the current levee wall separating Pond A8 from Alviso Slough. These modeling results, coupled with known mercury contamination in Alviso Slough, and concerns regarding wetland habitats being effective zones of MeHg production, raise a number of questions regarding the Pond A8 levee notch scenario. These questions include: How much mercury is in Alviso Slough and what are its dominant chemical forms? How much mercury will be mobilized as a function of sediment scour? Will the chemical form of mercury currently buried change if remobilized? Where will the remobilized sediment and mercury ultimately end up? Will remobilized mercury have any net effect on local or regional MeHg production and bioaccumulation?

To begin to answer some of these questions, a multi-year investigation of mercury-cycling and bioaccumulation in Alviso Slough and Pond A8 was undertaken by researchers from the San Francisco Estuary Institute (SFEI), U.S. Geological Survey (USGS), the Santa Clara Valley Water District (SCVWD) and the University of California, Berkeley (UC Berkeley). The current report focuses on Phase I objectives of this project, which include:

1. Determining the quantity and speciation of mercury in Alviso Slough;
2. Quantifying mercury species mobilization based upon the 20-foot and 40-foot levee notch scenario proposed for Pond A8; and
3. Conducting a sediment scour simulation experiment aimed at determining if the chemical speciation of currently buried mercury is affected by remobilization.

Purpose and Scope

This non-interpretive report provides complete tabular and graphical data associated with 15 two-meter deep sediment core profiles collected from the Alviso Slough main channel and the adjacent fringing marsh plain during September 2006. Field sampling methods and laboratory analytical methods are described for the following sediment constituents: total mercury (THg), methylmercury (MeHg), reactive mercury ($Hg(II)_R$), magnetic susceptibility, gamma and bulk sediment density, organic content, grain size, pH, and oxidation-reduction potential. Mercury species mobilization estimates are made based on the 20-foot and 40-foot levee notch scenario proposed for Pond A8. Results are given from a series of sediment scour simulation experiments aimed at determining if the $Hg(II)_R$ pool associated with currently buried sediment layers is affected by remobilization and resuspension under oxic, anoxic, high salinity and low salinity overlying water conditions. Photography and lithographic descriptions are provided for each core segment collected.

Methods

Study Area and Sample Collection

Sediment cores were collected between September 21 and 26, 2006 from 15 stations along Alviso Slough in South SFB (**Figure 2**). Five sampling transects were established (T1 to T5), along the slough salinity gradient, from the least saline upstream transect cluster (T1) near the town of Alviso, to the most saline transect cluster (T5) near the slough mouth. Three sites were sampled along each transect, which included one site each from the right and the left vegetated marsh plain that fringes either side of the slough (A and C series cores, respectively), as well as one site in the main slough channel (B series cores). Series B cores were collected from a portable floating work platform anchored in the slough channel. Sediment collection was conducted using a hand-operated 5.1 cm diameter piston coring device (Livingstone, 1955). Each core deployment recovered up to 100 cm of sediment. Three to four core segments (coded D1 to D4; total length ranging from 24 cm to 98 cm each) were required to reach the desired maximum depth of approximately 200 cm at a single site, with the individual segments slightly offset from each other to allow for overlapping depths (**Figure 3**). Specific sampling locations and core segment sampling depths are given in **Table 1** and **Table 2**, respectively.

Initial Post-Collection Sediment Core Processing

Within 3 – 7 days of field collection, sediment cores were characterized and sub-sampled. Each core section (50 in all) went through a five-step process which included a) initial non-destructive imaging of whole core sediment density and magnetic susceptibility, b) core splitting, c) physical description of the 'working' half split-core lithography and entering that information into a database, d) sub-sampling parameters of interest, and e) photographing the 'archive' half split-core.

Multi-Sensor Core Logger

Sediment wet bulk density (via the gamma irradiation method) and magnetic susceptibility (a measure of magnetic mineral content) were first made using the Multi-Sensor Core Logger (MSCL) (Model MSCL-75), which is owned and operated by the Coastal Marine Geology unit of the USGS (Menlo Park, CA). By measuring and studying the variation of these two state properties, an 'inside look' of each core was obtained prior to actually splitting the core tubes. Since down-core variation in these parameters is often not readily apparent to the naked eye, even once the cores are split and inspected, the MSCL data were critical in helping to decide exactly how to space the specific sediment intervals to be sub-sampled.

The MSCL-system is described in detail elsewhere (Gardner and others, 1995; Kayen and others, 1999). The MSCL consists of a four meter long tracking system that holds three sequential measurement devices: 1) a gamma ray wet bulk density sensor, 2) a primary compression-wave (P-wave) velocity and core-diameter sensor, and 3) a magnetic susceptibility sensor. A Macintosh computer driven by data acquisition software controls the system. Whole core sections up to 1.5 m in length can be logged. Core movement along the tracking system is run by a computer-controlled stepper motor that advances the core section at 1-cm intervals during logging. Each core section was run consecutively through the sensors, starting with the top of the section and progressing through to the bottom of the core. Core caps at each end (approximately 3 cm at the top and bottom of each core section) generate spurious data, which was subsequently excluded in the sediment profiles depicted in this report.

The sediment density sensor functions by sending a beam of gamma radiation (emitted from a $^{137}CsCl$ solid source) through the diameter (width) of the whole core. A scintillation detector coupled to a photomultiplier measures the attenuated radiation that passes through the core diameter. This attenuated gamma radiation signal is converted to sediment density (g/cm^3) by applying a two-point calibration curve based on the attenuated gamma radiation signal produced by a similar core tube filled with either pure water or a solid cylinder of aluminum (both of accurately known densities: 1.0 g/cm^3 and 2.7 g/cm^3, respectively). Calibration cores containing water and aluminum were run daily to verify the accuracy and consistency of the instrument.

The magnetic susceptibility sensor is set electronically by the manufacturer, based on a single standard of stable iron oxide. Thus, this sensor is calibrated absolutely and requires no additional calibration during daily operation.

The quality of the P-Wave velocity data was inconsistent due to a combination of factors including: the lack of water-saturated sediment in some core sections, incomplete coupling of the sediment with the interior core liner wall in some core sections, and the comparatively high degree of flexibility of the thin-walled core liner that was used for sediment collection. Thus, P-wave velocity data generated by the MSCL were not used in the determination of sediment intervals to sub-sample, and are not presented in this report.

Core Splitting

After the data from the MSCL were obtained and assessed, each core section was split vertically into two equal halves, representing the ‘working’ and ‘archive’ split core halves. The core end-caps were first removed. The whole core section was then placed into an aluminum core cradle with an inner diameter that exactly matches the outer diameter of the core tube, and which includes a top and bottom half, and thus totally encases the core liner. The core cradle also has two slits running along the length of each half, which act as a straight-line guide for the cutting tool. A utility knife blade was inserted at one end of the guide-slit, cutting into the core liner. The blade was run along the guide-slit until the core liner was cut from the top to the bottom ends on one side. The whole cradle was rotated 180^{o}, and the core liner was again cut along a line that is parallel and exactly opposite (180^{o}) the first. The core was then removed from the cradle and a very thin stainless steel wire was run longitudinally through the center of the core, along its full length. The two halves were then carefully pried apart and laid open-faced on the work bench. A film of plastic-wrap was gently placed over the exposed sediment of the ‘archive’ split core to minimize drying and chemical oxidation. The archive split-core half was then stored in a walk-in cooler at 3^{o}C until it can be photographed.

Core Descriptions & Database

The ‘working’ half split-core was moved to the work table outfitted with bright ‘full spectrum’ lights. The surface of the sediment was gently smoothed with an acid-clean stainless steel spatula (motion perpendicular to the length of the core), removing the surface 1-2 mm of material to expose fresh sediment. Always measuring from the top of the core down, the following lithologic parameters were noted for the complete core section: sediment color (hue/chroma) using the standard Munsell® soil color chart , grain-size via texture to touch (e.g. sand, silt, clay), the position and nature of stratigraphic contacts, and sedimentary structures (e.g. plant roots, shell fragments, etc.). All of this information was input into a sediment profile description database created in FileMaker Pro 6.0 (FileMaker, Inc. Santa Clara, CA) by the Coastal Marine Geology group at USGS (Menlo Park, CA).

Core Sub-Sampling

After fully describing an individual core section and assessing the associated MSCL density and magnetic susceptibility data, a decision was made as to the specific intervals to be sampled. Depth intervals typically ranged 10 – 30 cm in length. Priority of interval placement was given to obvious peaks in density and/or magnetic susceptibility, and to visible changes in sediment color and/or texture. Such discrete features were bracketed and typically sampled in one interval. When no such obvious features were noted, specific intervals were typically set to 20 or 30 cm, depending on the total number of intervals already identified for that whole 2 m core profile. When core sections from the same site overlapped (which was typically the case), sub-sampling in the next lower core section would begin at the sediment depth associated with the bottom of the last interval from the core section just above it. This allowed for collection of sub-samples representing the complete 2 meter length of the core site, without overlapping data. The only exception to this was profile T5A, which was the first sampled, and where there was some depth overlap during the sub-sampling between core sections D1, D2 and D3.

Once all depth intervals had been determined for the whole core section, tape was placed on a ruler that ran along side the core to mark-off each interval. Beginning with the top interval, an acid cleaned 1x1x1 cm plastic U-shaped sampling channel was placed open-face down along the length of the desired interval (just left of center) and then pushed evenly into the sediment until the top edge was flush with the sediment surface. A thin acid-cleaned stainless steel wire was then run along the bottom edge of the sampling channel to make a clean cut between the sediment inside and outside of the sampling channel, which was then gently extracted from the core section. This approach ensured that no sediment was sub-sampled that had been in contact with the interior surface of the core liner. The sediment filling the channel was immediately scraped from the interior into a 4 ounce (114 cm^3) plastic Whirl-Pak™ bag. A second channel was similarly sub-sampled (just right of center), and the extracted sediment was added to the same plastic bag. This resulted in 20 cm^3 (for a 10 cm interval) to 60 cm^3 (for a 30 cm interval) of sediment for each sub-sample. All sediment was squeezed to the bottom of the bag and all air squeezed out of the bag, which was then sealed at the top. The sediment in the bag was then well homogenized by hand manipulation of the bag for approximately 1 minute.

The bag was reopened and sub-samples were taken with an acid-cleaned 3 cm^3 plastic syringe (with the needle-end cut off) for the following parameters: a) total mercury (THg) [3-6 cm^3, frozen immediately on dry ice, all intervals and sites], b) reactive mercury ($Hg(II)_R$) [3-6 cm^3, flushed with nitrogen gas then frozen immediately on dry ice, all intervals and sites associated with Transects 1, 3 and 5 only], c) MeHg (MeHg) [3-6 cm^3, flushed with nitrogen gas then frozen immediately on dry ice, all intervals and sites associated with Transects 1, 3 and 5 only], d) combined organic content and % dry weight [6 cm^3, refrigerated, all intervals and sites], and e) grain size [6 cm^3, refrigerated, all intervals and sites]. Collection vials for all THg, organic content and grain size were 10 ml glass serum bottles. Collection bottles for $Hg(II)_R$ and MeHg were acid cleaned pre-combusted 20 ml screw-top glass vials. Sub-sample duplicates were taken for all of the above constituents at a frequency of approximately 10% of all samples collected.

After sub-sampling for the above parameters, the sediment remaining in the Whirl-Pak™ bag was again squeezed back to the bottom, and sediment pH and oxidation-reduction potential measurements are immediately taken on this material (see procedure below). The excess sediment that remained in the core liner was used to fill a new Whirl-Pak™ bag that was saved as an archive sample for that particular core section / depth interval. Sediment was squeezed to the bottom of the bag, and air was squeezed out, prior to sealing (as above). These archived sub-samples are stored refrigerated. The above sub-sampling procedure was repeated for all core sections and depth intervals.

Core Photography and Archiving

The sediment surface of the archive half split-core was gently smoothed (perpendicular to core length) with an acid-clean stainless steel spatula, removing the surface 1-2 mm of material to expose fresh sediment. The core was returned to the MSCL-system (described above) which is equipped with an overhead mounted Geoscan-colorline scan digital camera (using 3x1024 pixel charge-couple device arrays, Pentex™ k mounting lens). The system takes a digital photograph of the whole core in one image, while the core is mechanically moved down the MSCL track by the computer-controlled stepper motor. The image processing software (Geoscan™ Digital Imaging, version 5.2) creates a high resolution (approximately 25 Mb) JPEG file. After photographing, the exposed sediment surface of the archive half split-core was again covered with plastic wrap, and the core was placed into a D-tube for long-term storage in the USGS (Menlo Park) core refrigerator (at 3^{o}C). A piece of wet sponge was added to the D-tube to maintain a high moisture atmosphere, and the end of the D-tube was sealed with duct-tape and appropriately labeled.

Laboratory Analysis

Mercury Speciation

Total Mercury

Sub-samples for THg were taken at every depth interval for all sites, and were frozen at the time of sampling and maintained frozen until analysis. The procedure used for THg analysis generally follows that of an approved USGS method (Olund and others, 2004). Once thawed, sediment samples (approximately 0.25 g wet weight) are initially digested in an aqua regia mixture (2 mL concentrated hydrochloric acid and 6 mL of concentrated nitric acid) for 24 hours then a 5 % bromide monochloride solution is added to the sediment slurry which is then heated to 50 ^{o}C in an oven overnight. After samples are cooled, a sub-sample is transferred into a pre-combusted glass container and held until further analysis. Each batch of 10 environmental samples is accompanied with analysis of the following Quality Assurance (QA) samples: a) 1 certified reference material, b) 1 matrix spike sample, c) 1 analytical duplicate, and d) 1 method blank. The digestate is then analyzed on an Automated Mercury Analyzer (Tekran Model 2600), according to EPA Method 1631, Revision E (USEPA, 2002). This method is based on the reduction of Hg(II) to gaseous Hg^0 with tin chloride, trapping Hg^0 on gold sand, thermal desorption and quantification of Hg^0 via cold vapor atomic fluorescence spectrometry. Calibration standards are prepared from a NIST-certified commercially obtained $HgCl_2$ standard. The USGS Mercury laboratory in Menlo Park has been taking part in the QA/QC program overseen by Van Buuren Consulting LLC, for the CALFED/CBDA Ecosystem Restoration Program funded Mercury studies throughout the San Francisco Bay region. Participation in this program includes: a) standard operating procedure documentation review, b) conducting a mean detection limit prove-out exercise, and c) inter-laboratory comparison analysis of THg in sediment and water matrices (VBC, 2005; VBC and CDFG, 2005).

Reactive Mercury

Sediment “reactive” mercury ($Hg(II)_R$) is methodologically defined as the fraction of THg in a sediment sample that has not been chemically altered (e.g. digested, oxidized or chemically preserved) and that is readily reduced to elemental Hg^0 by an excess of tin chloride ($SnCl_2$) over a defined (short) exposure time. This operationally defined parameter was developed as a surrogate measure of the fraction of inorganic Hg(II) that is most likely available to Hg(II)-methylating bacteria responsible for

MeHg production. While there is no standard method for this parameter, the procedure described below is modified from that described elsewhere (Kieu, 2004), and has been used extensively in a number of research studies led by USGS researchers (Marvin-DiPasquale and others, 2006).

Recent experimental evidence suggests that the $Hg(II)_R$ assay effectively measures the fraction of Hg(II) that is associated with simple anions (e.g. $HgSO_4$, $HgCl_2$) in sediment pore water and/or Hg(II) that is weakly adsorbed to particle surfaces (Marvin-DiPasquale and others, 2006). Both of these fractions are indeed likely available to sediment microbes for Hg(II)-methylation. In a related set of experiments, the concentration of $Hg(II)_R$ measured in a suite of freeze-dried and homogenized environmental samples ranging over four-orders of magnitude in THg (1-24,000 ppm), was strongly correlated ($r^2 = 0.97$) with the amount of MeHg produced when these freeze-dried samples were mixed (at a constant THg amendment level) with fresh sediment containing active populations of Hg(II)-methylating bacteria (Bloom and others, 2006). These results suggest that the $Hg(II)_R$ fraction, as measured below, does provide a reasonable surrogate measure of the fraction of THg that is potentially available for Hg(II)-methylation.

Upon thawing in an anaerobic chamber (N_2 flushed), sediment sub-samples were initially homogenized in the original collection vial using an acid cleaned stainless steel spatula. A small amount of sediment (0.1-1.0 g) was then accurately weighed into 15 ml plastic centrifuge tubes, to which 10 ml of anoxic 0.5 % HCl solution was added. The tubes were capped and the resulting sediment slurry was homogenized using a vortex shaker. Samples were then removed from the anaerobic chamber and immediately refrozen on dry ice to minimize any oxidation reactions prior to transfer into the reaction bubblers. The reaction bubbler rig, the dual gold trap analytical set-up, and the cold vapor atomic fluorescence spectrophotometer (CVAFS) detection system employed for the remainder of the assay is the same as is described in EPA Method 1631 (USEPA, 2002) for the analysis of THg in an aqueous samples.

A set of four environmental samples were allowed to thaw for approximately 15 minutes prior to the actual analysis. The 200 ml glass gas-flushing bottles (bubbler flasks) are filled with 40 ml of anoxic 0.5 % HCl. The sample slurry was briefly remixed and the entire contents of a single centrifuge tube were quickly and completely transferred to a single bubbler. A 0.5 ml aliquot of 20 % (w/v) $SnCl_2$ was added to each and the system was sealed and purged with nitrogen gas for exactly 15 minutes while gently shaking. The evolved gaseous Hg^0 is subsequently trapped on a gold-sand trap. A soda-lime trap is located between the bubbler and the gold trap to protect the latter from acid fumes, as detailed in EPA Method 1631. The Hg^0 is then thermally desorbed from the gold trap to the analytical system and detected using CVAFS detector (Brooks Rand Model III Mercury Analyzer). Peak integration software (Peak Simple, Chrom Tech, Inc. Apple Valley, MN) is used to convert the analog signal output from the CVAFS to an integrated peak area value. Standard curves generated from aqueous $HgCl_2$ calibration standards, assayed as above, were used to calculate $Hg(II)_R$ concentrations.

Daily analytical batches consisted of a set of 4 (minimum) calibration standards, 8-16 $Hg(II)_R$ samples, 1-2 additional replicates of a single randomly picked $Hg(II)_R$ sample, and 4 bubbler blanks. Bubbler blanks consisted of 50 ml of 0.5% HCl and the $SnCl_2$ amendment only (no sediment). Calibration standards are prepared by dilution of a NIST-certified commercially obtained $HgCl_2$ standard. In addition, a precisely calculated amount of gaseous elemental Hg^0 is injected into the analytical rig to verify the results (peak area vs. total mercury added) of the aqueous standards.

Methylmercury

A standard USGS approved method was used for the sediment MeHg extraction and quantification (DeWild and others, 2004). In summary, MeHg is first extracted from sediment (0.5 to

1.0 g) with a mixture of potassium bromide, copper sulfate, and methylene chloride. A sub-sample of the organic phase (methylene chloride) is added to a container of water, which is then slowly heated. This results in the evaporation of the organic phase and the back-extraction of the MeHg into the aqueous phase. The pH is adjusted to 4.9 using acetate buffer. The extractant is then ethylated using sodium tetraethyl borate. The volatile ethylated mercury species are purged from solution with N_2 gas, collected on a carbon-trap, thermally desorbed, separated using a gas chromatographic (GC) column, reduced using a pyrolytic column, and detected using CVAFS.

Additional Sediment Characterization

Sediment pH

Measurements were made with a pH electrode used in conjunction with a hand held pH/mV multi-meter (Model 59002-00, Cole Parmer®). The electrode was calibrated daily with fresh commercial pH = 7 phosphate buffer and then rinsed clean with reagent water. The probe was then fully inserted into the homogenized sediment, which was squeezed into a ball around the probe tip (to exclude any air bubbles) in the bottom of the plastic Whirl-Pak™ bag.

Oxidation-Reduction Potential (ORP)

Measurements of sediment ORP were made with a platinum band ORP electrode (Model EW05990-55, Cole Parmer®) used in conjunction with a hand held pH/mV multi-meter (as above). The electrode's accuracy was tested daily with freshly made buffer solutions (pH = 7 and pH = 4) saturated with quinhydrone, as per the manufacturer's instructions (Cole-Parmer document #P1937). The ORP potential for each solution is measured and the difference between them calculated. If this value fell within the range of 173 ± 4 mV, the probe was determined to be functioning properly. After cleaning thoroughly with reagent water and drying, the probe was then fully inserted into the homogenized sediment, which was squeezed into a ball around the probe tip (to exclude any air bubbles) in the bottom of the plastic Whirl-Pak™ bag. The ORP meter was allowed to equilibrate for a minimum of 10 minutes, until a stable reading is achieved, prior to recording the milli-volt (mV) value. All measurements were taken while sediment was at room temperature (19-22 °C). The ORP meter values were converted to E_h values (a standard convention that adjusts the value assuming a normal hydrogen reference electrode), using the following conversion provided by the electrode manufacturer:

$$E_h = ORP + E_R$$

$$E_R = (-0.718 \times T) + 220$$

Where: ORP = the oxidation-reduction potential value directly from the meter (millivolts); E_R = is the standard potential for a normal hydrogen reference electrode (millivolts); T = temperature (°C)

Bulk Density, Percent Dry Weight, Porosity and Organic Content

Sediment bulk density, dry weight, porosity and organic content were all assayed in order from a single sediment sample. An exact 3.0 cm^3 of wet sediment was removed from the sample vial using a 3.0 cm^3 plastic syringe that has the needle end cut off of the syringe barrel. This sub-sample was transferred into a small crucible and weighed. Sediment bulk density (g/cm^3) was then calculated as the weight-to-volume ratio.

Sediment dry weight and porosity were measured using standard drying techniques (APHA, 1981a).The crucible was then placed in an oven over-night at 105 °C. The next day, the sample was placed in a dedicator to cool, and was then reweighed. The sediment percent dry weight was then calculated as [dry sed wt./wet sed wt. x 100]. Sediment porosity (ml porewater per cm^3 of wet sediment) was calculated as the volume of water lost upon drying divided by the original sediment wet volume.

Organic content was calculated via the weight Loss on Ignition (LOI) standard assay (APHA, 1981b). The crucible was then placed in a combustion oven at 500 ^{o}C for four hours. This completely burns off any organic constituents, leaving only mineral material. After recooling and reweighing, the weight loss was calculated, which is a measure of total organic content.

Grain Size

Grain size, greater or less than 63 microns (the sand/silt split), was assayed using a standard wet sieve method (Matthes and others, 1992).

Sediment and Mercury Inventory and Mobilization Calculations

A model analysis of predicted changes in Alviso Slough geometry, based upon the 20-foot and 40-foot notch scenarios for Pond A8, was previously conducted by PWA and presented in Appendix G of the draft Environmental Impact Study / Report for the South Bay Salt Ponds Restoration Project (EDAW and others, 2007). This report includes information regarding existing channel depth, width and cross sectional area, as well as predicted changes in these parameters associated with the two different notch scenarios, at five cross channel transects along the slough length (**Figure 2**). Based upon the location of these five transect lines, four sections of Alviso Slough were defined (Sections A through D; including slough channel plus fringing marsh), which were bounded by the transect lines on either end and the existing levee walls (**Figure 2**). The area of each section was determined from aerial photographic images of the study area, using two independent approaches. The first involved map digitization and subsequent area calculation using ArcMap software (Environmental System Research Institute, Redlands, CA). The second approach involved carefully cutting out (in triplicate) the defined sections from printed map images, weighing them to an accuracy of ± 0.0001 g, and calibrating these to similarly cut and weighed squares representing an area of 1 km^2 that was derived from the map distance scale. The two approaches to calculating the area of each section agreed to within 2.7 ± 1.4 % The length of the slough channel for each section was measured from aerial photographic images using the perimeter tool in Adobe Acrobat® (version 7.0 Professional).

The current inventory of each mercury species in each segment of Alviso Slough (A through D) was calculated as follows: (a) The concentration of each species was calculated on an aerial basis (e.g. mg/m^2) for each depth profile by integrating the cumulative volumetric concentrations to a common depth of exactly 0-200 cm. (b) Depth integrated concentrations from all sediment sampling sites that fell within a defined slough section were averaged to calculate a single 0-200 cm depth integrated value for that segment (e.g. all six sediment sampling sites associated with T2 and T3 were used to calculate a single 0-200 cm depth integrated THg value for slough segment C, see **Figure 2**). The exception to this grouping approach was for slough segment A, in which no sediment was sampled within its defined boundaries. In this case the three profiles associated with the T1 sediment sampling were used. (c) The average 0-200 cm depth integrated mercury species concentration (calculated in (b)) for a given slough section was then multiplied by the area of that section to calculate the total current inventory for that species in that slough segment. The resulting mercury inventory of all slough sections were added to calculate the complete mercury species inventory for Alviso Slough, between the uppermost PWA transect line (A8 Notch) and the lowermost one (Mouth).

To calculate the volume of sediment mobilized for each slough section and for each notch scenario the following approach was taken: (d) the change in slough cross sectional area (m^2) of each was first calculated for each transect from the data provided in the PWA report, (e) the average change in cross sectional area (m^2) for each slough segment (A through D) was than calculated as the average (± deviation; n =2) of the upper and lower bounding transect lines for that slough segment, (f) the value from (e) was multiplied by the measured slough length for that segment to calculate total cubic meters (m^3) of sediment mobilized under each scenario. The error associated with calculation (e) was carried through the rest of the calculation for sediment and mercury mobilization. Based on modeling results and for the purposes of these calculations, the assumption is made that the predicted change in the slough cross sectional area for the downstream most transect line (Mouth) is zero for both notch scenarios (i.e. no change) (Don Danmeier, PWA, personal communication).

To calculate the amount of each mercury species mobilized for each section and notch scenario, the following approach was taken: (g) the sediment volumetric mercury species concentration (e.g. mg/m^3) was first calculated for each discrete sample, based on the weight-based concentration (e.g. ng/g wet sediment) and the sediment bulk density (g/cm^3). (h) A single average (± standard error) value of volumetric mercury species concentration was then calculated as the average of all of the discrete samples that comprised the sediment profiles associated with that particular slough section (grouped as described in (b)). (i) To calculate the absolute mass of each mercury species mobilized for each slough segment (A through D), the specific volumetric mercury species concentration (calculated in (h)) was multiplied by the volume of sediment mobilized (calculated in (f)) for that section and notch scenario. The error associated with both (f) and (h) were propagated through these calculations. The mercury species mass mobilized in each slough segment was added to calculate the total mercury species mass mobilized between the uppermost PWA transect line (A8 Notch) and the lowermost one (Mouth).

Sediment Scour Simulation Experiment

Excess sediment from the 150-175 cm depth horizon of core AS-T2B-D3 was transferred into an acid cleaned glass mason jar at the time of initial sub-sampling and was stored refrigerated at 5 ^{o}C for 109 days prior to the initiation of the scour simulation experiment.. Surface water from Alviso Slough was collected as part of routine sampling by the SCVWD in late January 2007. The water from two sites (ASW1 and ASW3) was filtered (0.45 µm) and stored refrigerated at 5 ^{o}C for 7 days prior to the initiation of the scour simulation experiment. The salinity between these two sites varied more than two-fold, with the upstream ASW1 site being less saline (11 ppt) than ASW3 (26.5 ppt), the latter being located closer to the slough mouth. These two source waters were subsequently sub-sampled such that 1.0 liter of each was transferred into two large glass flasks equipped with a rubber stopper that had a) a port for a fritted glass gas purging rod that extended to the bottom of the flask, b) a gas venting tube, and c) a liquid sampling FEP tube that extended to the bottom of the flask and that had a stopcock above the stopper to close it off when not in use. The filtered slough water from both sites was purged for 24 hours with either compressed air or inert nitrogen (N_2) gas, while stirring with a magnetic stir bar. Thus, four treatment conditions were established with Alviso Slough water: a) low salinity / oxic, b) low salinity / anoxic, c) high salinity / oxic, and d) high salinity / anoxic. After establishing these initial conditions, two 50 ml samples of water were removed from each flask for initial aqueous $Hg(II)_R$ concentration analysis. The AS-T2B-D3 sediment was then sub-sampled and accurately weighed in an anaerobic chamber, and 27 g was added to each of the four flasks, resulting in final total suspended sediment concentration of 14.3 g dry sediment per liter (based upon 48.0 % sediment dry weight initially measured). Duplicate sub-samples of sediment (approximately 2 g each) were also taken and frozen for subsequent whole sediment $Hg(II)_R$ concentration analysis, and triplicate sub-samples were take for sediment dry weight analysis. Immediately after adding sediment to all four flasks, gas purging and aqueous phase stirring was resumed and continued thus throughout the remainder of the experiment. After approximately 1 hour, an initial (Day 0) sample was taken from each flask. Sub-sampling consisted of attaching a 60 ml syringe to the liquid sampling tube, opening the stopcock and pulling approximately 50 ml of the suspended sediment slurry into the syringe, which was subsequently weighed so that the exact sediment mass sampled could be calculated. The slurry in the syringe was immediately assayed for $Hg(II)_R$, as described above. Duplicate 50 ml sub-samples were taken from each flask during each sampling event, which was similarly repeated on days 1, 3, 5, and 7.

Results

Sediment Core Descriptions

Photographs, lithographic and accessory descriptions, and MSCL scans of sediment gamma density and magnetic susceptibility profiles are provided in **Appendix A** for of all 50 core segments collected.

Mercury Speciation and Quantification

Site and depth specific concentration data (dry weight) for THg, $Hg(II)_R$ and MeHg are summarized in **Table 2,** along with the quantity of $Hg(II)_R$ and MeHg expressed as a percentage of THg and summary statistics for the complete dataset. Concentration profiles for THg are graphically illustrated in **Figure 4** on a whole sediment basis ($\mu g/cm^3$), with the 0-200 cm depth integrated value (g/m^2) provided for each profile. Similarly, the whole sediment concentration profile for MeHg (ng/cm^3) is graphically illustrated in **Figure 5**, with the 0-200 cm depth integrated (mg/m^2) value provided for each site. Site specific profiles of % $Hg(II)_R$ are presented ($\log_{10}$ scale) in **Figure 6**, along with the 0-200 cm depth integrated $Hg(II)_R$ concentration (mg/m^2) at each site.

Quality assurance metrics for mercury species concentrations were as follows: The average percentage difference for THg samples run in duplicate was (mean ± std. dev.) 6.1 ± 5.1 % (N = 23). A 5 ng/L daily quality check standard (QCS), prepared from a different stock $HgCl_2$ solution than for the normal daily standard curve, was 97.4 ± 5.7 % of the theoretical value (N = 11). Recoveries of certified reference material (IAEA-405, estuarine sediment, THg certified value = 0.81 µg/g dry weight) were 103 ± 6 % (N =7) of the certified value. Matrix spike recoveries for THg were 103 ± 29 % (N = 6) of the calculated amount of Hg(II) added. The average percentage difference for $Hg(II)_R$ samples run in duplicate was 12.9 ± 9.5 % (N = 6). There is no certified reference material for $Hg(II)_R$ and matrix spikes do not provide reliable results due to the rapid binding of some fraction of the added Hg(II) spike to dissolved and solid organic phases. The average percentage difference for MeHg samples run in duplicate was 11.6 ± 9.1 % (N = 13). Recoveries of certified reference material (IAEA-405, estuarine sediment, MeHg certified value = 5.49 ng/g dry weight) were 83 ± 24 % (N = 16) of the certified value. Matrix spike recoveries for MeHg were 66 ± 45 % (N = 20) of the calculated amount of MeHg added.

Ancillary Sediment Parameters

Site and depth specific data for sediment pH, oxidation-reduction potential (E_h), dry weight, organic content (as % LOI), bulk density, porosity and grain size are summarized in **Table 3,** along with summary statistics for the individual profiles and the complete dataset. The following ancillary sediment parameter data are also given graphically: pH (**Figure 7**), E_h (**Figure 8**), LOI (**Figure 9**), and grain size (**Figure 10**). MSCL scan data are graphically depicted for sediment density via gamma irradiation (**Figure 11**) and magnetic susceptibility (**Figure 12**). In addition, discrete interval measurements of sediment bulk density, as directly measured via sub-sample weights and volumes, are superimposed on MSCL profiles of gamma density (**Figure 11**). The average percentage difference for samples run in duplicate was as follows (mean ± std. dev.): dry weight, 0.5 ± 0.7 % (N = 26); LOI, 2.6 ± 3.1 % (N = 25); bulk density, 1.5 ± 1.5 % (N = 26); porosity, 1.5 ± 1.6 % (N = 26); and grain size 1.4 ± 1.0 % (N = 8). Due to time constraints and equipment limitations during initial sample processing only one measurement was made for pH and E_h for each individual sample.

Sediment and Mercury Mobilization Estimates

Previously reported (EDAW and others, 2007) Alviso Slough current cross sectional areas, and those predicted for the 20-foot and 40-foot Pond A8 notch scenarios, are given in **Table 4** along with the calculated change in cross sectional area associated with both notch scenarios. The area and channel length measurements for the defined slough sections A-D (**Figure 2**) are given in **Table 5**, along with the volume of sediment mobilized as calculated for both notch scenarios.

Sediment Scour Simulation Experiment

The experimental mixing of deeply buried (150-175 cm depth interval) Alviso Slough main channel sediment with overlying slough water was conducted to simulate the scenario under which increased tidal energy in Alviso slough leads to the deepening of the slough channel, thus mobilizing sediment and currently buried mercury. The specific question addressed by this experiment is whether or not the operationally defined $Hg(II)_R$ fraction in buried (and chemically reducing) sediment changes (increases or decreases) as a result of being exposed to oxygenated overlying water of either high or low salinity. The anoxic treatments serve as a type of control, as the oxic treatments are more reflective of typical field conditions since the overlying slough water is tidally mixed and anoxic water conditions have not been observed in any of the five sampling events that have been conducted as part of the larger study between November 2006 and July 2007 (dissolved oxygen = 5.3 ± 0.8; n = 30 [5 sampling events x 3 sites along the salinity gradient x 2 depth (surface and deep)]).

The initial wet sediment $Hg(II)_R$ concentration was 0.14 ± 0.01 ng/g (0.30 ± 0.03 ng/g on a dry weight basis; n = 2). Initial aqueous $Hg(II)_R$ concentrations in the four treatment flasks, sampled immediately prior to the addition of sediment, ranged from 0.30 – 0.84 ng/L. Based on these measurements and the exact initial volumes used, the theoretical $Hg(II)_R$ concentration in the sediment/water slurry would be approximately 4.4 – 5.0 ng/L, assuming homogeneous mixing and no changes in the pool of $Hg(II)_R$ due to oxidation or reduction reactions. Within 1-2 hours of adding sediment to the flasks (Day 0), the actual $Hg(II)_R$ concentration measured for the individual slurry solutions ranged from 1.5 ng/L (high salinity / anoxic) to 4.0 ng/L (low salinity / anoxic). However, within 24 hours (Day 1) concentrations began to increase, and ranged from 25 ng/L (high salinity / anoxic) to 179 ng/L (high salinity / oxic). Over the next six days, the concentrations in both anoxic slurries remained in the comparatively narrow and low range of 17-29 ng/L, while the oxic treatments either remained elevated or continued to increase, ending at concentrations of 169 ng/L (high salinity / oxic) and 265 ng/L (low salinity / oxic) by Day 7 (**Figure 13**). Relative to the theoretical slurry $Hg(II)_R$ concentrations of 4.4 – 5.0 ng/L, based solely on the mixing of Alviso Slough sediment and water at initial concentrations, the approximate factor increase by the end of the experiment for each of the four treatments was as follows: 4X (low salinity / anoxic), 6X (high salinity / anoxic), 53X (low salinity / oxic), 35X (high salinity / oxic) Thus, these results indicate that the mixing of chemically reducing buried sediment with oxygenated overlying slough water significantly increases the fraction of $Hg(II)_R$. This experiment does not address how long these conditions are maintained beyond 7 days or the ultimate fate of this $Hg(II)_R$ pool.

Acknowledgments

The authors gratefully acknowledge the following individuals and organizations: J.L. Agee, E. Kakouros, S.L. Wren, J. Kanerva, K. Akstin (USGS, Menlo Park, CA) and C.N. Alpers (USGS, Sacramento, CA) for laboratory analytical support; J. Collins, L. Grenier, J. Hunt, S. Bezalel (SFEI, Oakland, CA) for collaborative, field and logistical support; D. Drury and B. Calhoun (SCVWD, San Jose, CA) for field logistical support; B. Watson and L. Reidy (UC Berkeley, CA) for sediment core collection and laboratory assistance; B. Edwards and B. Carkin (USGS, Menlo Park, CA) for use of the Multi-sensor core logger; D. Danmeier (PWA, San Francisco, CA) for assistance with sediment scour estimates, and S. Ritchie (California Coastal Conservancy, Oakland, CA) and M. Singer (USGS, Menlo Park, CA) for providing constructive reviews of this report. The work described herein was funded by the California Coastal Conservancy under Interagency Agreement #06-004.

References

Ackerman, J., Eagles-Smith, C., Heinz, G., Wainwright-De La Cruz, S., Takekawa, J., Adelsbach, T., Miles, A., Hoffman, D.J., Schwarzbach, S.E., Suchanek, T.H., and Maurer, T.C., 2007, Mercury in birds of the San Francisco Bay-Delta: trophic pathways, bioaccumulation and ecotoxicological risk to avian reproduction. 2006 Annual Administrative Report to CALFED: U.S. Geological Survey, Western Ecological Research Center, and U.S. Fish and Wildlife Service, Environmental Contaminants Division, 41 p.

Ackerman, J.T., Eagles-Smith, C.A., Takekawa, J.Y., Demers, S.A., Adelsbach, T.L., Bluso, J.D., Miles, A.K., Warnock, N., Suchanek, T.H., and Schwarzbach, S.E., (in press), Mercury concentrations and space use of pre-breeding American avocets and black-necked stilts in San Francisco Bay: Science of The Total Environment.

Alpers, C.N., Hunerlach, M.P., May, J.T., and Hothem, R.L., 2005, Mercury contamination from historical gold mining in California: US Geological Survey, Fact Sheet 2005-3014, 6 p. On-line: *http://pubs.usgs.gov/fs/2005/3014/*

APHA, 1981a, Section 209 C: Total Nonfiltrable Residue Dried at 103-105 °C, *in* Franson, M.A.H., ed., Standard Methods for the Examination of Water and Wastewater, 15th Edition: Washington, D.C., Amer. Public Health Association, Amer. Water Works Assoc., Water Pollut. Control Fed., p. 94-95.

---, 1981b, Section 209 G: Volatile and Fixed Matter in Nonfilterable Residue and in Solid and Semisolid Samples, *in* Franson, M.A.H., ed., Standard Methods for the Examination of Water and Wastewater, 15th Edition: Washington, D.C., Amer. Public Health Association, Amer. Water Works Assoc., Water Pollut. Control Fed., p. 97-99.

Bloom, N., Bollen, A., Briscoe, M., Hall, G., Horvat, M., Kim, C., Lasorsa, B., Marvin-Dipasquale, M., and Parker, J., 2006, International Solid Phase Mercury Speciation Exercise (ISPMSE): Introduction and Preliminary Results, *in* Mercury 2006 Abstracts Book: Eighth International Conference on Mercury as a Global Pollutant, Madison, Wisconsin August 6-11, 2006.

Brumbaugh, W.G., Krabbenhoft, D.P., Helsel, D.R., Wiener, J.G., and Echols, K.R., 2001, A national pilot study of mercury contamination of aquatic ecosystems along multiple gradients: Bioaccumulation in fish: U.S. Geological Survey, USGS/BRD/BSR-2001-0009, 26 p.

Cargill, S.M., Root, D.H., and Bailey, E.H., 1980, Resource estimation from historical data: mercury, a test case: Statistics and Earth Sciences, no. 12, p. 489–522.

Compeau, G.C., and Bartha, R., 1985, Sulfate-reducing bacteria: Principal methylators of mercury in anoxic estuarine sediment: Applied and Environmental Microbiology, v. 50, no. 2, p. 498-502.

Conaway, C.H., S., S., Mason, R.P., and Flegal, A.R., 2003, Mercury speciation in the San Francisco Bay estuary: Marine Chemistry, v. 80, p. 199-225.

CRWQCB, 2006, Mercury in San Francisco Bay: Proposed Basin Plan Amendment and Staff Report for Revised Total Maximum Daily Load (TMDL) and Proposed Mercury Water Quality Objectives: California Regional Water Quality Control Board - San Francisco Bay Region, 116 p. On-line: *http://www.waterboards.ca.gov/sanfranciscobay/TMDL/sfbaymercurytmdl.htm*

Davis, J.A., Yee, D., Collins, J.N., Schwarzbach, S.E., and Luoma, S.N., 2003, Potential for Increased Mercury Accumulation in the Estuary Food Web: San Francisco Estuary and Watershed Science, v. 1, no. 1/ article 4, p. 1-36.

DeWild, J.F., Olund, S.D., Olson, M.L., and Tate, M.T., 2004, Methods for the preparation and analysis of solids and suspended solids for methylmercury. Chapter 7 of Book 5, Laboratory Analysis; Section A, Water Analysis: U.S. Geological Survey, USGS Techniques and Methods Report 5 A 7p.

EDAW, Philip Williams and Associates Ltd., H.T. Harvey and Associates, Brown and Caldwell, and Geomatrix, 2007, South Bay Salt Pond Restoration Project, Environmental Impact Statement / Report. Appendix G - Hydrology, Flood Management and Infrastructure Impact Analysis Support: Prepared for U.S. Army Corp of Engineers, U.S. Fish and Wildlife Service, and California Dept. of Fish and Game, DRAFT March 2007, 141 p. On-line: *http://www.southbayrestoration.org/EIR/downloads.html*

Gardner, J.V., Edwards, B.D., Dean, W.E., and Wilson, J., 1995, P-wave velocity, wet bulk density, magnetic susceptibility, acoustic impedance, and visual core descriptions of sediment recovered during Research Cruise EW9504: Data, techniques, and procedures: U.S. Geological Survey Open File Report 95-533, 288 p.

Kayen, R.E., Edwards, B.D., and Lee, H.J., 1999, Nondestructive laboratory measurements of geotechnical and geoacoustic properties through intact core-liner, *in* Marr, W.A., and Fairhurst, C.E., eds., Nondestructive and Automated Testing for Soil and Rock Properties, ASTMSTP 1350, American Society for Testing and Materials, p. 83-94.

Kieu, L.H., 2004, The Seasonal Influence of Saltmarsh Plants (*Salicornia virginica* and *Scirpus robustus*) on Methylmercury Production and Degradation Over Small Spatial Scales in South San Francisco Bay: San Francisco, San Francisco State University, Master's Thesis, 72 p.

Krabbenhoft, D.P., Wiener, J.G., Brumbaugh, W.G., Olson, J.F., DeWild, J.F., and Sabin, T.J., 1999, A national pilot study of mercury contamination of aquatic ecosystems along multiple gradients.: U. S. Geological Survey - Toxic Substance Hydrology Program., 99-4018B, 145-146 p.

Lacerda, L.D., and Fitzgerald, W.F., 2001, Biogeochemistry of mercury in wetlands: Wetlands Ecol. Manag., v. 9, p. 291-293.

Life_Science!, 2003, South Bay Salt Ponds Initial Stewardship Plan: Prepared by Life Science! Inc. in cooperation with California Dept. of Fish and Game, and U.S. Fish and Wildlife Service, 251 p. On-line: *http://www.southbayrestoration.org/ISPNews.html*

Livingstone, D.A., 1955, A Lightweight Piston Sampler for Lake Deposits: Ecology, v. 36, no. 1, p. 137-139.

Marvin-DiPasquale, M., Hall, B.D., Flanders, J.R., Ladizinski, N., Agee, J.L., Kieu, L.H., and Windham-Myer, L., 2006, Ecosystem Investigations of Benthic Methylmercury Production: A Tin-Reduction Approach for Assessing the Inorganic Mercury Pool Available for Methylation, *in* Mercury 2006 Abstracts Book: Eighth International Conference on Mercury as a Global Pollutant, Madison, Wisconsin August 6-11, 2006.

Matthes, W.J.J., Sholar, C.J., and George, J.R., 1992, Quality-Assurance Plan for the Analysis of Fluvial Sediment by Laboratories of the U.S. Geological Survey: U.S. Geological Survey, Open-File Report 91-467, 37 p.

McKee, L., Leatherbarrow, J., and Oram, J., 2005, Concentrations and loads of mercury, PCBs, and OC pesticides in the lower Guadalupe River, San Jose, California: Water Years 2003 and 2004. A Technical Report of the Regional Watershed Program: San Francisco Estuary Institute, SFEI Contribution 409, 72 p.

Olund, S.D., DeWild, J.F., Olson, M.L., and Tate, M.T., 2004, Methods for the preparation and analysis of solids and suspended solids for total mercury. Chapter 8 of Book 5, Laboratory Analysis; Section A, Water Analysis: U.S. Geological Survey, USGS Techniques and Methods Report 5 A 8p.

PWA, H.T. Harvey & Associates, EDAW, and Brown and Caldwell, 2006, South Bay Salt Ponds Restoration Project: Final Alternatives Report: Prepared for: California State Coastal Conservancy, U.S. Fish and Wildlife Service, California Department of Fish and Game., 47 p. On-line: *http://www.southbayrestoration.org/Alternatives.html*

Thomas, M.A., Conaway, C.H., Steding, D.J., Marvin-DiPasquale, M., Abu-Saba, K.E., and Flegal, A.R., 2002, Mercury contamination from historic mining in water and sediment, Guadalupe River and San Francisco Bay, California: Geochemistry: Exploration, Environment, Analysis, v. 2, p. 211-217.

USEPA, 2002, Method 1631, Revision E: Mercury in water by oxidation, purge and trap, and cold vapor atomic fluorescence spectrometry: U.S. Environmental Protection Agency, Office of Water, EPA-821-R-02-019, 36 p.

VBC, 2005, The California Bay-Delta Authority Mercury Studies Quality Assurance Program. Kick-Off Meeting. May 19, 2005. Information Packet: Van Burren Consulting, LLCp. On-line: *www.vanbuurenconsulting.com*

VBC, and CDFG, 2005, Programmatic Quality Assurance and Quality Control for California Bay-Delta Authority (CBDA) Mercury Research and Monitoring Projects: Van Buuren Consulting, LLC and the California Department of Fish and Game, Annual Report for the California Bay-Delta Authority Projectp. On-line: *http://www.calwater.ca.gov/content/erp_calfed_mercury_2005_project_annual_reports_content.asp*

Wiener, J.G., Krabbenhoft, D.P., Heinz, G.H., and Scheuhammer, A.M., 2003, Ecotoxicology of mercury, Chapt. 16, *in* Hoffman, D.J., Rattner, B.A., Burton, G.A., Jr., and Cairns, J., Jr., eds., Handbook of Ecotoxicology, 2nd edition: Boca Raton, CRC Press, p. 409-463.

Zillioux, E.J., Porcella, D.B., and Benoit., J.M., 1993, Mercury cycling and effects in freshwater wetland ecosystems: Environ. Toxicol. Chem., v. 12, p. 2245-2264.

Figures

Figure 1. Map of South San Francisco Bay, Alviso Slough and the New Almaden Mining District

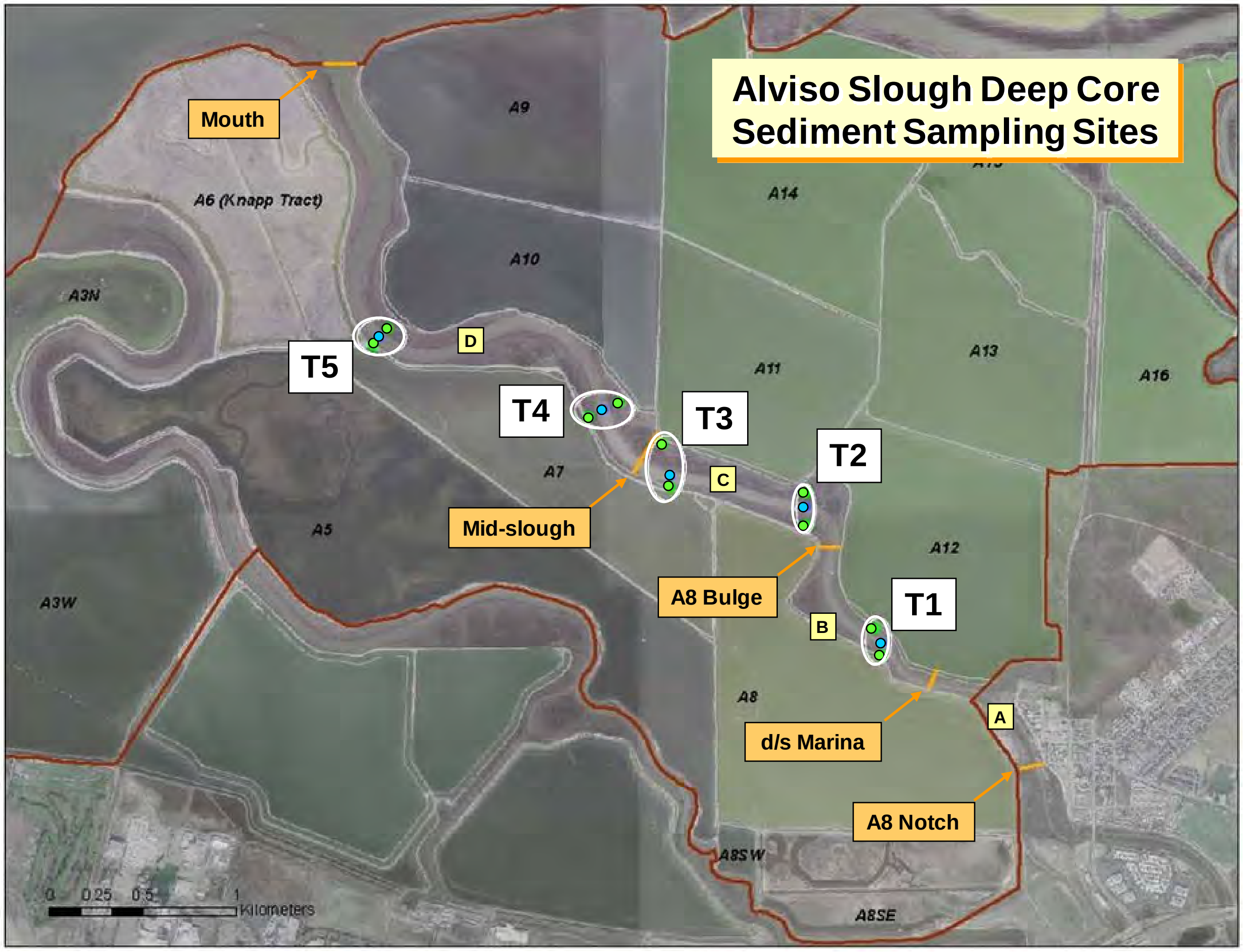

Figure 2. Map showing location of Alviso Slough sediment sampling sites

Sediment samples were collected between September 21 and 26, 2006, and included five transect groupings (T1 – T5). Each T# series consisted of three sampling locations, one in the primary slough channel (blue circle; B-series sites on Figures 3-12), one each on the right and left fringing marsh plains (green circles; A and C-series sites, respectively, on Figures 3-12). Also depicted are the PWA cross channel transect locations (orange lines) where slough geometry was previously determined, along with the transect line names (orange text boxes). The four slough segments (A – D, yellow text boxes) are bounded by the upper and lower cross channel transect lines and the existing levee wall, and include the slough channel plus the fringing marsh plain.

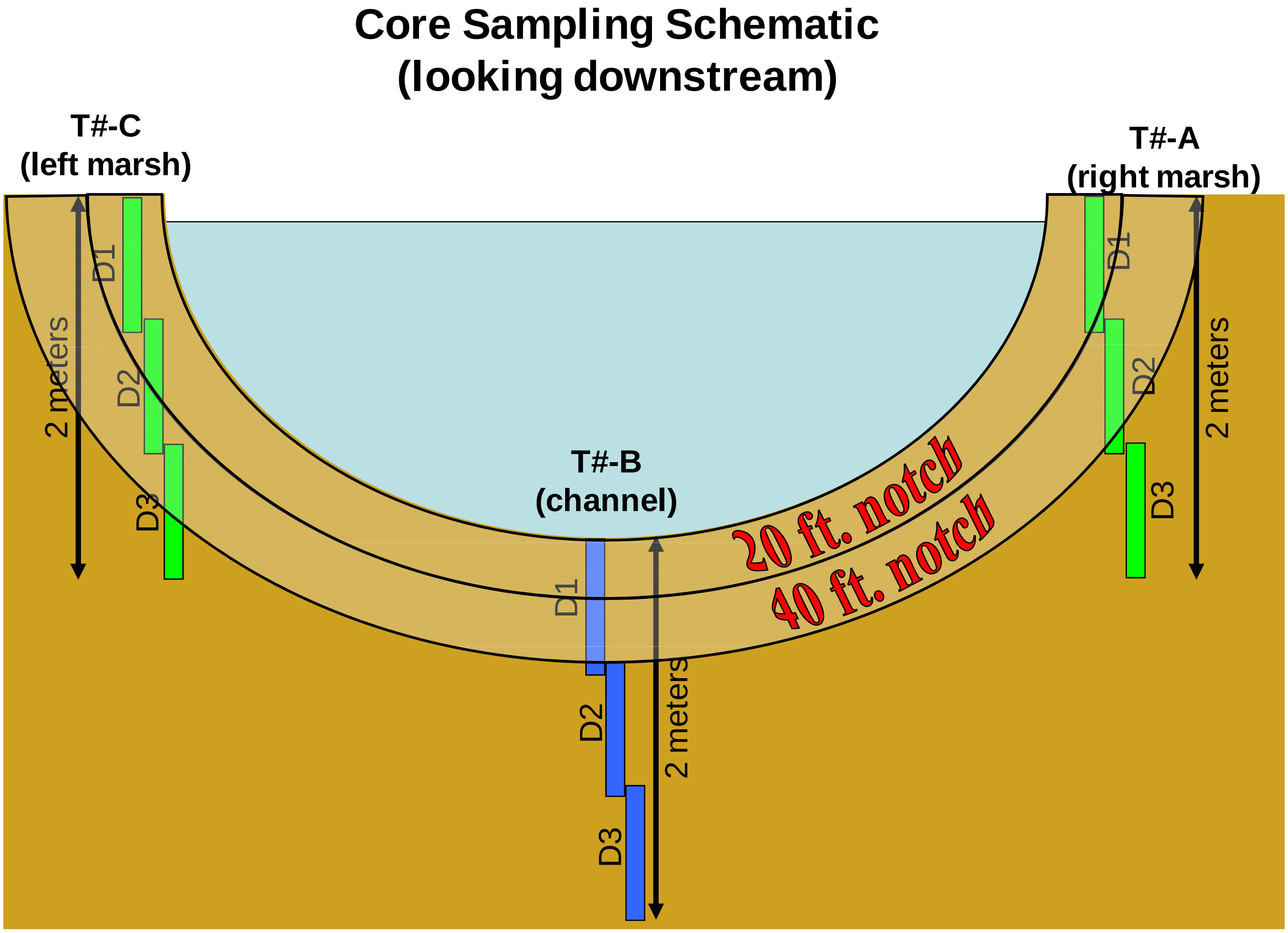

Figure 3. Illustration of slough cross section and sediment sampling design

The slough cross section illustration is orientated facing downstream and depicts the sediment sampling design associated with a generic sediment Transect (T#), including A (right marsh), B (slough channel), and C (left marsh) series sites. In the vertical, multiple cores were taken to a total depth of approximately 200 cm, from discrete depth intervals (D1-D3) that were slightly offset to allow for interval overlap. Also depicted is the theoretical slough scour (not to scale) associated with the two proposed Pond A8 levee notch scenarios (e.g. 20-foot and 40-foot wide notches).

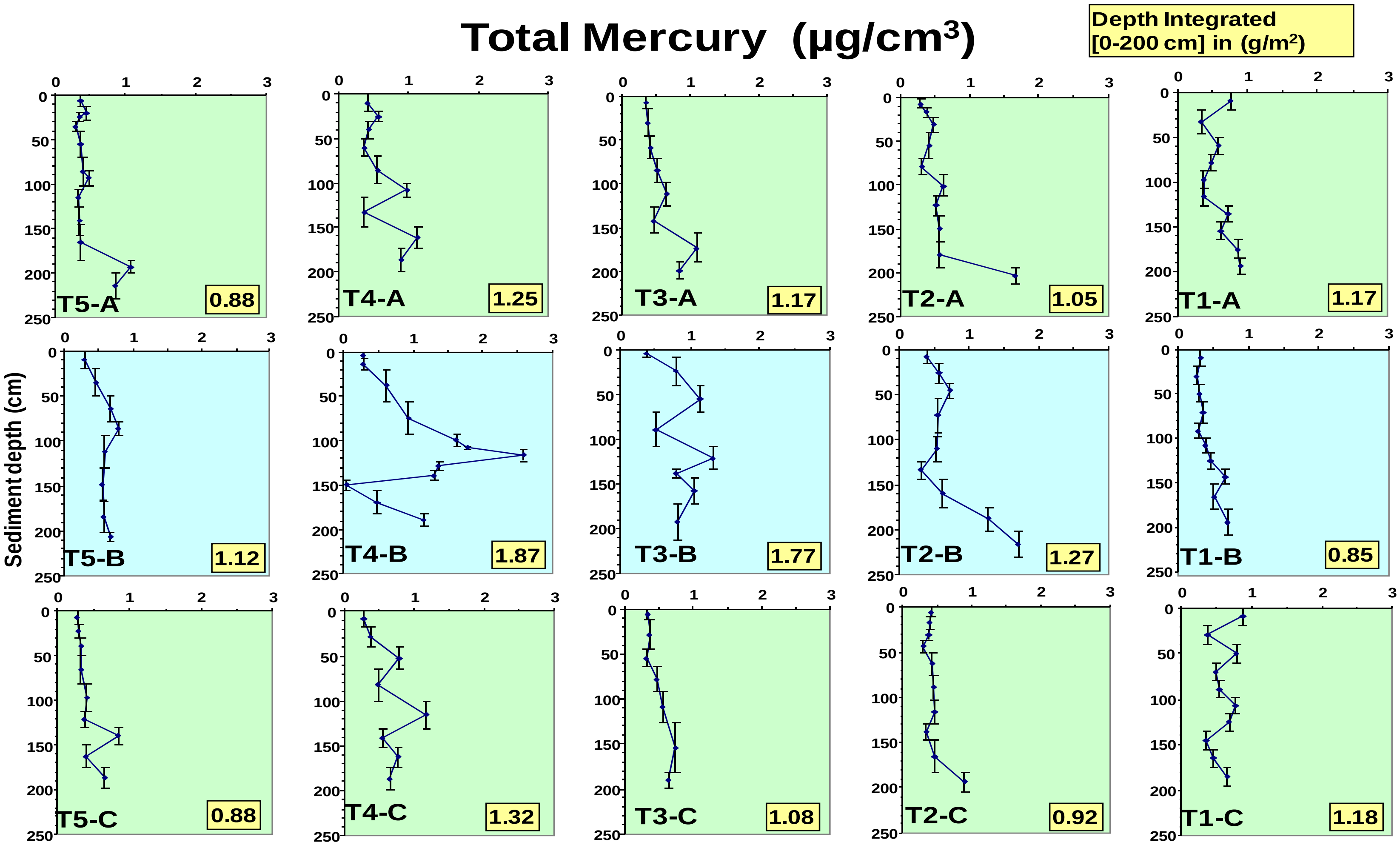

Figure 4. Depth profiles of sediment total mercury concentration

Alviso Slough total mercury (THg) concentration as a function of sediment dep th, where the symbol identifies the mid-point of each depth interval sampled and the associated vertical bars indicate the total interval vertical width. The aerial 0-200 cm depth integrated THg concentration (in g/m^2) is also given for each profile. Panel layout parallels the approximate orientation of the individual sites as depicted in **Figure 2**, and individual background colors (blue or green) reflect marsh or slough channel sites, respectively.

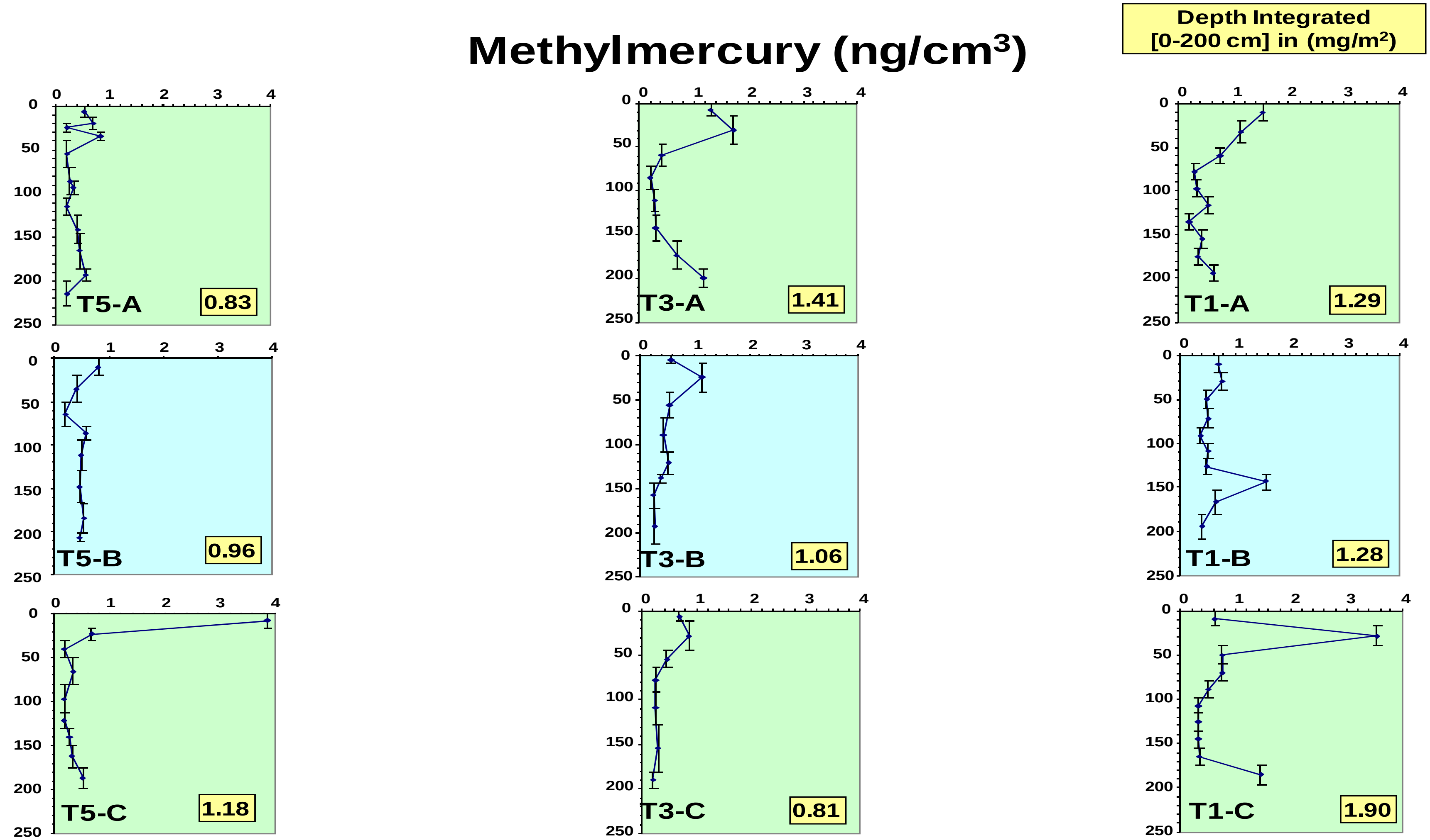

Figure 5. Depth profiles of sediment methylmercury concentration

Alviso Slough methylmercury (MeHg) concentration as a function of sediment depth, where the symbol identifies the mid-point of each depth interval sampled and the associated vertical bars indicate the total interval width. The aerial 0-200 cm depth integrated MeHg concentration (in mg/m^2) is also given for each profile. Panel layout parallels the approximate orientation of the individual sites as depicted in **Figure 2**, and individual background colors (blue or green) reflect marsh or slough channel sites, respectively.

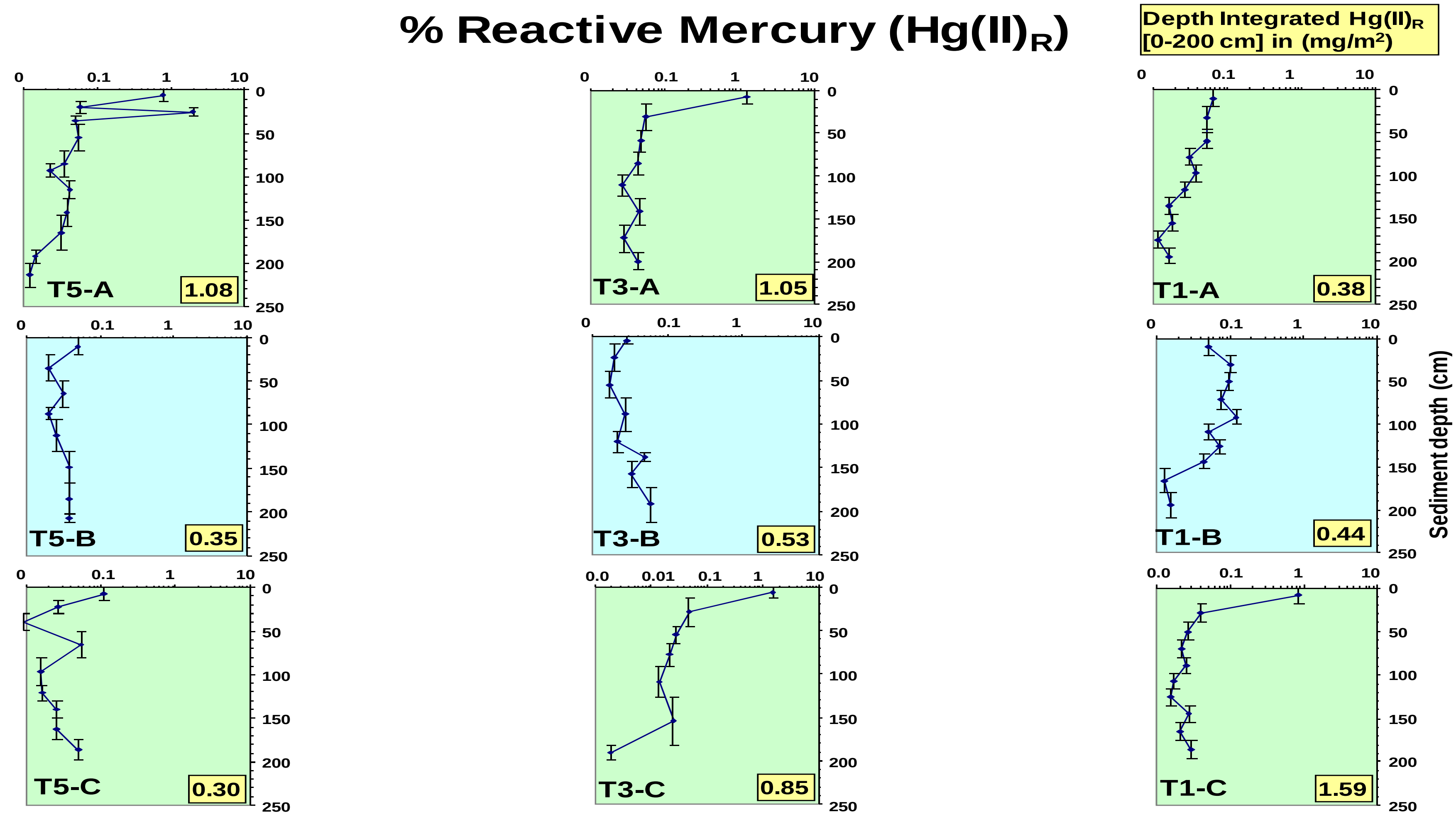

Figure 6. Depth profiles of sediment reactive inorganic mercury as a percentage of total mercury

Alviso Slough reactive inorganic mercury ($Hg(II)_R$) concentration as a percentage (%) of total mercury and as a function of sediment depth, where the symbol identifies the mid-point of each depth interval sampled and the associated vertical bars indicate the total interval width. The aerial 0-200 cm depth integrated $Hg(II)_R$ concentration (in mg/m^2) is also given for each profile. Panel layout parallels the approximate orientation of the individual sites as depicted in **Figure 2**, and individual background colors (blue or green) reflect marsh or slough channel sites, respectively.

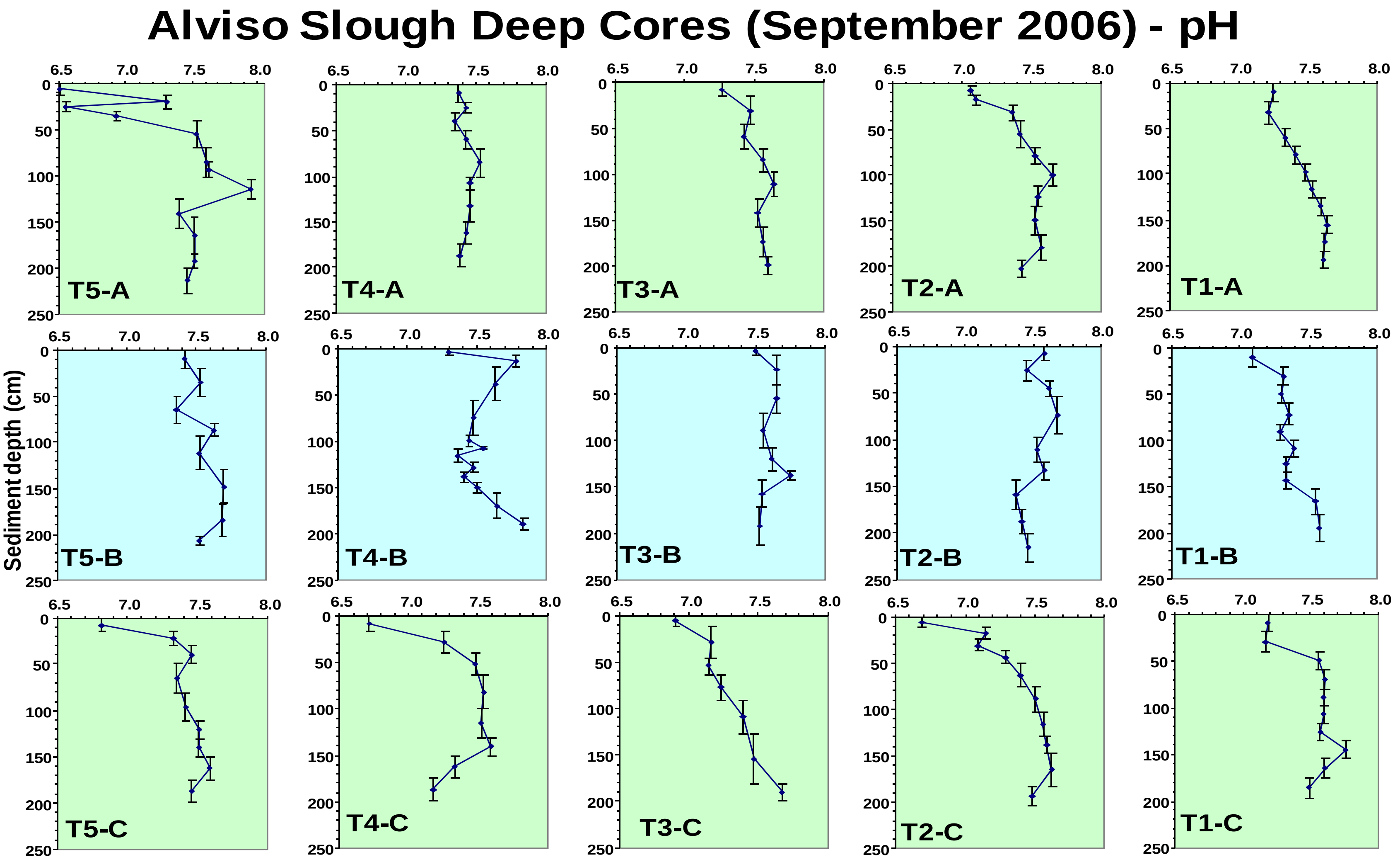

Figure 7. Depth profiles of sediment pH

Alviso Slough pH as a function of sediment depth, where the symbol identifies the mid-point of each depth interval sampled and the associated vertical bars indicate the total interval width. Panel layout parallels the approximate orientation of the individual sites as depicted in **Figure 2**, and individual background colors (blue or green) reflect marsh or slough channel sites, respectively.

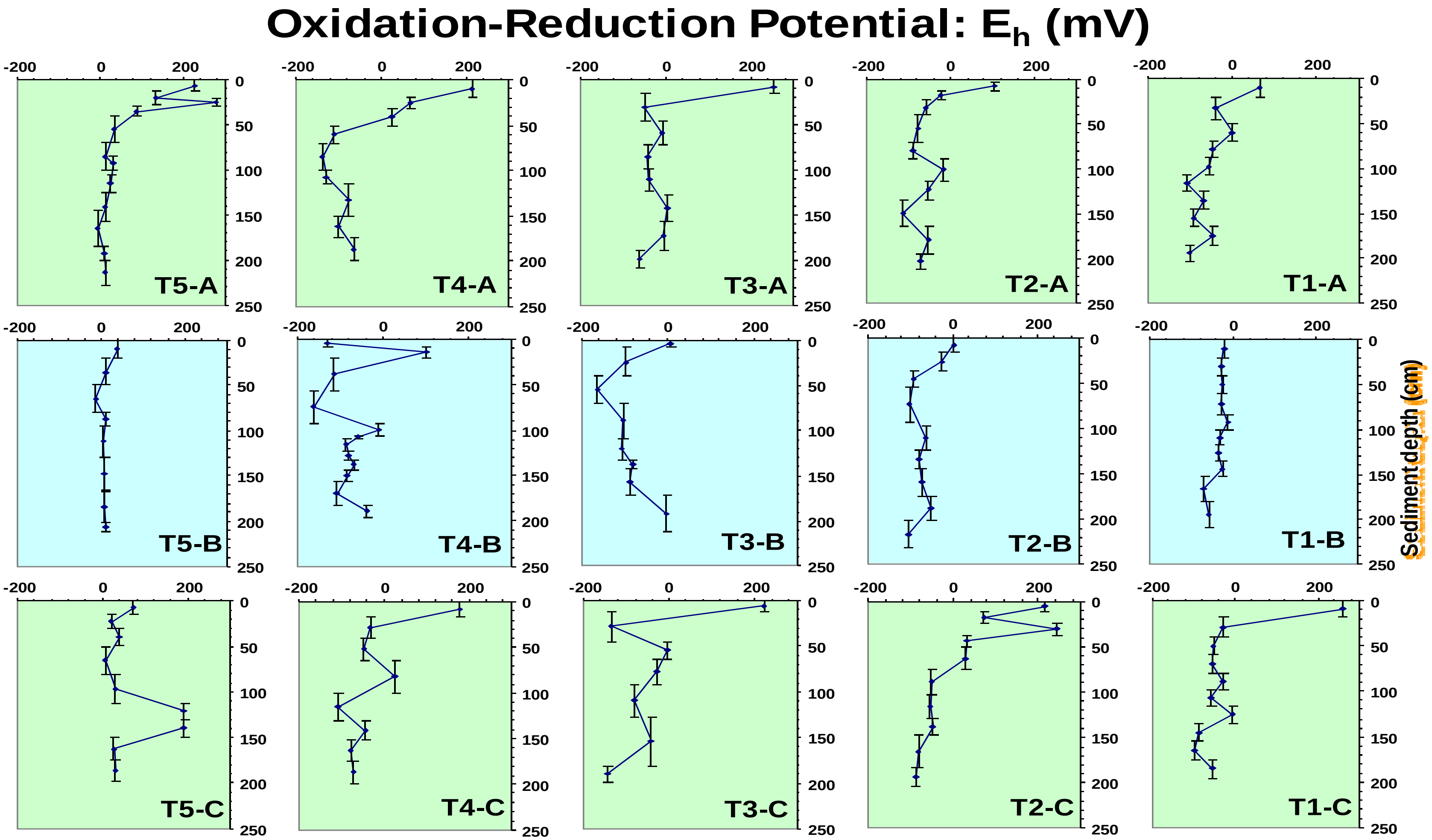

Figure 8. Depth profiles of sediment oxidation-reduction potential

Alviso Slough oxidation-reduction measurement (expressed as E_h) as a function of sediment depth, where the symbol identifies the mid-point of each depth interval sampled and the associated vertical bars indicate the total interval width. Panel layout parallels the approximate orientation of the individual sites as depicted in **Figure 2**, and individual background colors (blue or green) reflect marsh or slough channel sites, respectively.

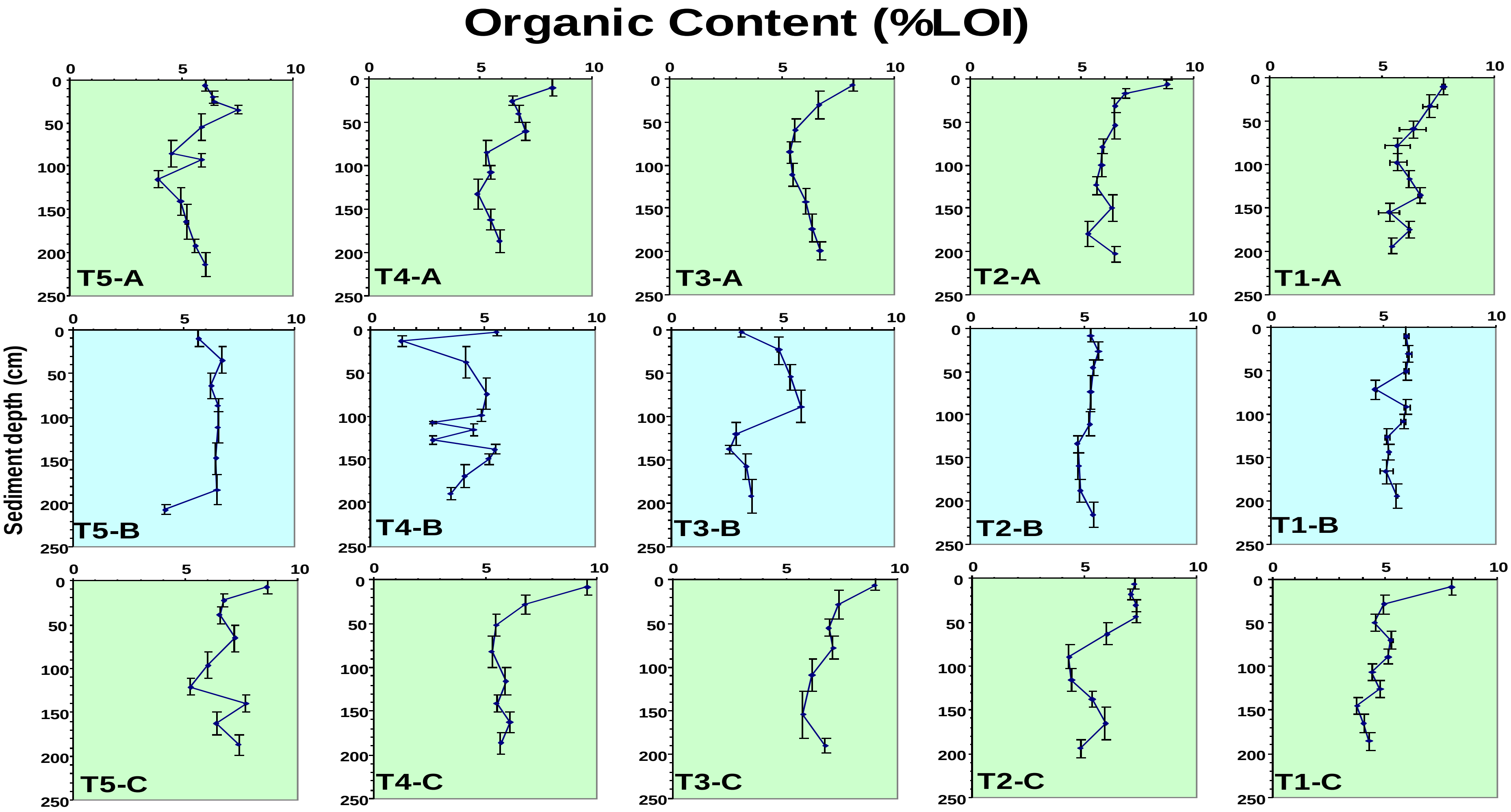

Figure 9. Depth profiles of sediment organic content

Alviso Slough sediment organic content (expressed as percent weight loss on ignition (% LOI)) as a function of sediment depth, where the symbol identifies the mid-point of each depth interval sampled and the associated vertical bars indicate the total interval width. Panel layout parallels the approximate orientation of the individual sites as depicted in **Figure 2**, and individual background colors (blue or green) reflect marsh or slough channel sites, respectively.

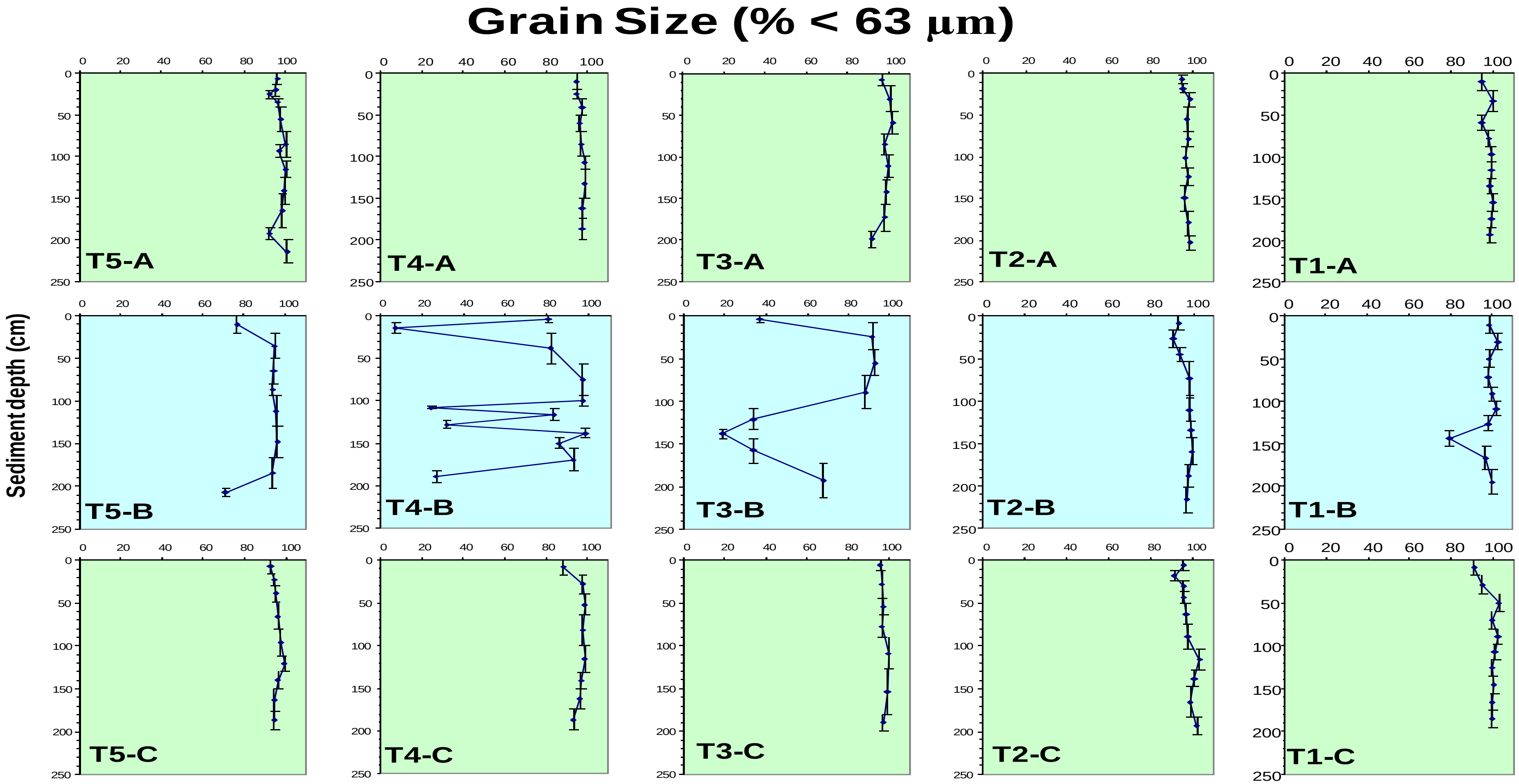

Figure 10. Depth profiles of sediment grain size

Alviso Slough sediment grain size (expressed as weight percent less than 63 micrometers (% < 63 µm)) as a function of sediment depth, where the symbol identifies the mid-point of each depth interval sampled and the associated vertical bars indicate the total interval width. Panel layout parallels the approximate orientation of the individual sites as depicted in **Figure 2**, and individual background colors (blue or green) reflect marsh or slough channel sites, respectively.

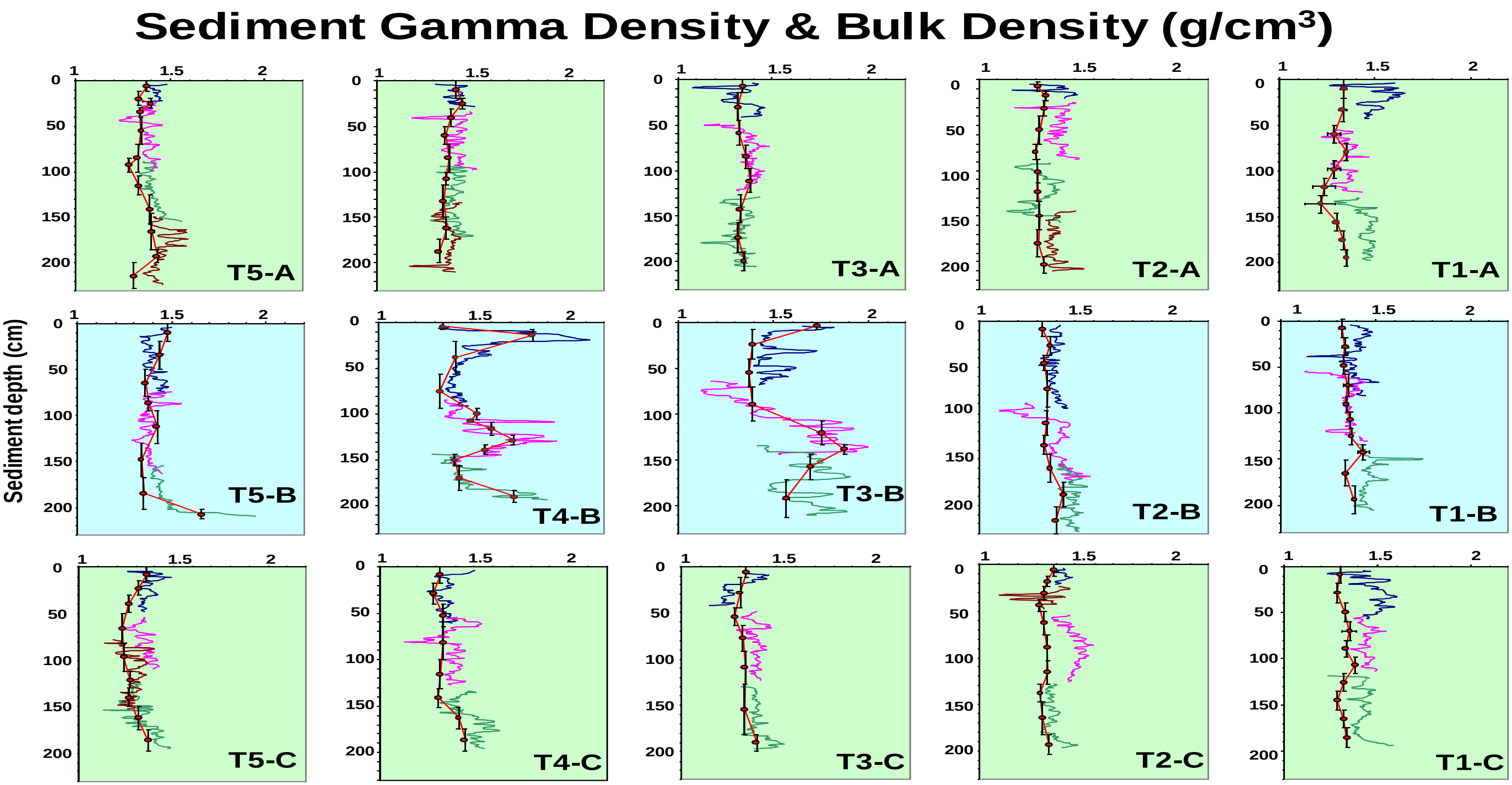

Figure 11. Depth profiles of sediment density

Alviso Slough sediment density as a function of sediment depth. Two approaches are depicted: a) Multi-Sensor core logger (MSCL) non-invasive scans conducted with gamma irradiation, where the various colors represent data from individual cores, and b) bulk density measured as the ratio of directly measured sediment weight to volume for discrete depth intervals, where the symbol identifies the mid-point of each depth interval sampled and the associated vertical bars indicate the total interval width. Panel layout parallels the approximate orientation of the individual sites as depicted in **Figure 2**, and individual background colors (blue or green) reflect marsh or slough channel sites, respectively.

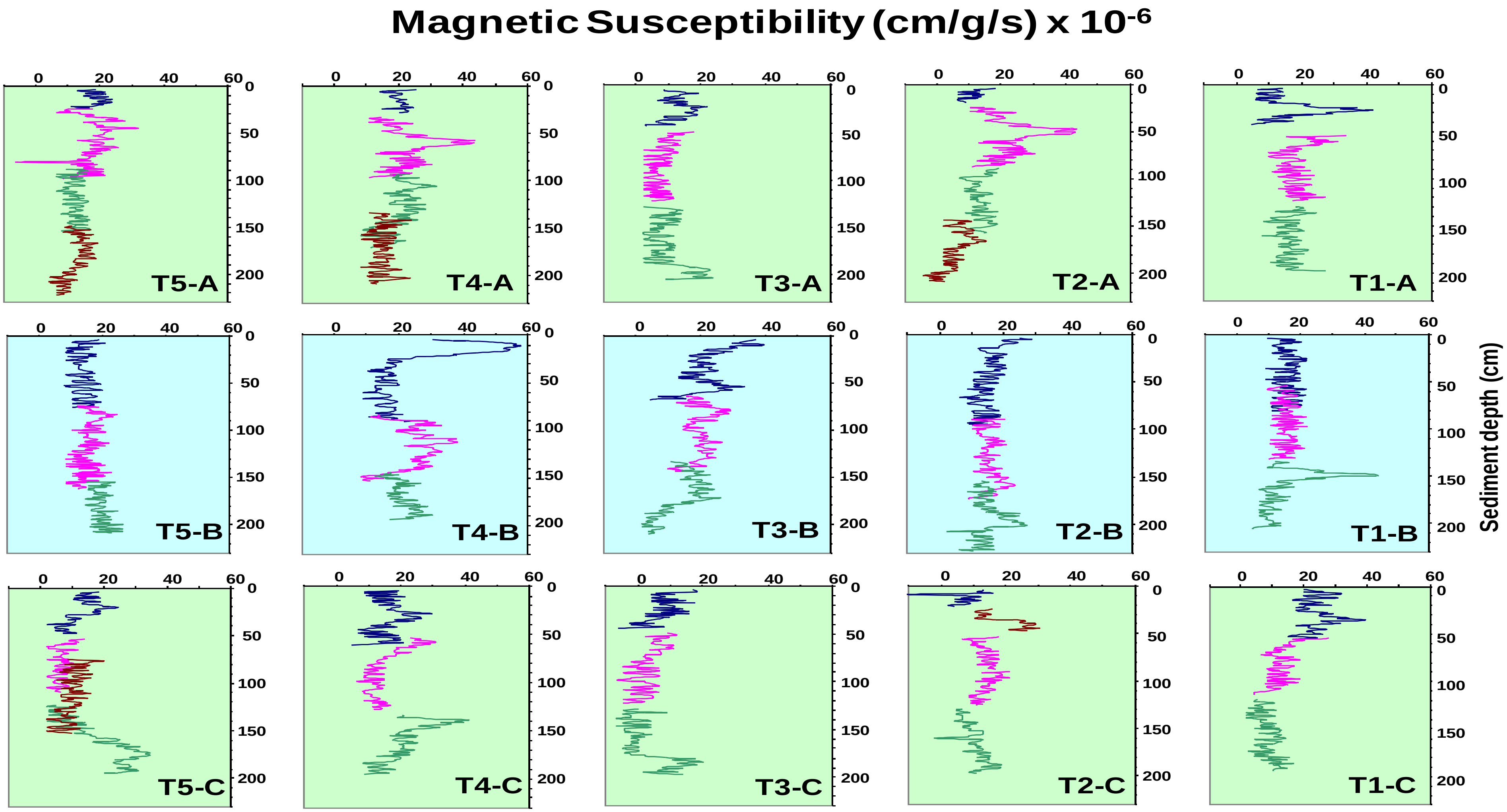

Figure 12. Depth profiles of sediment magnetic susceptibility

Alviso Slough sediment magnetic susceptibility scans as a function of sediment depth, as measured with the non-invasive Multi-Sensor core logger (MSCL), where the various colors represent data from individual cores. Panel layout parallels the approximate orientation of the individual sites as depicted in **Figure 2**, and individual background colors (blue or green) reflect marsh or slough channel sites, respectively.

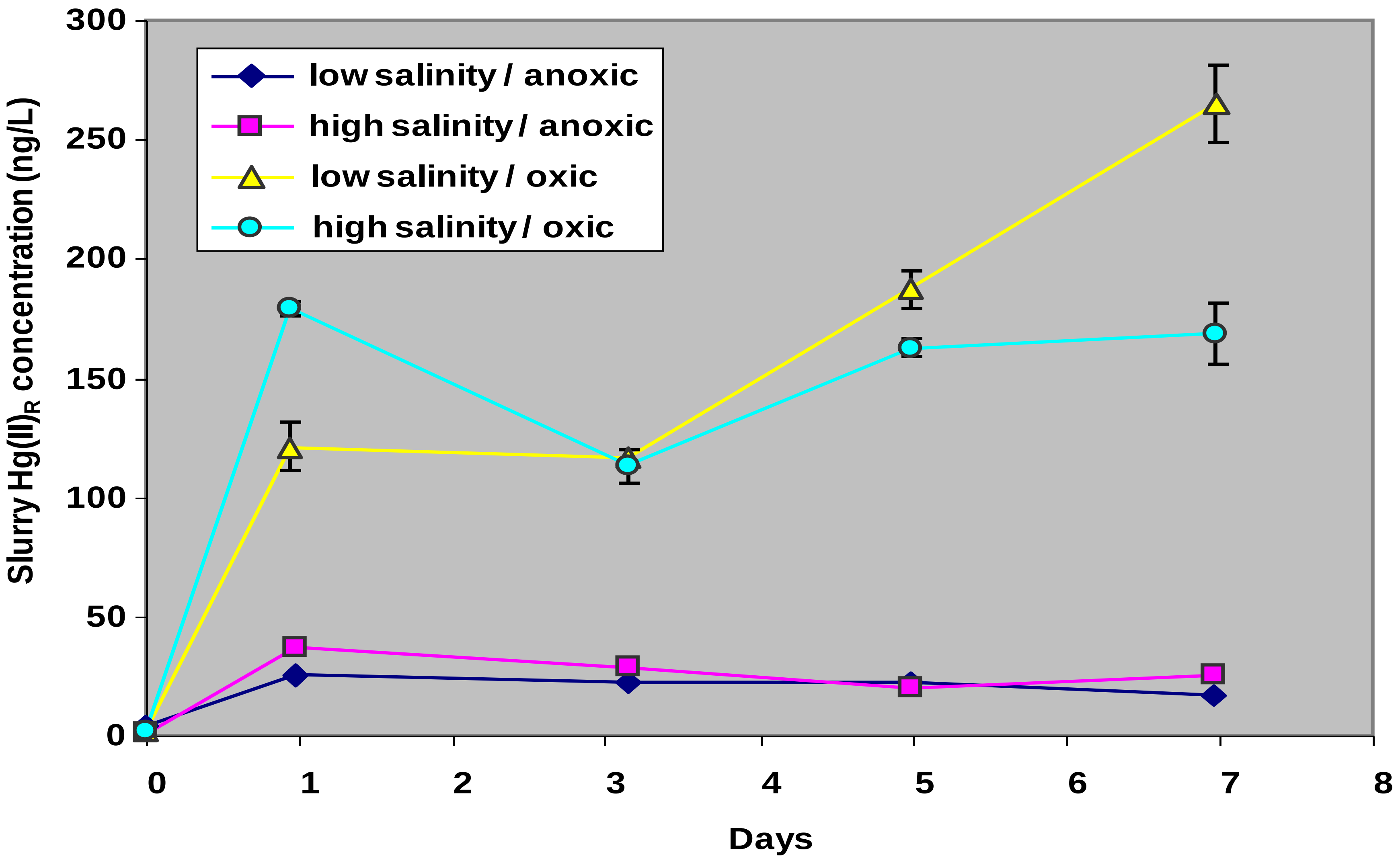

Figure 13. Time course plot of reactive mercury concentrations associated with the slough scour simulation experiment

Changes in reactive inorganic mercury ($Hg(II)_R$) concentrations in sediment / overlying slough water slurries repeatedly sampled over 7 days, under four treatment conditions (see inset legend). Error bars reflect the relative difference of n=2 sub-samples per treatment and time point. When not shown, error bars were smaller than the treatment symbol.

Tables

Table 1. Sediment sampling locations, Alviso Slough, September 2006

Site Name	Site Description[1]	Latitude[2]	Longitude[2]
AS-T1A	Right Marsh	37° 25’ 57.0”	121° 59’ 19.1”
AS-T1B	Slough Channel	37° 25’ 54.7”	121° 59’ 18.8”
AS-T1C	Left Marsh	37° 25’ 53.9”	121° 59’ 19.9”
AS-T2A	Right Marsh	37° 26’ 21.3”	121° 59’ 35.1”
AS-T2B	Slough Channel	37° 25’ 54.7”	121° 59’ 18.8”
AS-T2C	Left Marsh	37° 26’ 15.7”	121° 59’ 36.3”
AS-T3A	Right Marsh	37° 26’ 28.9”	122° 00’ 07.3”
AS-T3B	Slough Channel	37° 26’ 24.5”	122° 00’ 04.7”
AS-T3C	Left Marsh	37° 26’ 23.2”	122° 00’ 05.5”
AS-T4A	Right Marsh	34° 26’ 39.3”	122° 00’ 18.1”
AS-T4B	Slough Channel	37° 26’ 37.7”	122° 00’ 20.3”
AS-T4C	Left Marsh	37° 26’ 36.5”	122° 00’ 23.0”
AS-T5A	Right Marsh	37° 26’ 51.6”	122° 01’ 05.6”
AS-T5B	Slough Channel	37° 26’ 49.3”	122° 01’ 08.2”
AS-T5C	Left Marsh	37° 26’ 48.1”	122° 01’ 09.1”

[1] Site orientation looking downstream

[2] Datum, WGS 84

Table 2. Sediment Mercury Species Concentration

The deviation of n = 2 samples, when assayed, is given in parentheses ( ), and the type of replication is indicated by the cell color, where blue cells indicate analytical duplicates from the same sub-sample vial and green cell indicate sub-sample duplicates from the original core (separate vials) taken at the time of initial core processing. Profile averages (mean ± standard deviation) of mercury species concentrations are given in bold, with data weighted by depth interval width. Summary statistics for the complete data set are given at the bottom of the Table. [THg, total mercury; Hg(II)R, reactive mercury; MeHg, methylmercury; cm, centimeters; µg/g, micrograms per gram sediment (dry weight); ng/g, nanograms per gram sediment (dry weight); <, less than given detection limit; %, percentage of total mercury; NS, no sample collected].

Site ID and Core[1]	**Field: Depth interval[2] (cm)**	**Core: Depth Interval[3] (cm)**	**THg (µg/g)**		**$Hg(II)_R$ (ng/g)**		**MeHg (ng/g)**		**$Hg(II)_R$ (%)**	**MeHg (%)**
AS T1 A-D1	0-20	0-20	1.17		0.75		2.34		0.06	0.20
AS T1 A-D1	20-46	20-46	0.54		0.28		1.80		0.05	0.34
AS T1 A-D2	50-69	0-19	1.03	(0.02)	0.56		1.33		0.05	0.13
AS T1 A-D2	69-88	19-38	0.80		0.25		0.50		0.03	0.06
AS T1 A-D2	88-107	38-57	0.65		0.25		0.61		0.04	0.09
AS T1 A-D2	107-126	57-76	0.68		0.18		0.99		0.03	0.15
AS T1 A-D3	126-145	1-20	1.32		0.22		< 0.35		0.02	< 0.03
AS T1 A-D3	145-165	20-40	0.99		0.18		0.68		0.02	0.07
AS T1 A-D3	165-185	40-60	1.39		0.16		0.57		0.01	0.04
AS T1 A-D3	185-203	60-77.5	1.34		0.22		0.94		0.02	0.07
AS T1 A	**MEAN ±**	**(std. dev.)**	**0.98**	**(0.31)**	**0.31**	**(0.19)**	**1.04**	**(0.66)**	**0.03**	**0.11**
AS T1 B-D1	0-20	0-20	0.56		0.29		1.24		0.05	0.22
AS T1 B-D1	20-40	20-40	0.47		0.46		1.39		0.10	0.30
AS T1 B-D1	40-60	40-60	0.54		0.52		0.89		0.10	0.17
AS T1 B-D1	60-83	60-83	0.61	(0.06)	0.47	(0.10)	0.90	(0.05)	0.08	0.15
AS T1 B-D2	83-100	33-50	0.51	(0.04)	0.62		0.68		0.12	0.14
AS T1 B-D2	100-117	50-67	0.66		0.33		0.89		0.05	0.13
AS T1 B-D2	117-135	67-84.5	0.80		0.58		0.83		0.07	0.10
AS T1 B-D3	135-152	5-22	0.96		0.43		2.21		0.04	0.23

Site ID and Core[1]	Field: Depth interval[2] (cm)	Core: Depth Interval[3] (cm)	THg (µg/g)		$Hg(II)_R$ (ng/g)		MeHg (ng/g)		$Hg(II)_R$ (%)	MeHg (%)
AS T1 B-D3	152-180	22-50	0.84	(0.06)	0.11		1.10		0.01	0.13
AS T1 B-D3	180-209	50-78.5	1.13		0.17		0.62		0.02	0.06
AS T1 B	**MEAN ±**	**(std. dev.)**	**0.73**	**(0.22)**	**0.37**	**(0.16)**	**1.05**	**(0.45)**	**0.05**	**0.14**
AS T1 C-D1	0-18	0-18	1.37	(0.11)	11.73		0.97		0.86	0.07
AS T1 C-D1	18-40	18-40	0.64		0.26		6.10		0.04	0.95
AS T1 C-D1	40-60	40-60	1.36		0.35		1.33		0.03	0.10
AS T1 C-D2	60-80	10-30	0.79	(0.10)	0.17	(0.01)	1.22	(0.16)	0.02	0.15
AS T1 C-D2	80-98	30-48	0.91	(0.21)	0.23		0.85		0.02	0.09
AS T1 C-D2	98-116	48-66	1.22	(0.02)	0.21		0.50		0.02	0.04
AS T1 C-D3	116-135	1-20	1.12	(0.01)	0.17		0.55		0.02	0.05
AS T1 C-D3	135-155	20-40	0.60		0.16		0.56		0.03	0.09
AS T1 C-D3	155-175	40-60	0.75		0.15		0.59		0.02	0.08
AS T1 C-D3	175-196	60-81	1.04		0.30		2.34	(0.04)	0.03	0.22
AS T1 C	**MEAN ±**	**(std. dev.)**	**0.97**	**(0.28)**	**1.28**	**(3.39)**	**1.58**	**(1.80)**	**0.13**	**0.16**
AS T2 A-D1	2-12	2-12	0.52		NS		NS			
AS T2 A-D1	12-23	12-23	0.67		NS		NS			
AS T2 A-D2	23-40	3-20	0.84		NS		NS			
AS T2 A-D2	40-70	20-50	0.73	(0.01)	NS		NS			
AS T2 A-D2	70-88	50-68	0.60		NS		NS			
AS T2 A-D3	88-113	3-28	1.08		NS		NS			
AS T2 A-D3	113-134	28-49	0.90		NS		NS			
AS T2 A-D3	134-165	49-80	1.00	(0.12)	NS		NS			
AS T2 A-D4	165-194	25-54	1.02		NS		NS			
AS T2 A-D4	194-212	54-72	2.83		NS		NS			
AS T2 A	**MEAN ±**	**(std. dev.)**	**1.03**	**(0.67)**						
AS T2 B-D1	0-16	0-16	0.67		NS		NS			
AS T2 B-D1	16-37	16-37	0.91		NS		NS			

Site ID and Core[1]	Field: Depth interval[2] (cm)	Core: Depth Interval[3] (cm)	THg (µg/g)		$Hg(II)_R$ (ng/g)		MeHg (ng/g)		$Hg(II)_R$ (%)	MeHg (%)
AS T2 B-D1	37-54	37-54	1.17		NS		NS			
AS T2 B-D1	54-93	54-73	0.91	(0.15)	NS		NS			
AS T2 B-D2	97-124	12-39	0.87		NS		NS			
AS T2 B-D2	124-144	39-59	0.53		NS		NS			
AS T2 B-D2	144-175	59-90	0.99		NS		NS			
AS T2 B-D3	175-201	25-51	1.81	(0.01)	NS		NS			
AS T2 B-D3	201-231	51-81	2.47		NS		NS			
AS T2 B	**MEAN ±**	**(std. dev.)**	**1.19**	**(0.64)**						
AS T2 C-D1	0-12	0-12	0.60		NS		NS			
AS T2 C-D1	12-24	12-24	0.65		NS		NS			
AS T2 C-D1"	24-37	4-17	0.62		NS		NS			
AS T2 C-D1"	37-50	17-30	0.51		NS		NS			
AS T2 C-D2	50-75	0-25	0.75		NS		NS			
AS T2 C-D2	75-103	25-53	0.73	(0.05)	NS		NS			
AS T2 C-D2	103-129	53-79	0.77		NS		NS			
AS T2 C-D3	129-147	4-22	0.61		NS		NS			
AS T2 C-D3	147-183	22-58	0.79		NS		NS			
AS T2 C-D3	183-204	58-79	1.42	(0.19)	NS		NS			
AS T2 C	**MEAN ±**	**(std. dev.)**	**0.78**	**(0.26)**						
AS T3 A-D1	0-15	0-15	0.57		6.90		2.14		1.22	0.38
AS T3 A-D1	15-46	15-46	0.68		0.36		3.04		0.05	0.45
AS T3 A-D2	46-72	1-27	0.72	(0.03)	0.34		0.72		0.05	0.10
AS T3 A-D2	72-98	27-53	0.83		0.35		< 0.33		0.04	< 0.04
AS T3 A-D2	98-124	53-79	0.99		0.27		0.43		0.03	0.04
AS T3 A-D3	127-157	2-32	0.78		0.35		0.52		0.05	0.07
AS T3 A-D3	157-189	32-64	1.85		0.52		1.17		0.03	0.06
AS T3 A-D3	189-209	64-83	1.34		0.57		1.87		0.04	0.14
AS T3 A	**MEAN ±**	**(std. dev.)**	**0.99**	**(0.44)**	**0.87**	**(1.65)**	**1.24**	**(0.95)**	**0.09**	**0.12**

Site ID and Core[1]	Field: Depth interval[2] (cm)	Core: Depth Interval[3] (cm)	THg (µg/g)		$Hg(II)_R$ (ng/g)		MeHg (ng/g)		$Hg(II)_R$ (%)	MeHg (%)
AS T3 B-D1	0-8	0-8	0.31		0.09		0.47		0.03	0.15
AS T3 B-D1	8-40	8-40	1.16	(0.15)	0.24	(0.01)	1.66	(0.11)	0.02	0.14
AS T3 B-D1	40-70	40-70	1.75	(0.08)	0.30		0.85		0.02	0.05
AS T3 B-D2	70-108	10-48	0.75		0.21		0.64	(0.08)	0.03	0.08
AS T3 B-D2	108-133	48-73	1.07		0.24		0.42		0.02	0.04
AS T3 B-D2	133-143	73-83	0.54		0.27		0.27		0.05	0.05
AS T3 B-D3	143-172	13-42	0.89		0.30		< 0.21		0.03	< 0.02
AS T3 B-D3	172-212	42-82	0.85	(0.47)	0.52	(0.04)	< 0.28	(0.00)	0.06	< 0.03
AS T3 B	**MEAN ±**	**(std. dev.)**	**1.00**	**(0.47)**	**0.29**	**(0.12)**	**0.65**	**(0.52)**	**0.03**	**0.06**
AS T3 C-D1	0-12	0-12	0.55		8.17		1.07	(0.02)	1.50	0.20
AS T3 C-D1	12-45	12-45	0.67		0.32		1.55		0.05	0.23
AS T3 C-D2	45-64	0-19	0.62		0.18		0.87		0.03	0.14
AS T3 C-D2	64-91	19-46	0.86		0.18		0.45		0.02	0.05
AS T3 C-D2	91-127	46-82	0.97	(0.01)	0.14		0.43		0.01	0.04
AS T3 C-D3	127-181	2-56	1.31		0.33		0.53		0.02	0.04
AS T3 C-D3	181-199	56-74	0.94		0.02		< 0.30		0.00	< 0.03
AS T3 C	**MEAN ±**	**(std. dev.)**	**0.94**	**(0.29)**	**0.70**	**(1.59)**	**0.71**	**(0.43)**	**0.08**	**0.08**
AS T4 A-D1	0-19.5	0-19.5	0.54		NS		NS			
AS T4 A-D1	19.5-31	19.5-31	0.72		NS		NS			
AS T4 A-D2	31-50	1-20	0.62		NS		NS			
AS T4 A-D2	50-70	20-40	0.57		NS		NS			
AS T4 A-D2	70-100	40-70	0.83		NS		NS			
AS T4 A-D3	100-115	10-25	1.49		NS		NS			
AS T4 A-D3	115-150	25-60	0.59		NS		NS			
AS T4 A-D3	150-174	60-84	1.75		NS		NS			
AS T4 A-D4	174-200	44-70	1.45		NS		NS			
AS T4 A	**MEAN ±**	**(std. dev.)**	**0.95**	**(0.47)**						

Site ID and Core[1]	Field: Depth interval[2] (cm)	Core: Depth Interval[3] (cm)	THg (µg/g)		$Hg(II)_R$ (ng/g)	MeHg (ng/g)		$Hg(II)_R$ (%)	MeHg (%)
AS T4 B-D1	0-7.5	0-7.5	0.49		NS	NS			
AS T4 B-D1	7.5-20	7.5-20	0.20		NS	NS			
AS T4 B-D1	20-56	20-56	0.84	(0.00)	NS	NS			
AS T4 B-D1	56-93	56-93	1.52		NS	NS			
AS T4 B-D2	93-106	13-26	1.81		NS	NS			
AS T4 B-D2	106-109	26-29	1.51		NS	NS			
AS T4 B-D2	109-123	29-42.5	2.37		NS	NS			
AS T4 B-D2	123-133	42.5-52.5	1.12		NS	NS			
AS T4 B-D2	133-144	52.5-63.5	1.40		NS	NS			
AS T4 B-D2	144-156	63.5-76	0.08		NS	NS			
AS T4 B-D3	156-183	16-43	0.69		NS	NS			
AS T4 B-D3	183-196	43-56	0.91		NS	NS			
AS T4 B	**MEAN ±**	**(std. dev.)**	**1.08**	**(0.68)**					
AS T4 C-D1	0-17	0-17	0.48		NS	NS			
AS T4 C-D1	17-40	17-40	0.65	(0.02)	NS	NS			
AS T4 C-D1	40-64	40-64	1.26		NS	NS			
AS T4 C-D2	64-100	14-50	0.80		NS	NS			
AS T4 C-D2	100-131	50-81	1.97		NS	NS			
AS T4 C-D3	131-151	1-21	0.91		NS	NS			
AS T4 C-D3	151-174	21-44	1.01		NS	NS			
AS T4 C-D3	174-199	44-68.5	0.83		NS	NS			
AS T4 C	**MEAN ±**	**(std. dev.)**	**1.03**	**(0.48)**					
AS T5 A-D1	0-12.5	0-12.5	0.54		4.17	0.79		0.78	0.15
AS T5 A-D1	12.5-27.3	12.5-27.3	0.73		0.41	1.14		0.06	0.16
AS T5 A-D2	20-30	0-10	0.50		10.02	< 0.30		2.01	< 0.06
AS T5 A-D2	30-40	10-20	0.49	(0.01)	0.25	1.38		0.05	0.28
AS T5 A-D2	40-70	20-50	0.59		0.33	< 0.33		0.06	< 0.06
AS T5 A-D2	70-101	50-81	0.67	(0.00)	0.24	0.46	(0.01)	0.04	0.07

Site ID and Core[1]	Field: Depth interval[2] (cm)	Core: Depth Interval[3] (cm)	THg (µg/g)		Hg(II)_R (ng/g)		MeHg (ng/g)		Hg(II)_R (%)	MeHg (%)
AS T5 A-D3	85-101	0-20	0.94		0.21		0.66	(0.04)	0.02	0.07
AS T5 A-D3	105-125	20-40	0.53		0.22		< 0.32		0.04	< 0.06
AS T5 A-D3	125-157	40-71	0.52		0.20		0.59		0.04	0.11
AS T5 A-D4	145-185	0-40	0.51	(0.02)	0.16	(0.01)	0.63	(0.02)	0.03	0.12
AS T5 A-D4	185-200	40-55	1.43	(0.00)	0.21		0.76		0.01	0.05
AS T5 A-D4	200-228	55-82	1.41		0.17		< 0.32		0.01	< 0.02
AS T5 A	**MEAN ±**	**(std. dev.)**	**0.73**	**(0.34)**	**0.80**	**(1.70)**	**0.58**	**(0.31)**	**0.11**	**0.08**
AS T5 B-D1	0-20	0-20	0.36		0.18		0.97	(0.02)	0.05	0.27
AS T5 B-D1	20-50	20-50	0.59		0.12		0.51		0.02	0.09
AS T5 B-D1	50-79	50-79	1.01		0.32		< 0.31		0.03	< 0.03
AS T5 B-D2	79-94	9-24	1.16		0.23		0.87		0.02	0.08
AS T5 B-D2	94-130	24-60	0.82	(0.04)	0.21		0.70		0.03	0.09
AS T5 B-D2	130-166	60-96	0.88		0.34		0.72		0.04	0.08
AS T5 B-D3	167-202	17-52	0.90	(0.00)	0.34	(0.10)	0.83	(0.02)	0.04	0.09
AS T5 B-D3	202-212	52-62	0.54		0.21		0.38		0.04	0.07
AS T5 B	**MEAN ±**	**(std. dev.)**	**0.80**	**(0.27)**	**0.25**	**(0.08)**	**0.67**	**(0.24)**	**0.03**	**0.08**
AS T5 C-D1	0-15	0-15	0.41		0.45		5.82		0.11	1.41
AS T5 C-D1	15-30	15-30	0.50		0.13		1.18	(0.05)	0.03	0.24
AS T5 C-D1	30-49	30-49	0.64		0.06		< 0.37		0.01	< 0.06
AS T5 C-D2	50-81	0-31	0.68		0.37		0.67		0.05	0.10
AS T5 C-D2	81-112	31-62	0.78		0.12		< 0.35		0.02	< 0.05
AS T5 C-D2"	112-130	40-58	0.68		0.11		< 0.35		0.02	< 0.05
AS T5 C-D3	130-150	10-30	1.75		0.44		0.56		0.03	0.03
AS T5 C-D3	150-175	30-55	0.66		0.16		0.53		0.03	0.08
AS T5 C-D3	175-198	55-78	0.99		0.49		0.78		0.05	0.08
AS T5 C	**MEAN ±**	**(std. dev.)**	**0.80**	**(0.40)**	**0.26**	**(0.17)**	**0.98**	**(1.46)**	**0.03**	**0.12**
ALL DATA		**MEAN**	**0.93**		**0.35**		**0.56**		**0.04**	**0.06**

Site ID and Core[1]	Field: Depth interval[2] (cm)	Core: Depth Interval[3] (cm)	THg (µg/g)	$Hg(II)_R$ (ng/g)	MeHg (ng/g)	$Hg(II)_R$ (%)	MeHg (%)
ALL DATA		**STD. DEV.**	**0.45**	**0.91**	**0.56**	**0.32**	**0.19**
ALL DATA		**STD. ERR.**	**0.04**	**0.10**	**0.06**	**0.04**	**0.02**
ALL DATA		**MEDIAN**	**0.80**	**0.25**	**0.69**	**0.03**	**0.08**
ALL DATA		**MINIMUM**	**0.08**	**0.02**	**< 0.21**	**0.00**	**< 0.02**
ALL DATA		**MAXIMUM**	**2.83**	**11.73**	**6.10**	**2.01**	**1.41**
ALL DATA		**TOTAL N**	**140**	**82**	**82**	**82**	**82**

[1] Core coding: AS T# [A, B or C]-D#; where AS = Alviso Slough; T# = Transect number (1 thru 5); [A, B or C] = Site description as per Table 1 (left marsh, right marsh or slough channel, respectively); D# = depth specific core segment

[2] Field depth interval measured from the sediment / water interface

[3] Core depth interval measured from the top of the individual core liner

Table 3. Ancillary Sediment Parameters

Profile averages (mean ± standard deviation) for each parameter are given in bold, with data weighted by depth interval width. Summary statistics for the complete data set are given at the bottom of the Table. [pH in standard units; E_h, oxidation-reduction potential corrected for the standard hydrogen reference half-reaction; LOI, loss on ignition, a measure of sediment organic content; cm, centimeters; mV, millivolts; %, percentage; g/cm^3, grams of wet sediment per cubic centimeter; ml/cm^3, milliliters of pore water per cubic centimeter of wet sediment; % <63 µm; percentage of sediment (by weight) less than 63 micrometers, representing the sand/silt size fraction cut-off].

Site ID and Core Section[1]	Field: Depth interval[2] (cm)	Core: Depth Interval[3] (cm)	pH	Eh (mV)	Dry weight (%)	LOI (%)	Bulk Density (g/cm^3)	Porosity (ml/cm^3)	Grain size (% < 63 µm)
AS T1 A-D1	0-20	0-20	7.25	65	49.2	7.78	1.33	0.68	94.7
AS T1 A-D1	20-46	20-46	7.21	-40	46.9	7.17	1.33	0.71	99.8
AS T1 A-D2	50-69	0-19	7.33	-2	44.5	6.42	1.28	0.71	94.8
AS T1 A-D2	69-88	19-38	7.41	-46	43.9	5.71	1.35	0.76	98.2
AS T1 A-D2	88-107	38-57	7.48	-55	43.6	5.72	1.28	0.72	99.5
AS T1 A-D2	107-126	57-76	7.53	-108	43.7	6.25	1.23	0.69	99.5
AS T1 A-D3	126-145	1-20	7.59	-68	45.7	6.72	1.21	0.66	98.7
AS T1 A-D3	145-165	20-40	7.64	-91	48.2	5.34	1.30	0.67	100.2
AS T1 A-D3	165-185	40-60	7.62	-48	47.0	6.27	1.33	0.71	99.3
AS T1 A-D3	185-203	60-77.5	7.61	-101	49.9	5.46	1.35	0.67	98.8
AS T1 A		**MEAN**	**7.46**	**-48**	**46.3**	**6.32**	**1.30**	**0.70**	**98.4**
		Std. Dev.	**0.16**	**50**	**2.4**	**0.78**	**0.05**	**0.03**	**2.0**
AS T1 B-D1	0-20	0-20	7.09	-20	44.1	6.04	1.28	0.71	98.4
AS T1 B-D1	20-40	20-40	7.32	-28	43.3	6.15	1.29	0.73	102.6
AS T1 B-D1	40-60	40-60	7.3	-26	42.4	6.04	1.28	0.74	98.8
AS T1 B-D1	60-83	60-83	7.36	-29	44.6	4.65	1.30	0.72	98.2
AS T1 B-D2	83-100	33-50	7.29	-11	42.5	6.04	1.30	0.74	100.2
AS T1 B-D2	100-117	50-67	7.39	-32	43.7	5.90	1.32	0.74	102.3
AS T1 B-D2	117-135	67-84.5	7.34	-34	44.0	5.18	1.32	0.74	97.8
AS T1 B-D3	135-152	5-22	7.34	-25	50.7	5.26	1.39	0.69	79.6
AS T1 B-D3	152-180	22-50	7.55	-71	46.2	5.15	1.29	0.70	96.5
AS T1 B-D3	180-209	50-78.5	7.58	-58	46.1	5.61	1.34	0.72	99.7

Site ID and Core Section[1]	Field: Depth interval[2] (cm)	Core: Depth Interval[3] (cm)	pH	Eh (mV)	Dry weight (%)	LOI (%)	Bulk Density (g/cm^3)	Porosity (ml/cm^3)	Grain size (% < 63 µm)
AS T1 B		**MEAN**	**7.37**	**-36**	**44.8**	**5.57**	**1.31**	**0.72**	**97.6**
		Std. Dev.	**0.14**	**19**	**2.5**	**0.51**	**0.03**	**0.02**	**6.6**
AS T1 C-D1	0-18	0-18	7.19	259	48.9	7.95	1.30	0.67	91.1
AS T1 C-D1	18-40	18-40	7.17	-28	45.0	4.97	1.29	0.71	94.6
AS T1 C-D1	40-60	40-60	7.56	-53	43.5	4.57	1.33	0.75	103.0
AS T1 C-D2	60-80	10-30	7.61	-55	46.0	5.26	1.35	0.73	99.3
AS T1 C-D2	80-98	30-48	7.6	-30	44.2	5.13	1.33	0.74	101.9
AS T1 C-D2	98-116	48-66	7.6	-57	46.0	4.45	1.38	0.75	100.6
AS T1 C-D3	116-135	1-20	7.57	-5	46.1	4.82	1.32	0.71	99.2
AS T1 C-D3	135-155	20-40	7.76	-86	44.1	3.78	1.29	0.72	99.9
AS T1 C-D3	155-175	40-60	7.61	-97	45.3	4.05	1.32	0.72	99.6
AS T1 C-D3	175-196	60-81	7.49	-55	46.3	4.34	1.34	0.72	99.7
AS T1 C		**MEAN**	**7.51**	**-24**	**45.5**	**4.90**	**1.33**	**0.72**	**98.9**
		Std. Dev.	**0.19**	**115**	**1.5**	**1.15**	**0.03**	**0.02**	**3.5**
AS T2 A-D1	2-12	2-12	7.06	104	44.4	8.80	1.29	0.72	95.0
AS T2 A-D1	12-23	12-23	7.1	-25	45.5	6.97	1.28	0.70	95.8
AS T2 A-D2	23-40	3-20	7.36	-60	44.5	6.50	1.31	0.72	99.2
AS T2 A-D2	40-70	20-50	7.42	-79	43.2	6.49	1.30	0.74	97.9
AS T2 A-D2	70-88	50-68	7.53	-91	41.3	5.98	1.28	0.75	98.3
AS T2 A-D3	88-113	3-28	7.65	-19	43.7	5.88	1.34	0.75	96.8
AS T2 A-D3	113-134	28-49	7.55	-53	43.7	5.66	1.31	0.74	98.4
AS T2 A-D3	134-165	49-80	7.53	-112	45.1	6.38	1.29	0.71	96.0
AS T2 A-D4	165-194	25-54	7.57	-52	43.5	5.27	1.30	0.73	98.2
AS T2 A-D4	194-212	54-72	7.43	-73	44.0	6.48	1.34	0.75	98.9
AS T2 A		**MEAN**	**7.47**	**-58**	**43.8**	**6.24**	**1.30**	**0.73**	**97.6**
		Std. Dev.	**0.20**	**75**	**1.2**	**0.93**	**0.02**	**0.02**	**1.5**
AS T2 B-D1	0-16	0-16	7.58	3	45.7	5.35	1.33	0.72	93.1
AS T2 B-D1	16-37	16-37	7.46	-25	46.0	5.66	1.37	0.74	90.7

Site ID and Core Section[1]	Field: Depth interval[2] (cm)	Core: Depth Interval[3] (cm)	pH	Eh (mV)	Dry weight (%)	LOI (%)	Bulk Density (g/cm^3)	Porosity (ml/cm^3)	Grain size (% < 63 μm)
AS T2 B-D1	37-54	37-54	7.62	-91	46.0	5.46	1.34	0.72	93.7
AS T2 B-D1	54-93	54-73	7.68	-100	45.1	5.32	1.36	0.74	98.2
AS T2 B-D2	97-124	12-39	7.53	-63	45.5	5.27	1.35	0.73	98.3
AS T2 B-D2	124-144	39-59	7.58	-79	44.2	4.76	1.34	0.75	98.6
AS T2 B-D2	144-175	59-90	7.38	-74	46.1	4.79	1.37	0.74	99.7
AS T2 B-D3	175-201	25-51	7.42	-50	49.3	4.83	1.43	0.73	97.4
AS T2 B-D3	201-231	51-81	7.47	-104	49.6	5.44	1.40	0.71	97.0
AS T2 B		**MEAN**	**7.52**	**-70**	**46.5**	**5.20**	**1.37**	**0.73**	**96.8**
		Std. Dev.	**0.10**	**39**	**1.8**	**0.33**	**0.03**	**0.01**	**3.1**
AS T2 C-D1	0-12	0-12	6.69	213	48.9	7.26	1.39	0.71	95.8
AS T2 C-D1	12-24	12-24	7.15	72	45.4	7.03	1.35	0.74	91.2
AS T2 C-D1"	24-37	4-17	7.09	242	46.3	7.32	1.33	0.72	96.0
AS T2 C-D1"	37-50	17-30	7.29	32	43.1	7.27	1.31	0.75	95.8
AS T2 C-D2	50-75	0-25	7.4	28	43.3	5.98	1.33	0.76	96.8
AS T2 C-D2	75-103	25-53	7.51	-50	45.5	4.31	1.35	0.74	98.0
AS T2 C-D2	103-129	53-79	7.56	-54	44.4	4.44	1.36	0.75	103.8
AS T2 C-D3	129-147	4-22	7.59	-49	43.0	5.37	1.32	0.75	100.8
AS T2 C-D3	147-183	22-58	7.62	-83	43.7	5.93	1.33	0.75	98.8
AS T2 C-D3	183-204	58-79	7.48	-91	46.0	4.81	1.36	0.74	102.0
AS T2 C		**MEAN**	**7.42**	**-4**	**44.7**	**5.68**	**1.34**	**0.74**	**98.6**
		Std. Dev.	**0.29**	**21**	**1.8**	**1.15**	**0.02**	**0.02**	**3.7**
AS T3 A-D1	0-15	0-15	7.27	252	45.4	8.21	1.34	0.73	96.2
AS T3 A-D1	15-46	15-46	7.47	-49	42.9	6.69	1.32	0.75	100.6
AS T3 A-D2	46-72	1-27	7.43	-9	42.5	5.59	1.32	0.76	101.6
AS T3 A-D2	72-98	27-53	7.56	-43	45.4	5.37	1.36	0.74	98.1
AS T3 A-D2	98-124	53-79	7.64	-39	46.9	5.51	1.38	0.73	100.0
AS T3 A-D3	127-157	2-32	7.53	5	43.8	6.06	1.33	0.75	98.5
AS T3 A-D3	157-189	32-64	7.56	-6	44.6	6.38	1.32	0.73	97.5
AS T3 A-D3	189-209	64-83	7.6	-61	46.5	6.72	1.35	0.72	91.2

Site ID and Core Section[1]	Field: Depth interval[2] (cm)	Core: Depth Interval[3] (cm)	pH	Eh (mV)	Dry weight (%)	LOI (%)	Bulk Density (g/cm^3)	Porosity (ml/cm^3)	Grain size (% < 63 μm)
AS T3 A		**MEAN**	**7.52**	**-7**	**44.6**	**6.21**	**1.34**	**0.74**	**98.3**
		Std. Dev.	**0.12**	**110**	**1.6**	**0.91**	**0.02**	**0.01**	**3.3**
AS T3 B-D1	0-8	0-8	7.5	5	69.4	3.15	1.73	0.53	37.0
AS T3 B-D1	8-40	8-40	7.65	-98	49.8	4.81	1.39	0.70	91.5
AS T3 B-D1	40-70	40-70	7.65	-161	47.4	5.33	1.38	0.72	93.0
AS T3 B-D2	70-108	10-48	7.56	-102	48.4	5.79	1.39	0.72	88.5
AS T3 B-D2	108-133	48-73	7.62	-107	70.1	2.91	1.76	0.53	34.1
AS T3 B-D2	133-143	73-83	7.75	-81	78.3	2.63	1.88	0.41	19.4
AS T3 B-D3	143-172	13-42	7.55	-89	69.5	3.37	1.70	0.52	34.2
AS T3 B-D3	172-212	42-82	7.53	-2	61.3	3.61	1.57	0.61	67.8
AS T3 B		**MEAN**	**7.59**	**-85**	**58.5**	**4.25**	**1.54**	**0.62**	**66.7**
		Std. Dev.	**0.08**	**59**	**11.3**	**1.28**	**0.19**	**0.12**	**34.7**
AS T3 C-D1	0-12	0-12	6.91	223	46.8	8.94	1.34	0.71	96.0
AS T3 C-D1	12-45	12-45	7.16	-134	42.9	7.33	1.31	0.75	96.7
AS T3 C-D2	45-64	0-19	7.14	-5	40.3	6.95	1.28	0.76	97.4
AS T3 C-D2	64-91	19-46	7.23	-30	41.7	7.09	1.32	0.77	96.8
AS T3 C-D2	91-127	46-82	7.39	-82	43.4	6.18	1.33	0.75	99.5
AS T3 C-D3	127-181	2-56	7.47	-40	42.9	5.80	1.33	0.76	99.5
AS T3 C-D3	181-199	56-74	7.67	-143	49.0	6.73	1.39	0.71	97.4
AS T3 C		**MEAN**	**7.32**	**-52**	**43.4**	**6.68**	**1.33**	**0.75**	**98.1**
		Std. Dev.	**0.25**	**213**	**3.0**	**0.96**	**0.03**	**0.02**	**1.4**
AS T4 A-D1	0-19.5	0-19.5	7.38	212	54.6	8.20	1.42	0.64	94.9
AS T4 A-D1	19.5-31	19.5-31	7.43	68	54.1	6.43	1.45	0.67	94.8
AS T4 A-D2	31-50	1-20	7.35	25	50.7	6.74	1.39	0.69	97.2
AS T4 A-D2	50-70	20-40	7.43	-112	48.8	7.02	1.36	0.70	96.1
AS T4 A-D2	70-100	40-70	7.53	-138	48.6	5.27	1.38	0.71	97.0
AS T4 A-D3	100-115	10-25	7.46	-130	47.6	5.48	1.37	0.72	98.4
AS T4 A-D3	115-150	25-60	7.46	-76	46.2	4.89	1.35	0.73	98.4

Site ID and Core Section[1]	Field: Depth interval[2] (cm)	Core: Depth Interval[3] (cm)	pH	Eh (mV)	Dry weight (%)	LOI (%)	Bulk Density (g/cm^3)	Porosity (ml/cm^3)	Grain size (% < 63 µm)
AS T4 A-D3	150-174	60-84	7.43	-100	47.0	5.45	1.37	0.73	97.3
AS T4 A-D4	174-200	44-70	7.39	-65	45.8	5.86	1.33	0.72	97.5
AS T4 A		**MEAN**	**7.43**	**-48**	**48.7**	**5.98**	**1.37**	**0.70**	**97.0**
		Std. Dev.	**0.05**	**160**	**3.2**	**1.02**	**0.04**	**0.03**	**1.3**
AS T4 B-D1	0-7.5	0-7.5	7.29	-130	44.5	5.61	1.34	0.75	80.6
AS T4 B-D1	7.5-20	7.5-20	7.78	100	80.3	1.38	1.82	0.36	7.6
AS T4 B-D1	20-56	20-56	7.63	-113	51.5	4.24	1.41	0.68	81.7
AS T4 B-D1	56-93	56-93	7.48	-162	46.2	5.12	1.33	0.72	96.9
AS T4 B-D2	93-106	13-26	7.44	-8	59.0	4.91	1.52	0.63	96.9
AS T4 B-D2	106-109	26-29	7.55	-58	79.2	2.75	1.49	0.31	24.6
AS T4 B-D2	109-123	29-42.5	7.36	-88	68.3	4.58	1.60	0.51	83.1
AS T4 B-D2	123-133	42.5-52.5	7.48	-81	71.6	2.74	1.72	0.49	32.0
AS T4 B-D2	133-144	52.5-63.5	7.41	-69	59.9	5.54	1.57	0.63	98.1
AS T4 B-D2	144-156	63.5-76	7.5	-82	50.9	5.26	1.41	0.69	85.7
AS T4 B-D3	156-183	16-43	7.64	-107	49.9	4.17	1.43	0.71	92.2
AS T4 B-D3	183-196	43-56	7.83	-38	74.6	3.52	1.72	0.44	26.9
AS T4 B		**MEAN**	**7.55**	**-88**	**57.0**	**4.32**	**1.49**	**0.62**	**76.5**
		Std. Dev.	**0.16**	**85**	**12.1**	**1.37**	**0.15**	**0.16**	**38.4**
AS T4 C-D1	0-17	0-17	6.72	178	45.7	9.54	1.32	0.72	88.0
AS T4 C-D1	17-40	17-40	7.25	-34	45.6	6.73	1.29	0.70	97.3
AS T4 C-D1	40-64	40-64	7.48	-49	46.3	5.43	1.34	0.72	98.6
AS T4 C-D2	64-100	14-50	7.54	24	45.1	5.27	1.34	0.73	97.2
AS T4 C-D2	100-131	50-81	7.52	-109	45.2	5.92	1.32	0.73	98.6
AS T4 C-D3	131-151	1-21	7.59	-45	46.9	5.53	1.31	0.70	96.9
AS T4 C-D3	151-174	21-44	7.33	-79	53.3	6.05	1.42	0.66	96.3
AS T4 C-D3	174-199	44-68.5	7.18	-72	54.1	5.66	1.45	0.67	93.2
AS T4 C		**MEAN**	**7.36**	**-30**	**47.6**	**6.09**	**1.35**	**0.70**	**96.2**
		Std. Dev.	**0.29**	**116**	**3.7**	**1.36**	**0.06**	**0.03**	**3.6**

Site ID and Core Section[1]	Field: Depth interval[2] (cm)	Core: Depth Interval[3] (cm)	pH	Eh (mV)	Dry weight (%)	LOI (%)	Bulk Density (g/cm^3)	Porosity (ml/cm^3)	Grain size (% < 63 µm)
AS T5 A-D1	0-12.5	0-12.5	6.46	229	50.1	6.03	1.37	0.69	96.1
AS T5 A-D1	12.5-27.3	12.5-27.3	7.26	134	45.6	6.37	1.33	0.72	95.8
AS T5 A-D2	20-30	0-10	6.5	278	49.3	6.47	1.40	0.71	92.3
AS T5 A-D2	30-40	10-20	6.88	88	45.8	7.51	1.34	0.72	96.9
AS T5 A-D2	40-70	20-50	7.49	33	46.1	5.86	1.34	0.72	98.4
AS T5 A-D2	70-101	50-81	7.56	13	45.7	4.55	1.33	0.72	100.5
AS T5 A-D3	85-101	0-20	7.58	29	39.7	5.89	1.28	0.77	97.5
AS T5 A-D3	105-125	20-40	7.89	23	46.7	3.92	1.33	0.71	100.9
AS T5 A-D3	125-157	40-71	7.35	13	48.3	4.96	1.39	0.72	100.2
AS T5 A-D4	145-185	0-40	7.47	-5	51.1	5.25	1.40	0.69	99.0
AS T5 A-D4	185-200	40-55	7.47	8	52.7	5.63	1.43	0.68	92.6
AS T5 A-D4	200-228	55-82	7.41	12	46.6	6.08	1.30	0.70	101.5
AS T5 A		**MEAN**	**7.38**	**45**	**47.5**	**5.48**	**1.35**	**0.71**	**98.5**
		Std. Dev.	**0.45**	**59**	**3.4**	**0.91**	**0.04**	**0.03**	**3.1**
AS T5 B-D1	0-20	0-20	7.42	39	57.0	5.67	1.48	0.64	76.6
AS T5 B-D1	20-50	20-50	7.53	12	53.7	6.76	1.43	0.66	95.0
AS T5 B-D1	50-79	50-79	7.36	-13	48.5	6.24	1.36	0.70	94.4
AS T5 B-D2	79-94	9-24	7.63	12	49.3	6.58	1.38	0.70	93.6
AS T5 B-D2	94-130	24-60	7.52	4	50.9	6.58	1.42	0.70	95.6
AS T5 B-D2	130-166	60-96	7.7	8	47.9	6.45	1.34	0.70	96.6
AS T5 B-D3	167-202	17-52	7.69	8	47.7	6.51	1.35	0.71	93.9
AS T5 B-D3	202-212	52-62	7.52	11	74.6	4.18	1.66	0.42	71.4
AS T5 B		**MEAN**	**7.56**	**9**	**51.5**	**6.32**	**1.40**	**0.68**	**92.2**
		Std. Dev.	**0.12**	**12**	**8.7**	**0.88**	**0.10**	**0.10**	**10.1**
AS T5 C-D1	0-15	0-15	6.82	72	48.7	8.65	1.36	0.70	92.7
AS T5 C-D1	15-30	15-30	7.33	20	43.6	6.71	1.31	0.74	94.5
AS T5 C-D1	30-49	30-49	7.46	39	40.6	6.53	1.26	0.75	95.2
AS T5 C-D2	50-81	0-31	7.35	5	40.4	7.22	1.23	0.73	96.5
AS T5 C-D2	81-112	31-62	7.41	29	42.5	5.98	1.24	0.71	97.8

Site ID and Core Section[1]	Field: Depth interval[2] (cm)	Core: Depth Interval[3] (cm)	pH	Eh (mV)	Dry weight (%)	LOI (%)	Bulk Density (g/cm^3)	Porosity (ml/cm^3)	Grain size (% < 63 µm)
AS T5 C-D2"	112-130	40-58	7.51	192	43.1	5.24	1.27	0.72	99.4
AS T5 C-D3	130-150	10-30	7.51	191	38.8	7.70	1.26	0.77	96.4
AS T5 C-D3	150-175	30-55	7.59	26	46.0	6.38	1.31	0.71	94.3
AS T5 C-D3	175-198	55-78	7.46	31	48.8	7.35	1.37	0.70	94.5
AS T5 C		**MEAN**	**7.40**	**60**	**43.4**	**6.81**	**1.28**	**0.73**	**95.9**
		Std. Dev.	**0.23**	**65**	**3.6**	**0.99**	**0.05**	**0.03**	**2.0**
ALL DATA		**MEAN**	**7.46**	**-28**	**47.6**	**5.7**	**1.4**	**0.71**	**93.9**
ALL DATA		**STD. DEV.**	**0.23**	**148**	**7.8**	**1.3**	**0.1**	**0.08**	**17.4**
ALL DATA		**STD. ERROR**	**0.02**	**12**	**0.7**	**0.1**	**0.0**	**0.01**	**1.5**
ALL DATA		**MEDIAN**	**7.48**	**-36**	**46.0**	**5.7**	**1.3**	**0.72**	**97.0**
ALL DATA		**MINIMUM**	**6.46**	**-162**	**38.8**	**1.4**	**1.2**	**0.31**	**7.6**
ALL DATA		**MAXIMUM**	**7.89**	**278**	**80.3**	**9.5**	**1.9**	**0.77**	**103.8**
ALL DATA		**TOTAL N**	**140**	**140**	**140**	**140**	**140**	**140**	**140**

[1] Core coding: AS T# [A, B or C]-D#; where AS = Alviso Slough; T# = Transect number (1 thru 5); [A, B or C] = Site description as per Table 1 (left marsh, right marsh or slough channel, respectively); D# = depth specific core segment

[2] Field depth interval measured from the sediment / water interface

[3] Core depth interval measured from the top of the individual core liner

Table 4. PWA Transects and Predicted Changes in Slough Cross Sectional Area

Data for current channel cross sectional areas and predicted cross sectional areas for the 20-foot (20') and 40-foot (40') levee notch scenarios proposed for Pond A8, as reported by Philip Williams and Associates (PWA)[1], have been converted from feet to meters. [XS, cross sectional; m^2, meters squared; ND, not determined]

Transect[1]	Current Channel XS Area (m^2)	20′ Notch Channel XS Area (m^2)	40′ Notch Channel XS Area (m^2)	20′Notch XS Area CHANGE (m^2)	40' Notch XS Area CHANGE (m^2)
I. A8 Notch	112.4	162.9	204.9	50.5	92.5
II. d/s Marina	100.9	143.9	179.8	43.0	79.0
III. A8 Bulge	126.9	154.0	178.7	27.1	51.8
IV. Mid-Slough	177.0	188.9	200.7	12.0	23.7
V. Mouth[2]	N.D.	N.D.	N.D.	0.0	0.0

[1] EDAW and others, 2007

[2] Model assumption is that there is no cross sectional area change for the Mouth transect

Table 5. Sediment Mobilization Predictions by Slough Segment

Slough channel length and slough segment areas, as measured from digital aerial photographs. The change in channel cross sectional (XS) area for each segment was based on the average of the two transect lines in **Table 4** that bound that defined slough segment. Sediment mobilized for the 20-foot (20') and 40-foot (40') Pond A8 notch scenarios were calculated as the product of the XS area change and the slough channel length for each segment. Propagated error for all calculations are given in parentheses ( ). [m, meters; m^2, meters squared; m^3, meters cubed]

Alviso Slough Segment	Slough Channel Length (m)	Segment Area (m^2)	20' Notch Channel XS Area CHANGE (m^2)		40' Notch Channel XS Area CHANGE (m^2)		20' Notch Sediment mobilized (m^3)		40' Notch Sediment mobilized (m^3)	
A	777	155,772	46.8	(3.8)	85.7	(6.8)	36,342	(2923)	66,621	(5269)
B	1020	166,342	35.1	(7.9)	65.4	(13.6)	35,769	(8101)	66,705	(13834)
C	1134	279,833	19.6	(7.6)	37.8	(14.1)	22,174	(8585)	42,821	(15959)
D	3419	794,437	6.0	(6.0)	11.8	(11.8)	20,485	(20485)	40,495	(40495)
TOTAL	**6350**	**1,396,384**					**114,771**	**(23,823)**	**216,642**	**(45,974)**

Table 6. Mercury Species Current Inventory and Mobilization Predictions by Slough Segment

Propagated error for all calculations is given in parentheses ( ). [THg, total mercury; MeHg, methylmercury; Hg(II)_R, reactive mercury; g/m^2, grams per meter squared; g/m^3, grams per meter cubed; kg, kilograms]

A. Total Mercury

Slough Segment	Sediment Core Data Used	0-200 cm Depth Integrated THg (g/m^2)	CURRENT INVENTORY 0-200 cm Depth Integrated THg (kg)	Average Sediment HgT Concentration by volume (g/m^3)	20' Notch THg mobilized (kg)	40' Notch THg mobilized (kg)
A	T1	1.07 (0.19)	166 (30)	0.54 (0.04)	19.6 (2.1)	36.0 (3.7)
B	T1	1.07 (0.19)	177 (32)	0.54 (0.04)	19.3 (4.6)	36.0 (7.9)
C	T2 & T3	1.21 (0.30)	339 (83)	0.62 (0.05)	13.7 (5.4)	26.4 (10.0)
D	T4 & T5	1.22 (0.37)	969 (292)	0.65 (0.06)	13.3 (13.3)	26.2 (26.3)
TOTAL			**1651 (307)**		**65.9 (15.2)**	**124.6 (29.5)**

B. Reactive Inorganic Mercury

Slough Segment	Sediment Core Data Used	0-200 cm Depth Integrated Hg(II)_R (mg/m^2)	CURRENT INVENTORY 0-200 cm Depth Integrated Hg(II)_R (kg)	Average Sediment Hg(II)_R Concentration by volume (mg/m^3)	20' Notch Hg(II)_R mobilized (kg)	40' Notch Hg(II)_R mobilized (kg)
A	T1	0.80 (0.68)	0.13 (0.11)	0.43 (0.24)	0.016 (0.009)	0.029 (0.016)
B	T1	0.80 (0.68)	0.13 (0.11)	0.43 (0.24)	0.015 (0.009)	0.029 (0.017)
C	T3	0.81 (0.26)	0.23 (0.07)	0.60 (0.27)	0.013 (0.008)	0.026 (0.015)
D	T5	0.58 (0.44)	0.46 (0.35)	0.49 (0.25)	0.010 (0.011)	0.020 (0.022)
TOTAL			**0.94 (0.39)**		**0.054 0.019**	**0.102 0.036**

C. Methylmercury

Slough Segment	Sediment Core Data Used	0-200 cm Depth Integrated MeHg (mg/m^2)	CURRENT INVENTORY 0-200 cm Depth Integrated MeHg (kg)	Average Sediment MeHg Concentration by volume (mg/m^3)	20' Notch MeHg mobilized (kg)	40' Notch MeHg mobilized (kg)
A	T1	1.49 (0.36)	0.23 (0.06)	0.72 (0.12)	0.026 (0.005)	0.048 (0.009)
B	T1	1.49 (0.36)	0.25 (0.06)	0.72 (0.12)	0.026 (0.007)	0.048 (0.013)
C	T3	1.09 (0.30)	0.31 (0.08)	0.57 (0.09)	0.013 (0.005)	0.025 (0.010)
D	T5	0.99 (0.18)	0.79 (0.14)	0.53 (0.12)	0.011 (0.011)	0.022 (0.022)
TOTAL			**1.57 (0.18)**		**0.076 (0.015)**	**0.142 (0.029)**

Appendix A—Sediment core descriptions, Alviso Slough, September 2006

Each page describes a single sediment core section, with the following information depicted (from left to right): whole core section photograph, dominant lithology, accessories, magnetic susceptibility and sediment density profiles. Refer to the **Symbol Legend** on page 49 for keys to lithology and accessories. The vertical length of the sediment depth interval that encompasses a noted accessory is depicted by the thin vertical black line immediately to the left of the accessory symbol. The approximate percentage of the depth interval occupied by that accessory is given in parentheses ( ) immediately below the accessory symbol. Both magnetic susceptibility and sediment density profiles were obtained from whole core scans using the multi-sensor core logger. The specific **core identification code** is given in the upper left corner of each page according to the format: T# [A, B or C] D#; where T# = Transect number (1 thru 5); [A, B or C] = Site description as per Table 1 (left marsh, right marsh or slough channel, respectively); D# = depth specific core segment. The specific core depth interval, measured in centimeters below the sediment/water interface is given in parentheses ( ) immediately following the core identification code. The sediment depth scale depicted on the photograph (black ruler) and the Y-axis associated with the plots of magnetic susceptibility and sediment density are precisely aligned.[1]

---

[1] This paragraph serves as the alternative text for all of the graphics in this appendix as the description for each is identical.

SYMBOL LEGEND

Lithology

■	**Clay**
▥	**Clayey Silt**
▩	**Clayey Sand**
▨	**Silty Clay**
⬚	**Silty Clay with Sand**
▤	**Silty Clay Sand**
🟨	**Sand**
▥	**Sandy Silt**
▤	**Sandy Silt Clay**

Accessories

•••	**Mottles, oxidized**
ōōo	**Mottles, reduced**
⍋	**Plant remains, undifferentiated**
⅄⅄	**Rootlets**
Fe	**Iron Stain, ferruginous**
υυυ	**Shell fragments**
⊖	**Molluscs, undifferentiated**
Wd	**Wood fragments**
ooo	**Pebbles/Granules**

T1A D1 (0-46 cm)

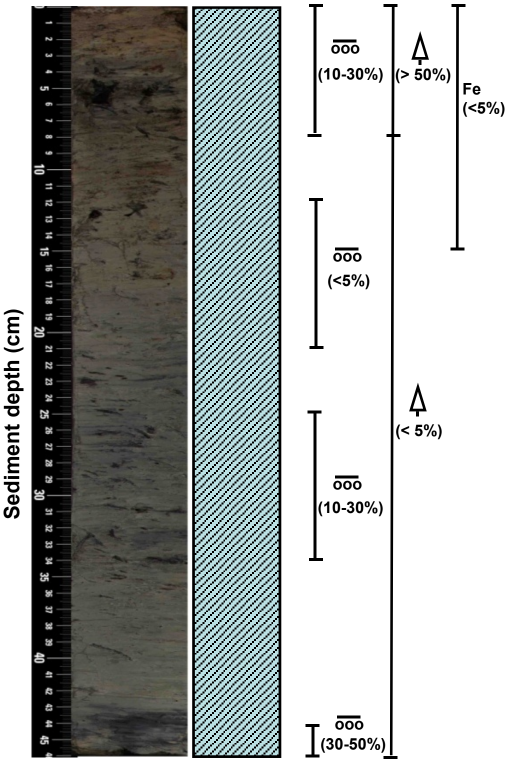
Sediment depth (cm)
ooo
(10-30%)
(> 50%)
Fe
(<5%)
ooo
(<5%)
(< 5%)
ooo
(10-30%)
ooo
(30-50%)

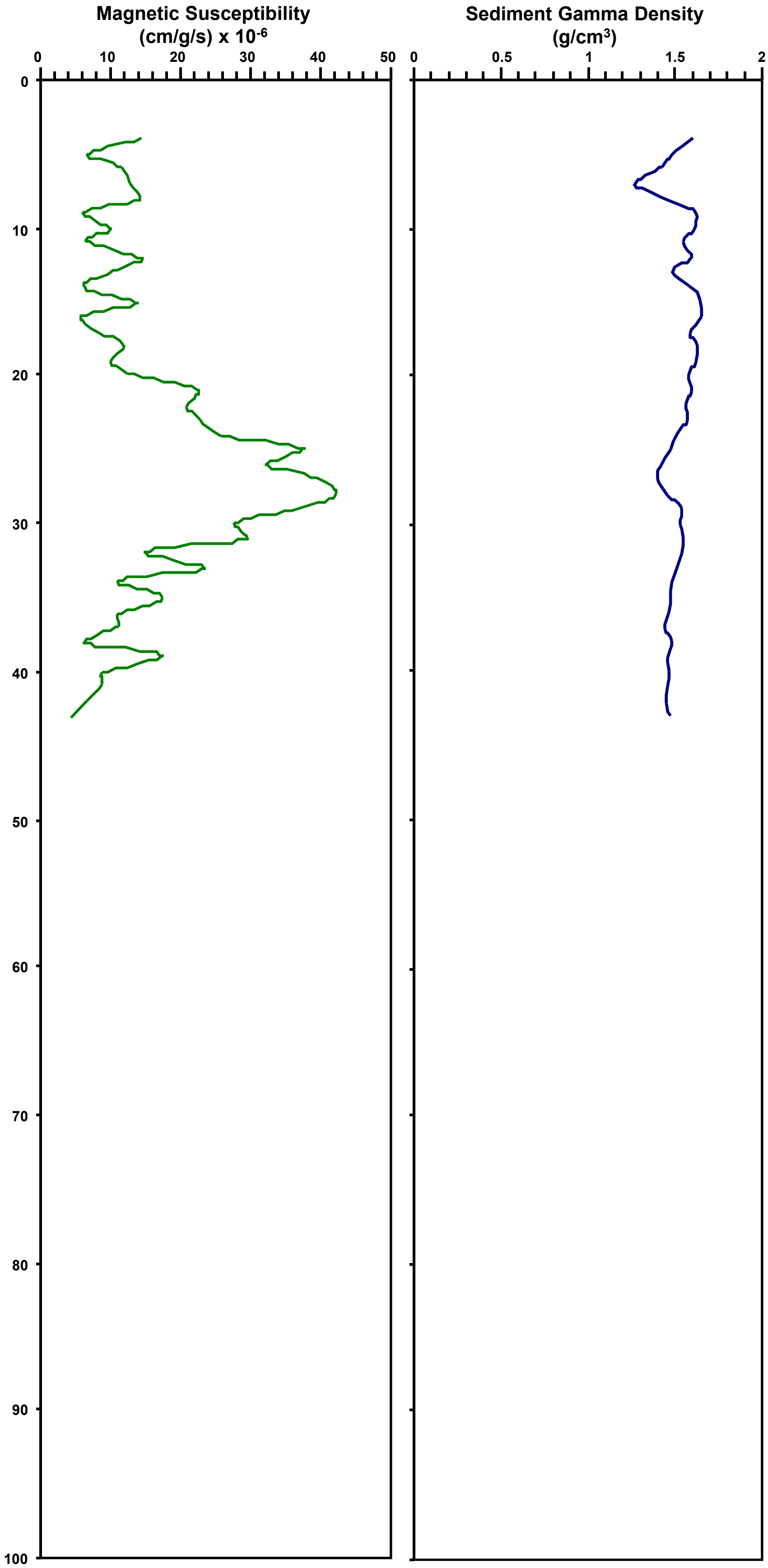
Magnetic Susceptibility
(cm/g/s) x 10-6
0
10
20
30
40
50
Sediment Gamma Density
(g/cm3)
0
0.5
1
1.5
2
0
10
20
30
40
50
60
70
80
90
100

T1A D2 (50-126 cm)

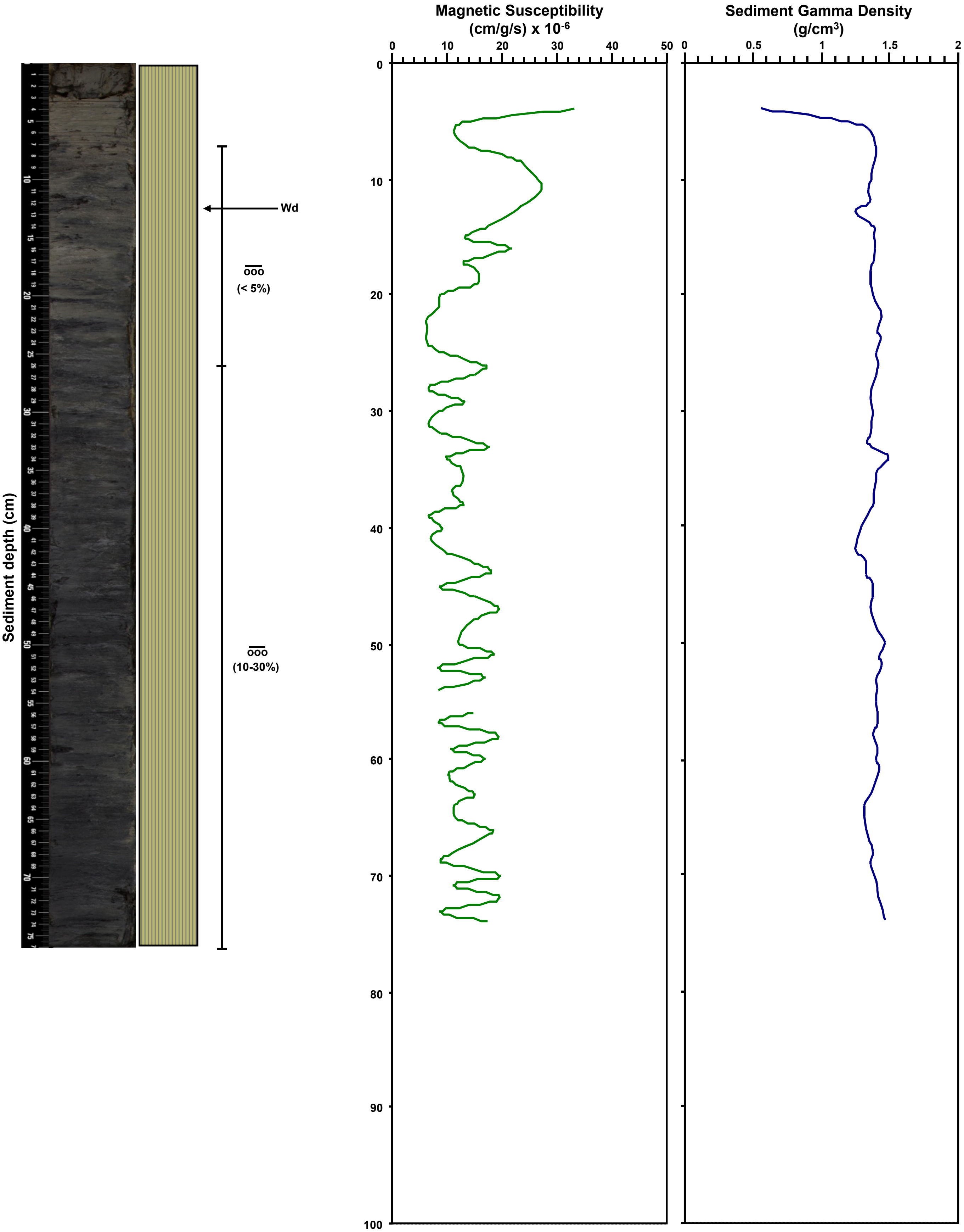

T1A D3 (125-203 cm)

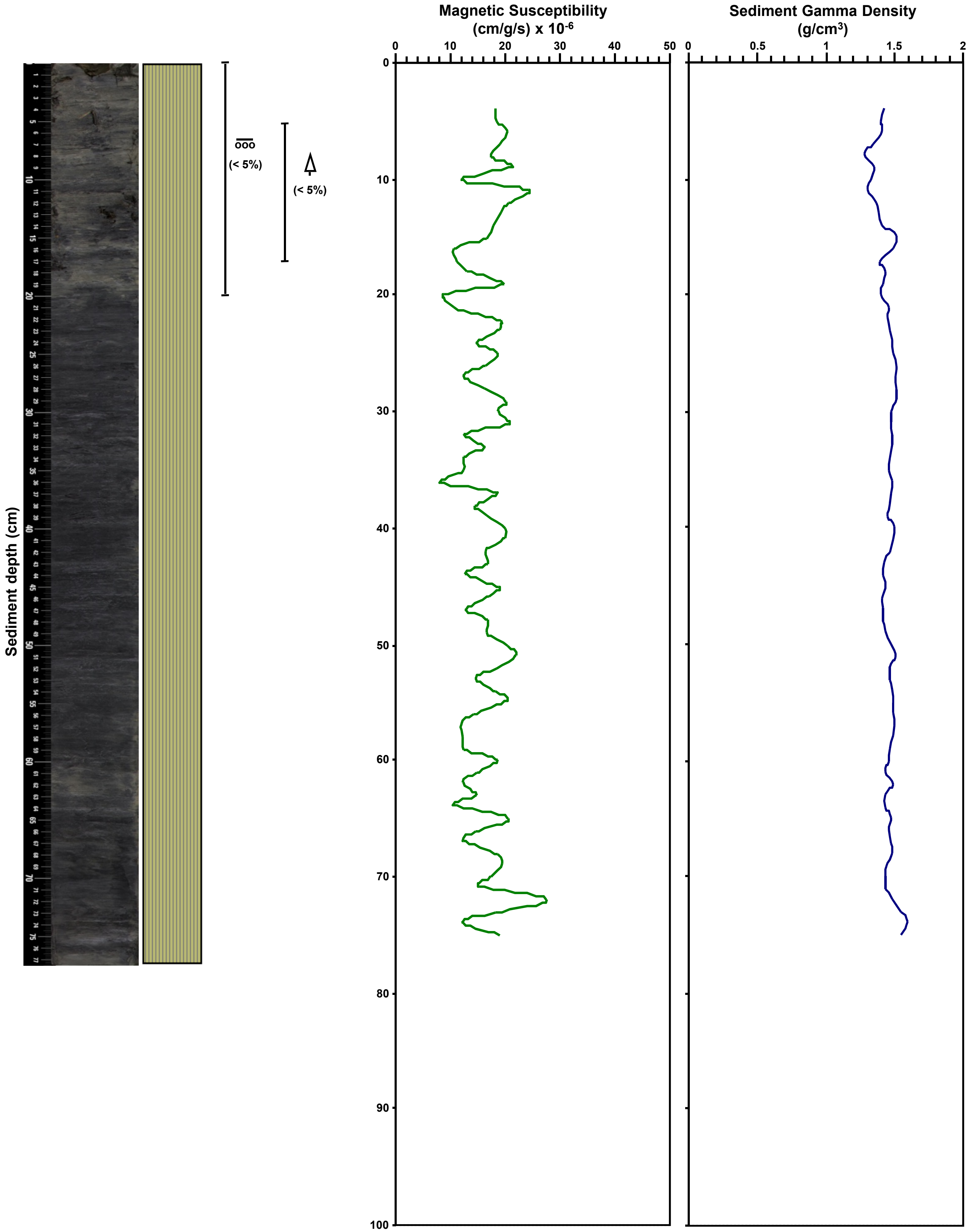

T1B D1 (0-83 cm)

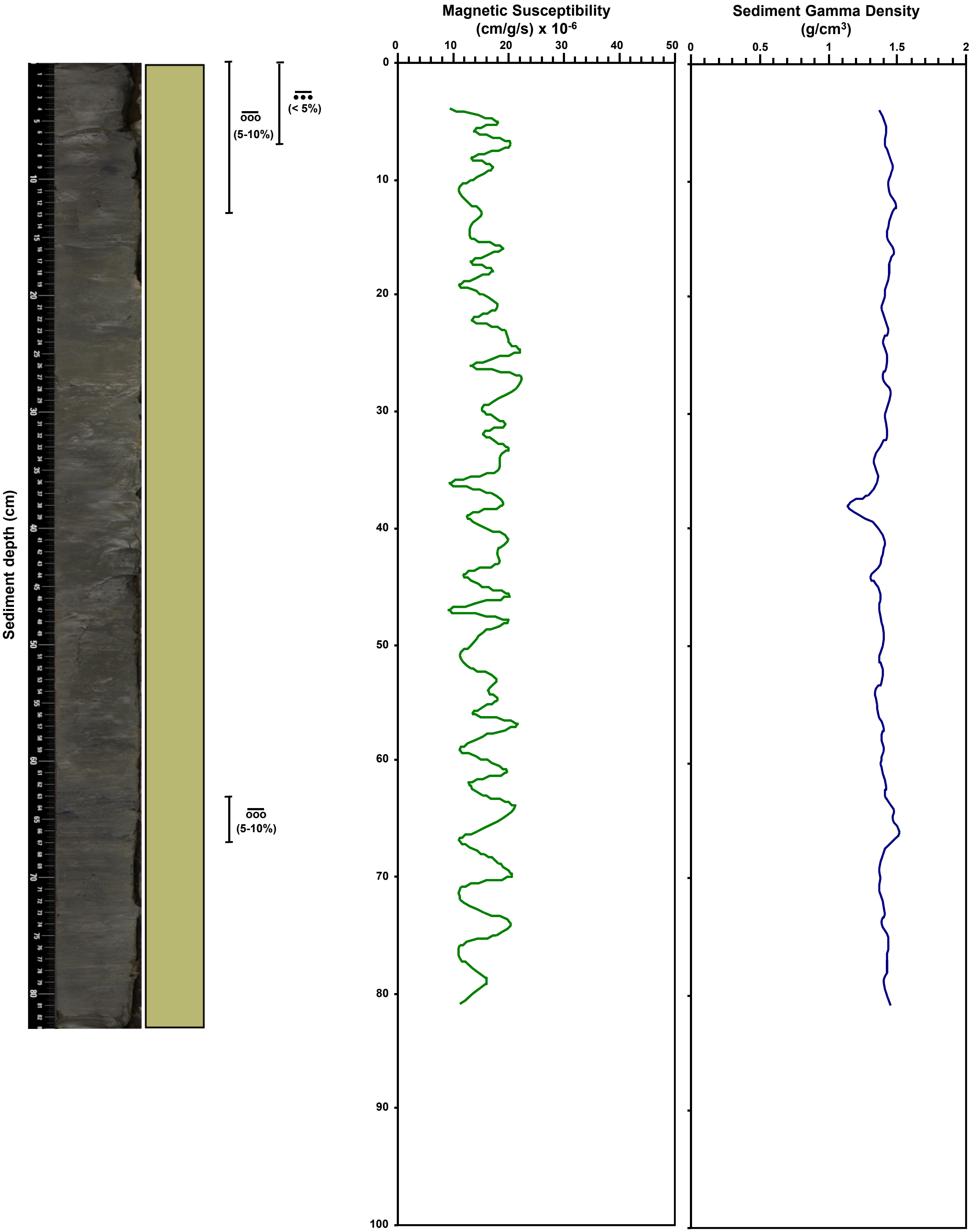
Sediment depth (cm)
ooo (5-10%)
••• (< 5%)
ooo (5-10%)
Magnetic Susceptibility
(cm/g/s) x 10^-6
0
10
20
30
40
50
Sediment Gamma Density
(g/cm³)
0
0.5
1
1.5
2
0
10
20
30
40
50
60
70
80
90
100

T1B D2 (50-135 cm)

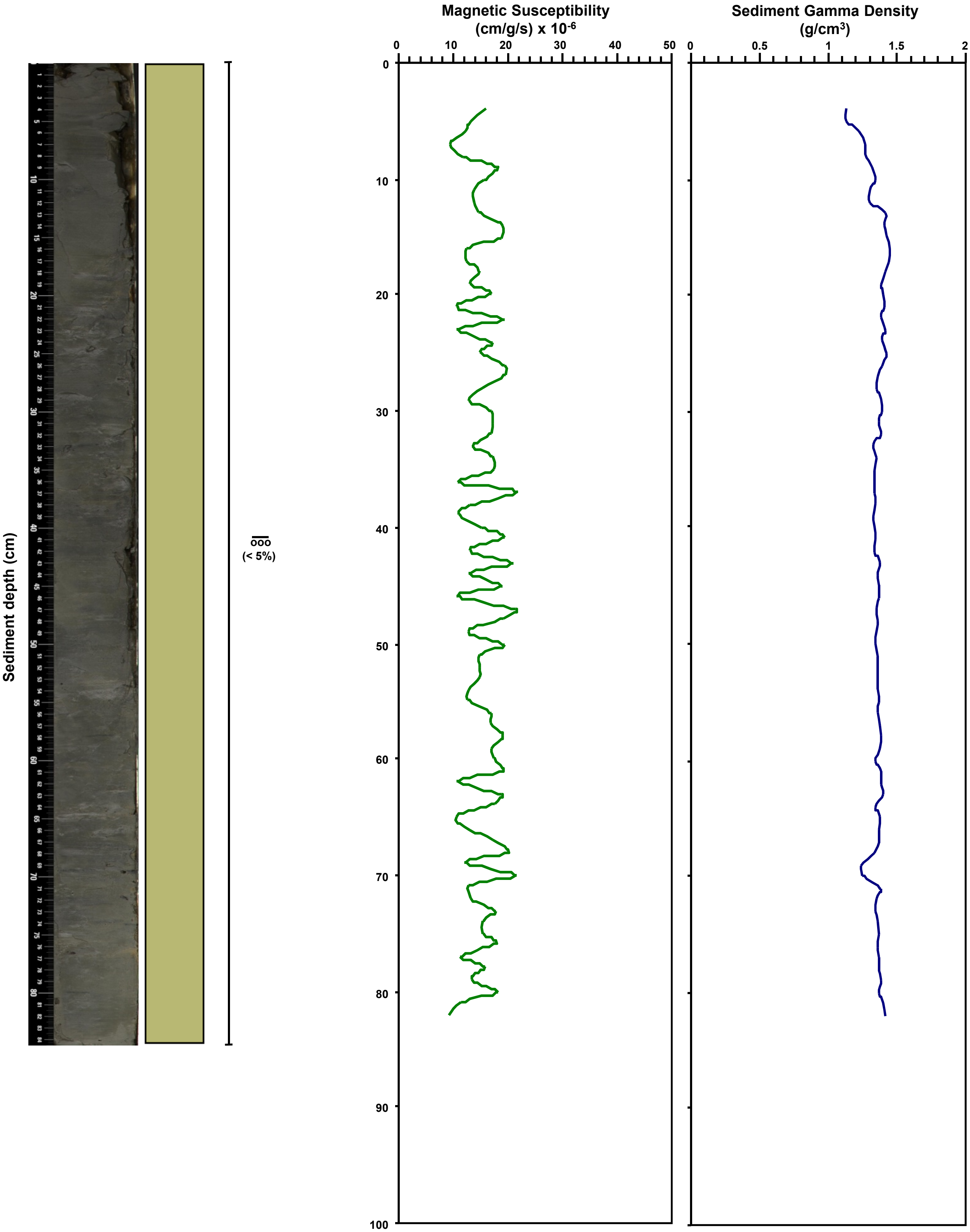

T1B D3 (130-209 cm)

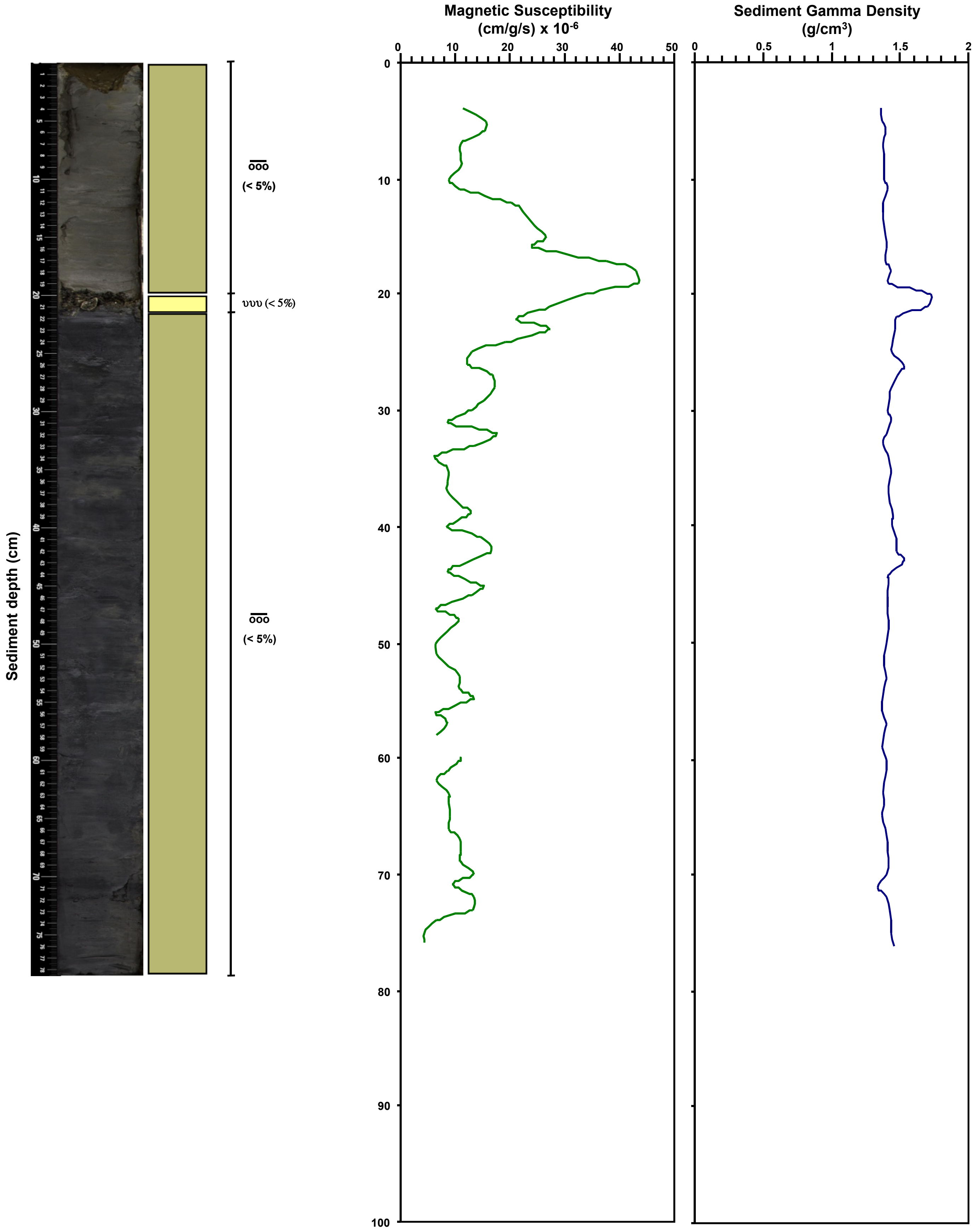

T1C D1 (0-60 cm)

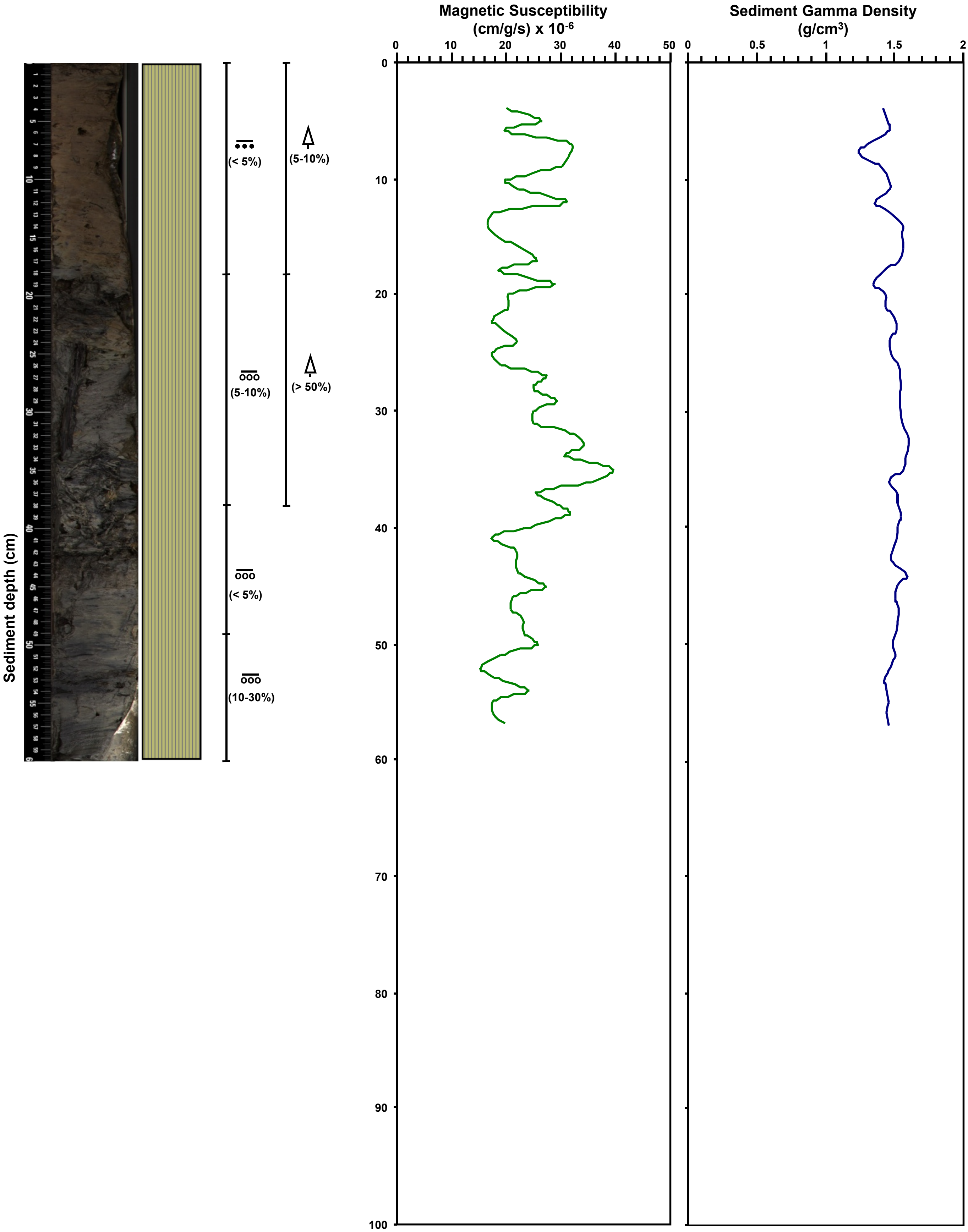
Sediment depth (cm)
(< 5%)
(5-10%)
(5-10%)
(> 50%)
(< 5%)
(10-30%)
Magnetic Susceptibility
(cm/g/s) x 10-6
0
10
20
30
40
50
Sediment Gamma Density
(g/cm3)
0
0.5
1
1.5
2
0
10
20
30
40
50
60
70
80
90
100

T1C D2 (50-116 cm)

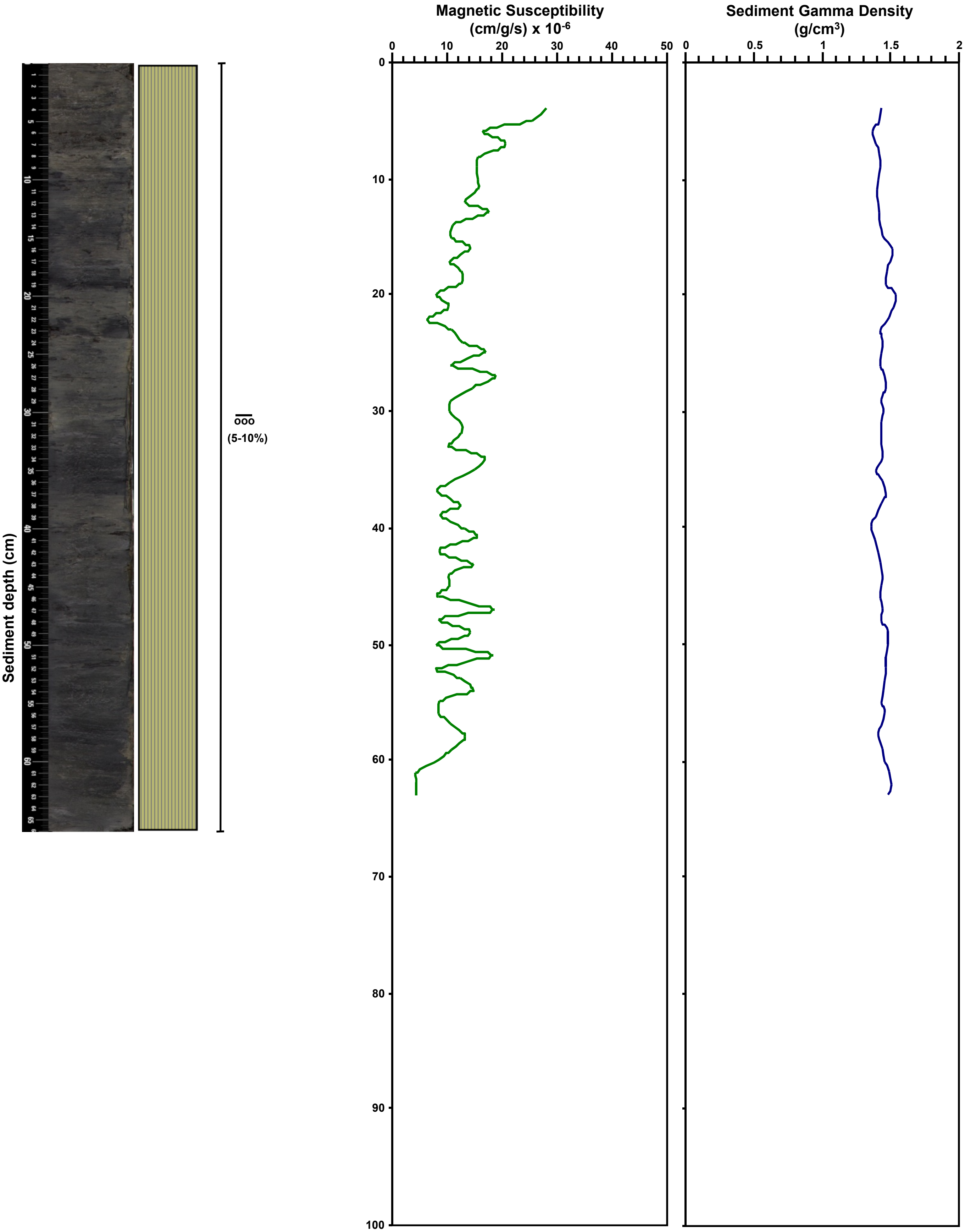

T1C D3 (115-196 cm)

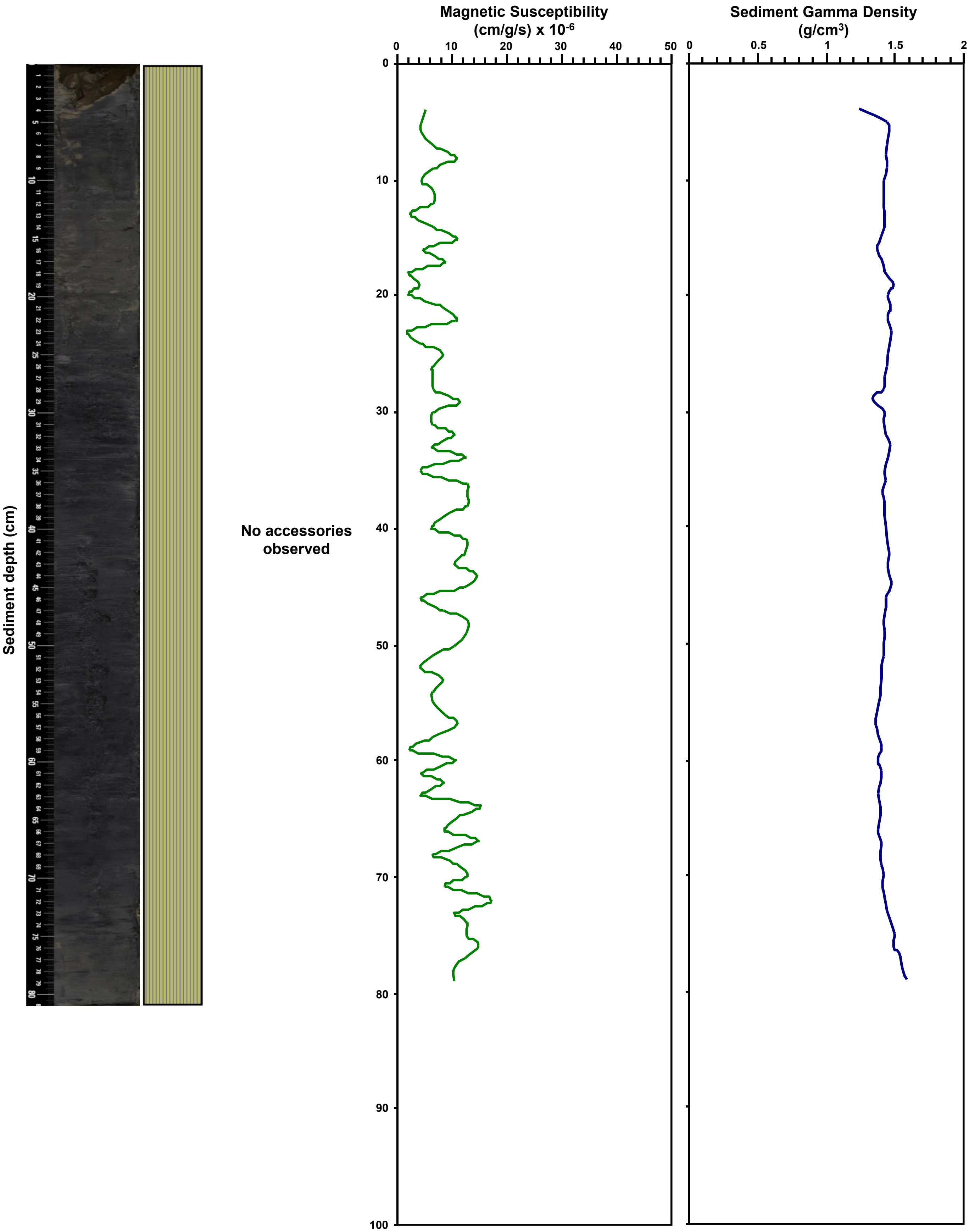

T2A D1 (0-23 cm)

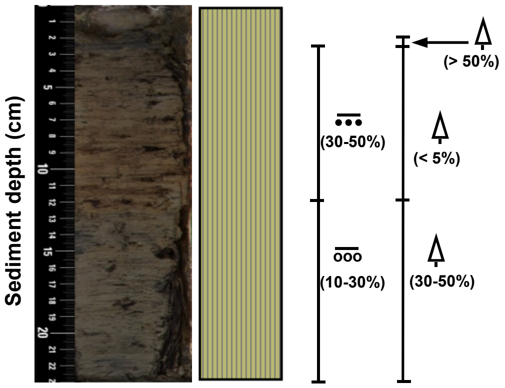
Sediment depth (cm)
(> 50%)
•••
(30-50%)
(< 5%)
ooo
(10-30%)
(30-50%)

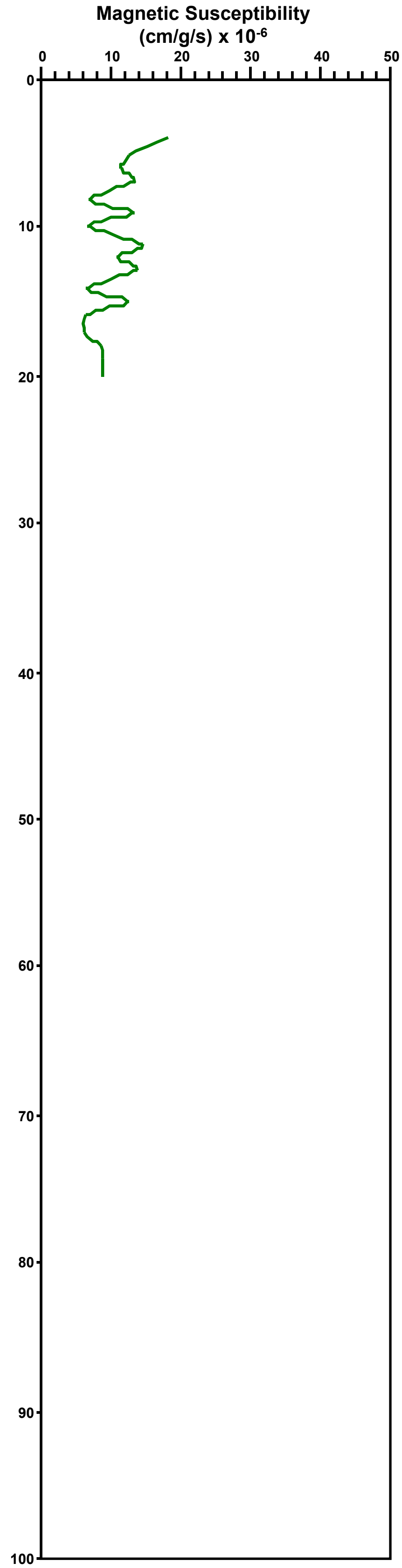
Magnetic Susceptibility
(cm/g/s) x 10-6
0
10
20
30
40
50
0
10
20
30
40
50
60
70
80
90
100

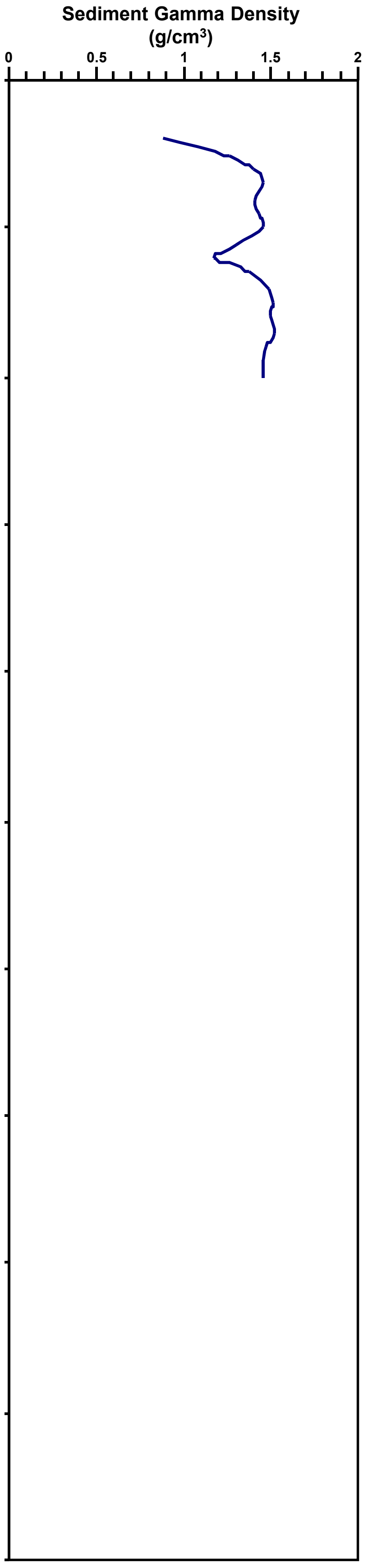
Sediment Gamma Density
(g/cm3)
0
0.5
1
1.5
2

T2A D2 (20-90 cm)

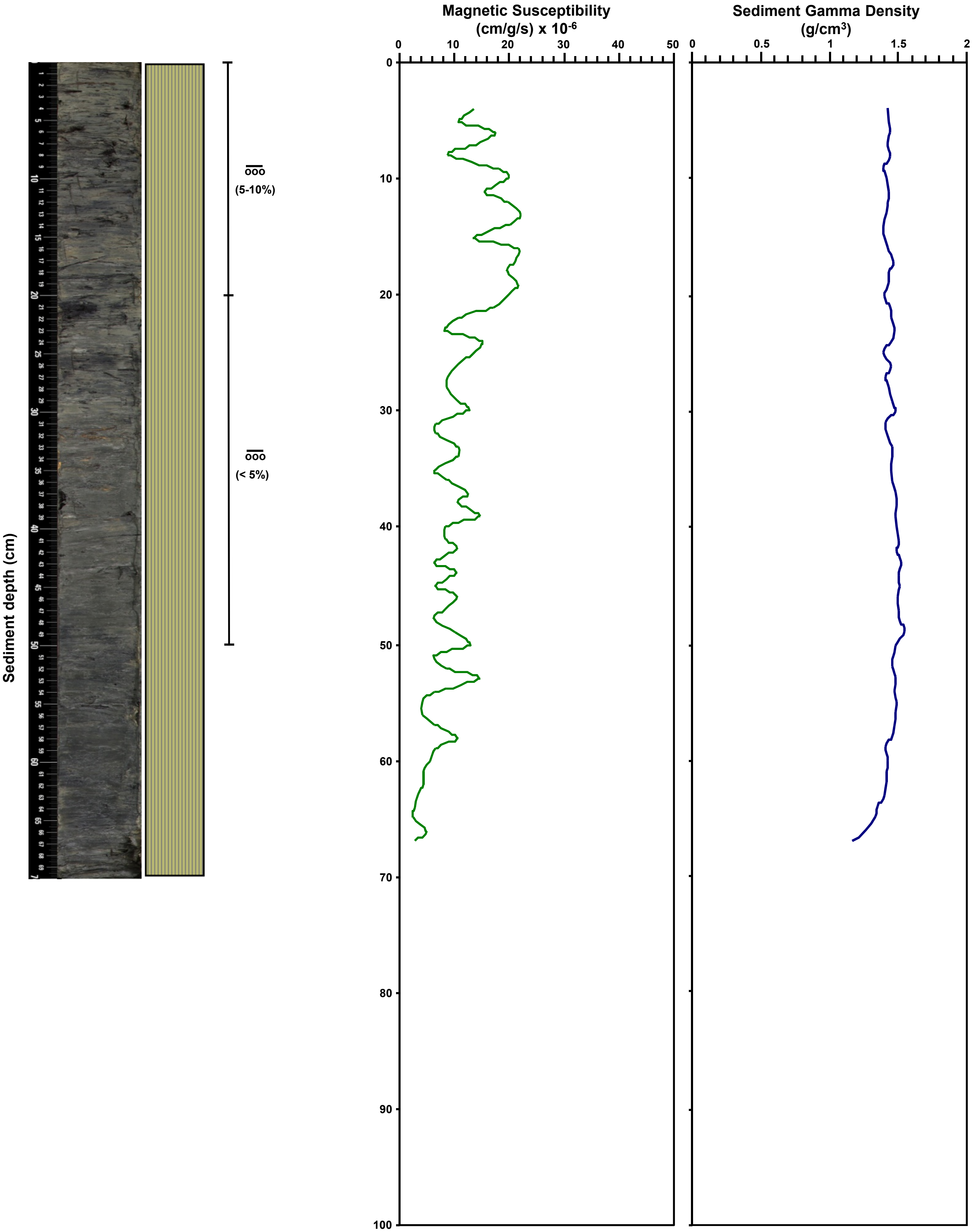

T2A D3 (85-166 cm)

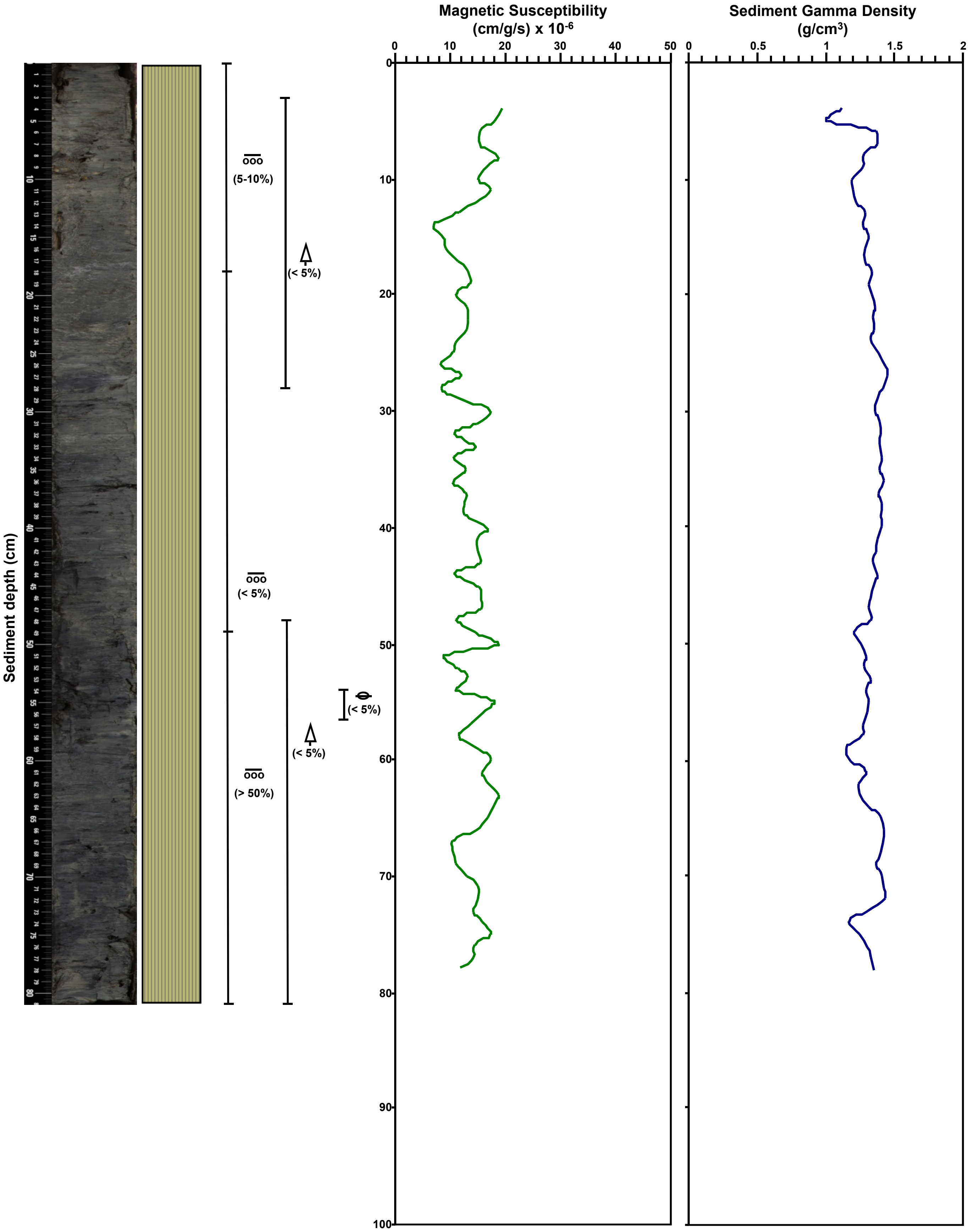

T2A D4 (140-212 cm)

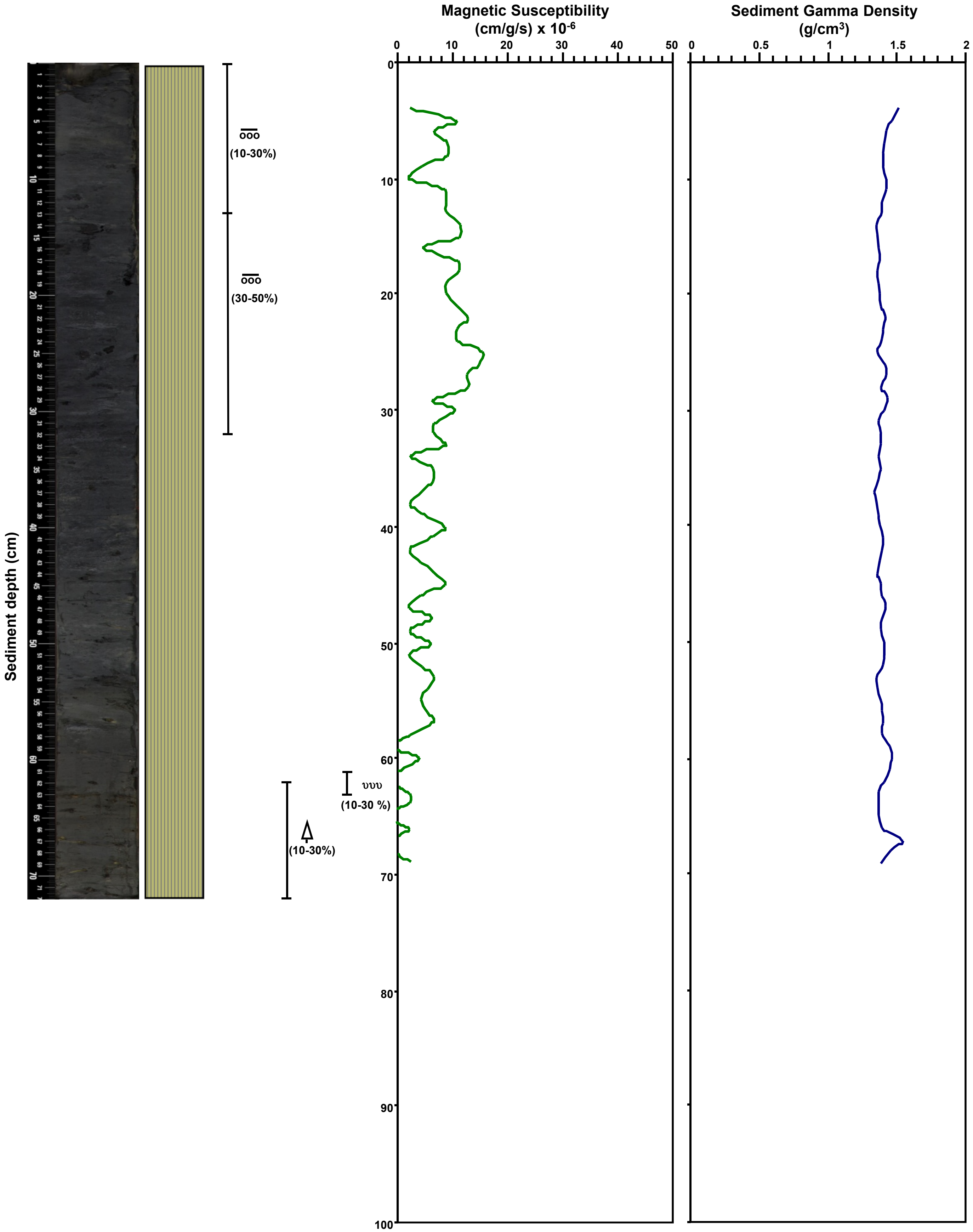

T2B D1 (0-97 cm)

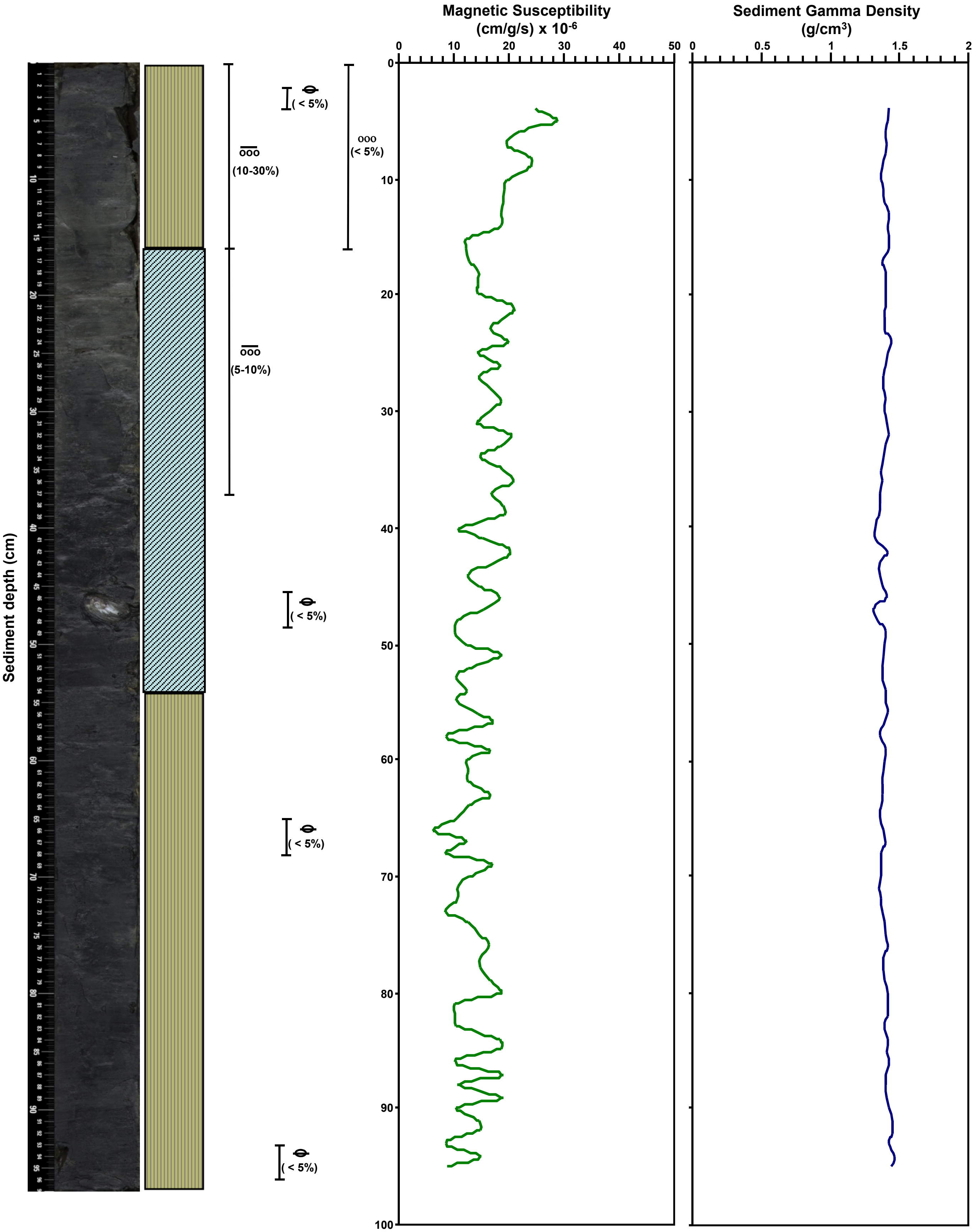
Sediment depth (cm)
ooo
(10-30%)
ooo
(5-10%)
ooo
(< 5%)
(< 5%)
(< 5%)
(< 5%)
(< 5%)
Magnetic Susceptibility
(cm/g/s) x 10-6
0
10
20
30
40
50
Sediment Gamma Density
(g/cm3)
0
0.5
1
1.5
2
0
10
20
30
40
50
60
70
80
90
100

T2B D2 (85-175 cm)

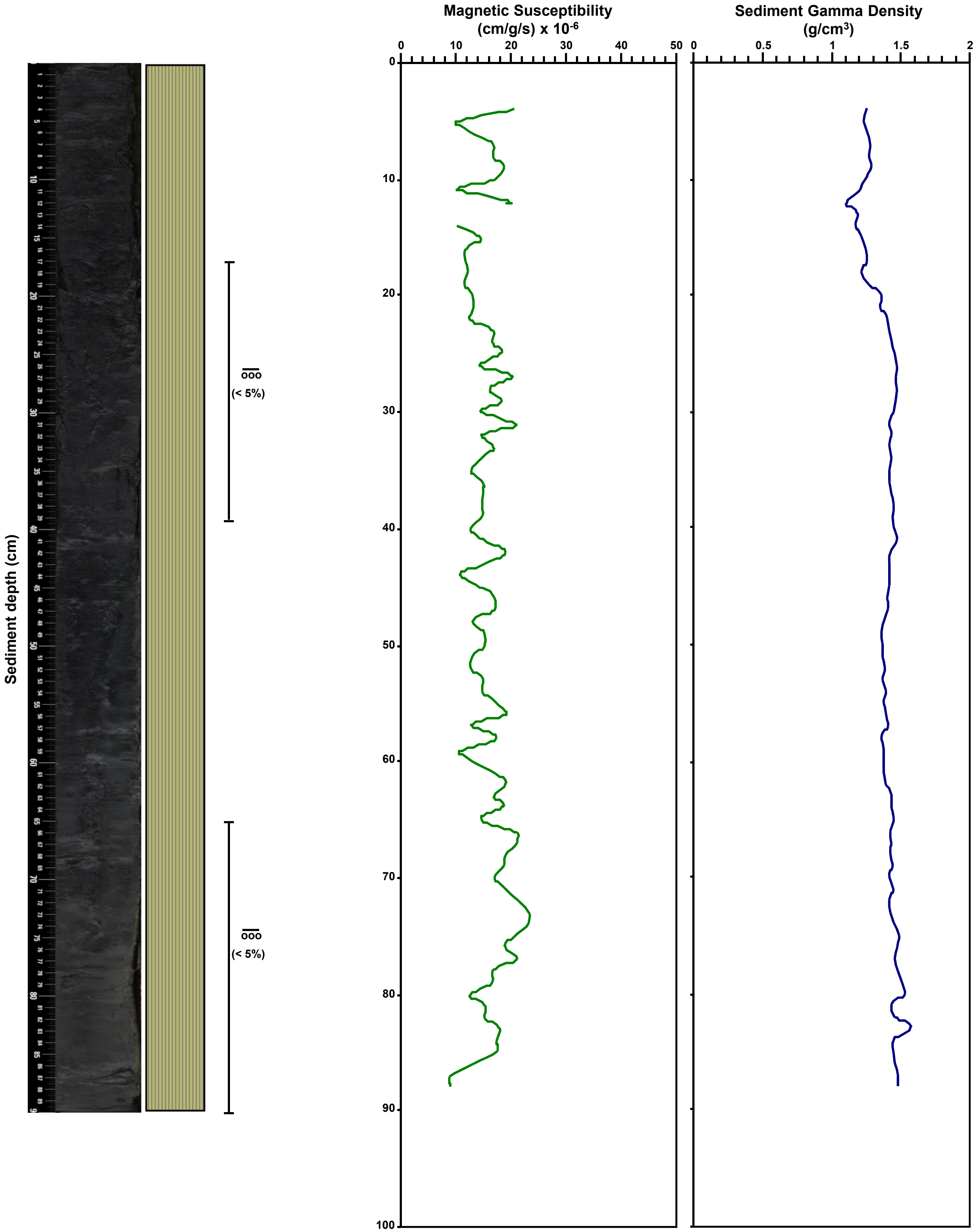

T2B D3 (150-231 cm)

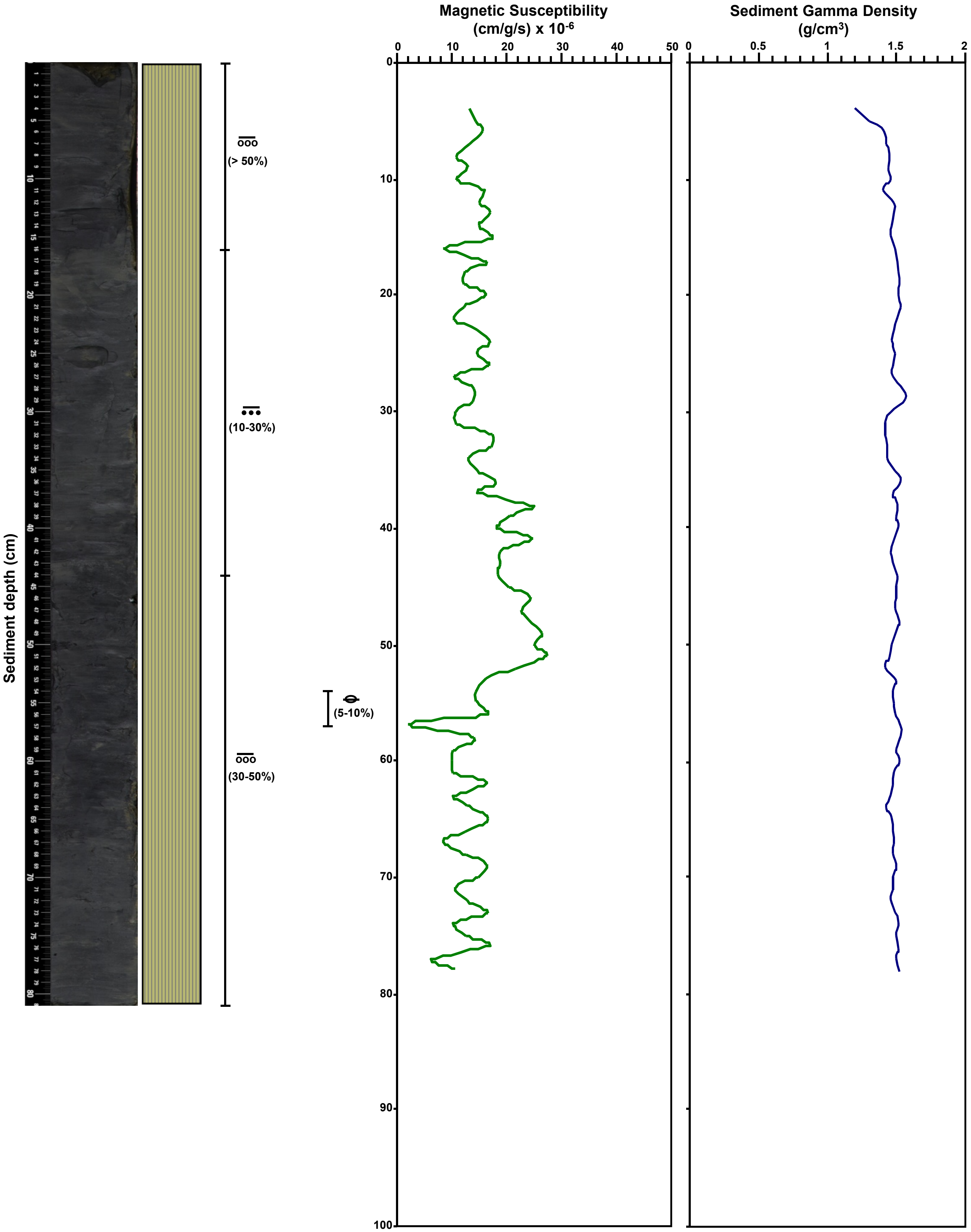

T2C D1 (0-25 cm)

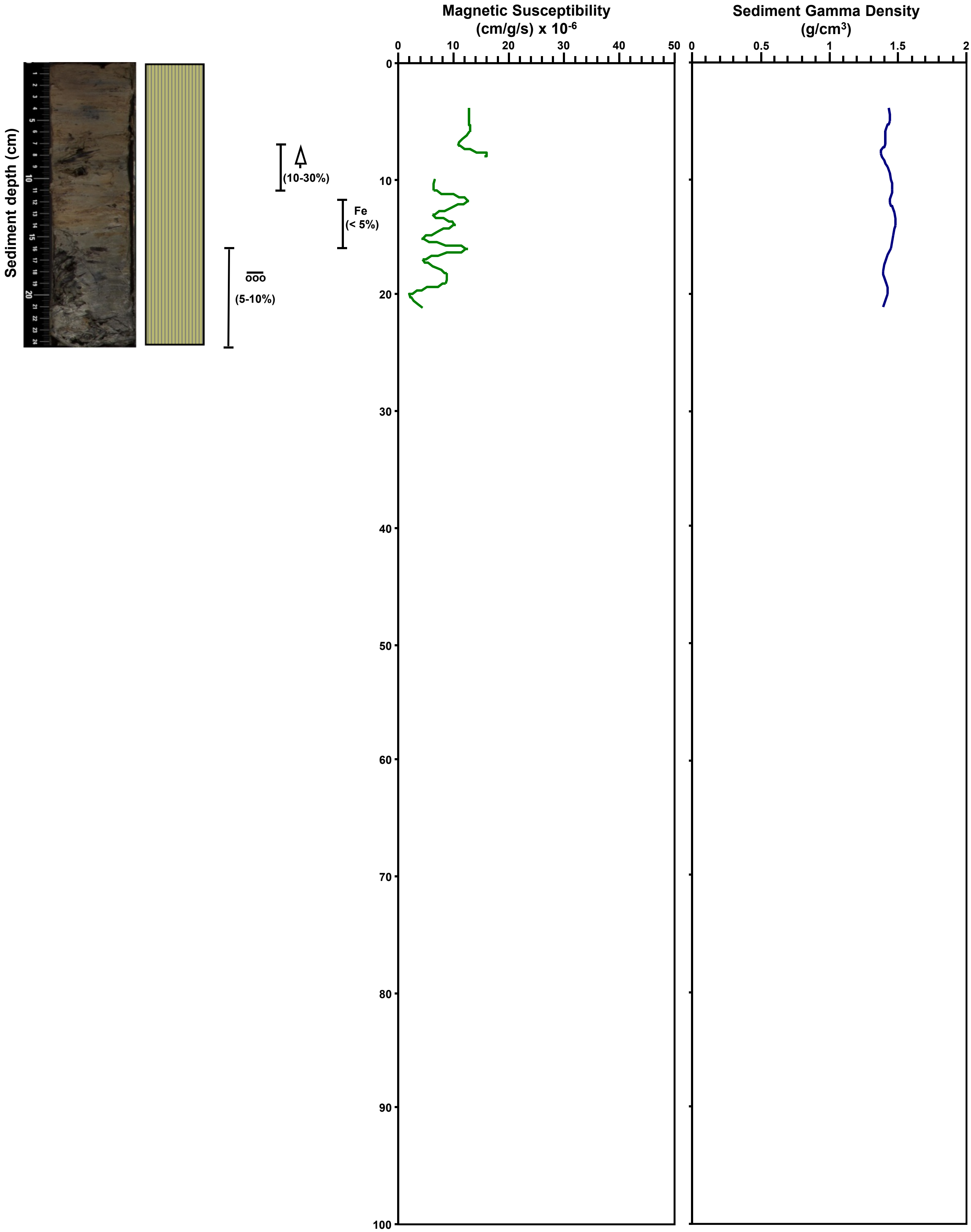
Sediment depth (cm)
(10-30%)
Fe
(< 5%)
ooo
(5-10%)
Magnetic Susceptibility
(cm/g/s) x 10-6
0
10
20
30
40
50
Sediment Gamma Density
(g/cm3)
0
0.5
1
1.5
2
0
10
20
30
40
50
60
70
80
90
100

T2C D1” (20-50 cm)

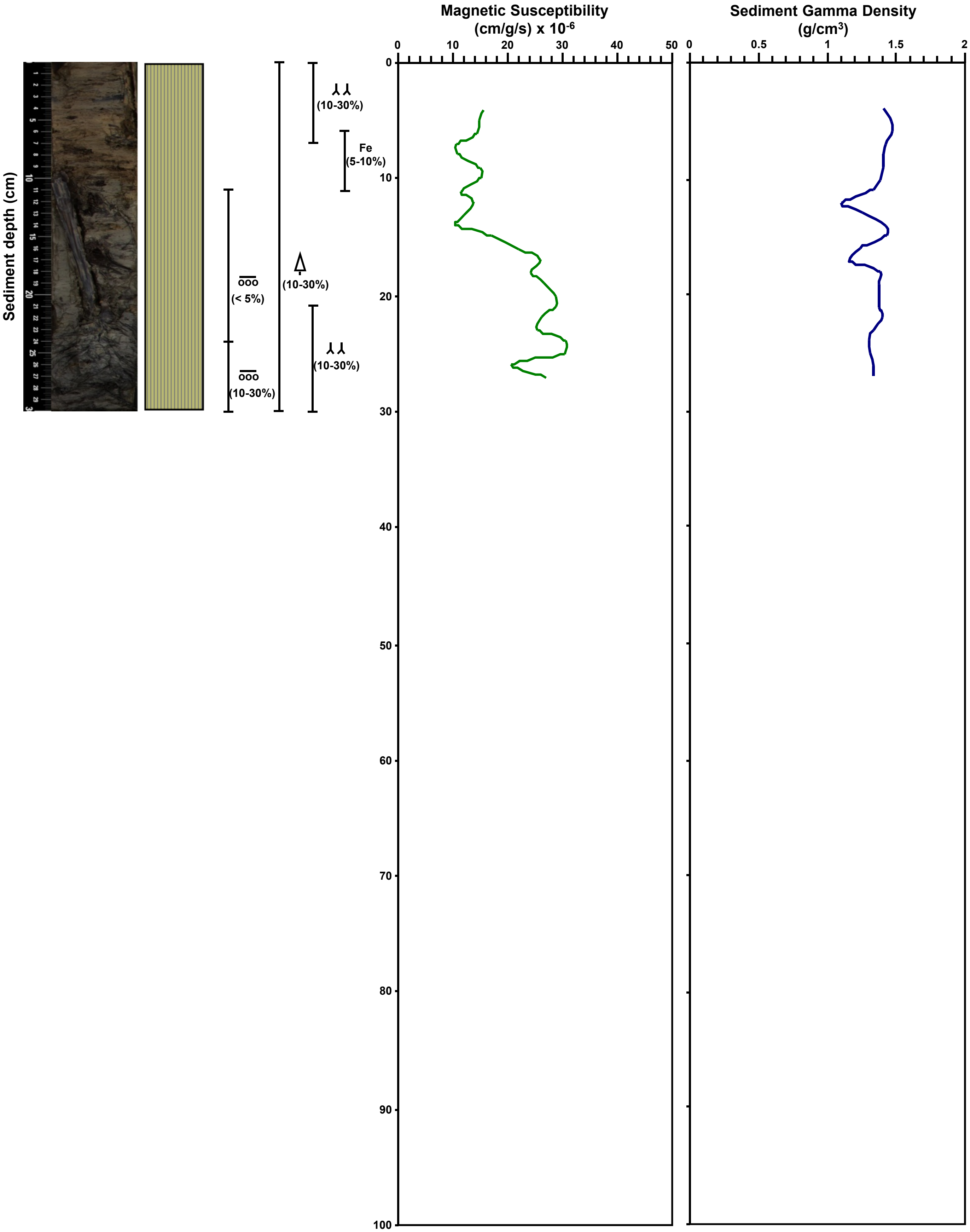

T2C D2 (50-130 cm)

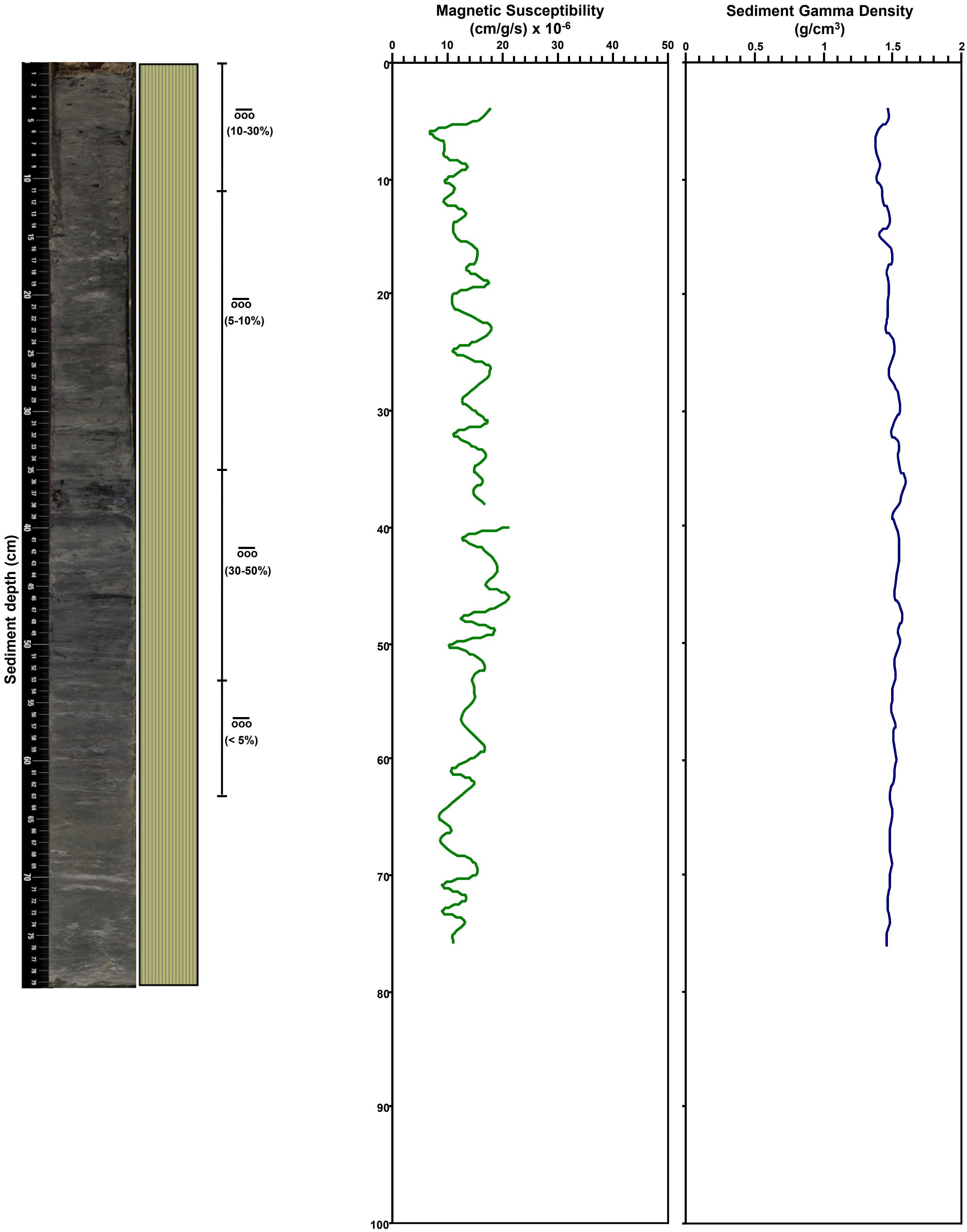

T2C D3 (125-204 cm)

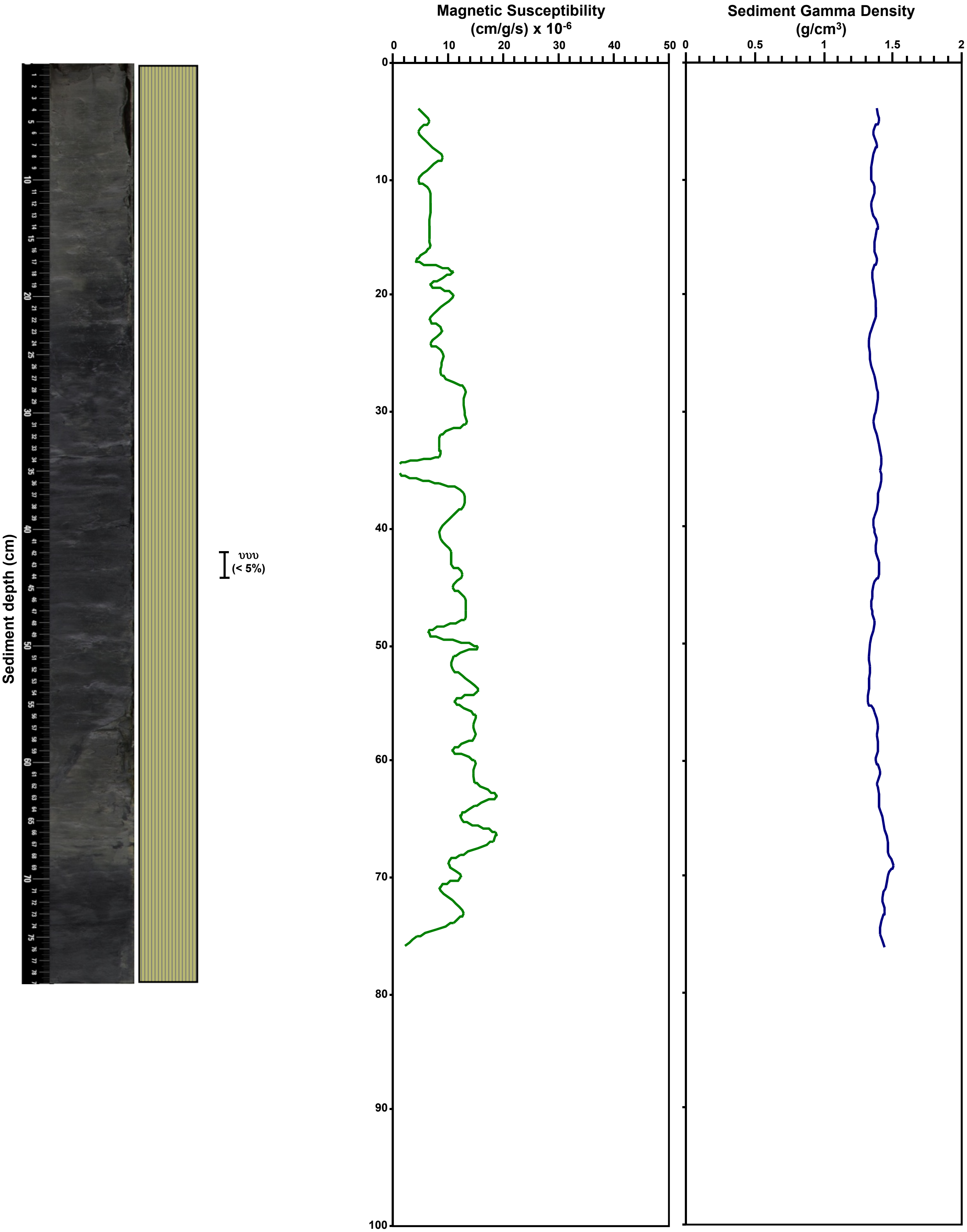

T3A D1 (0-46 cm)

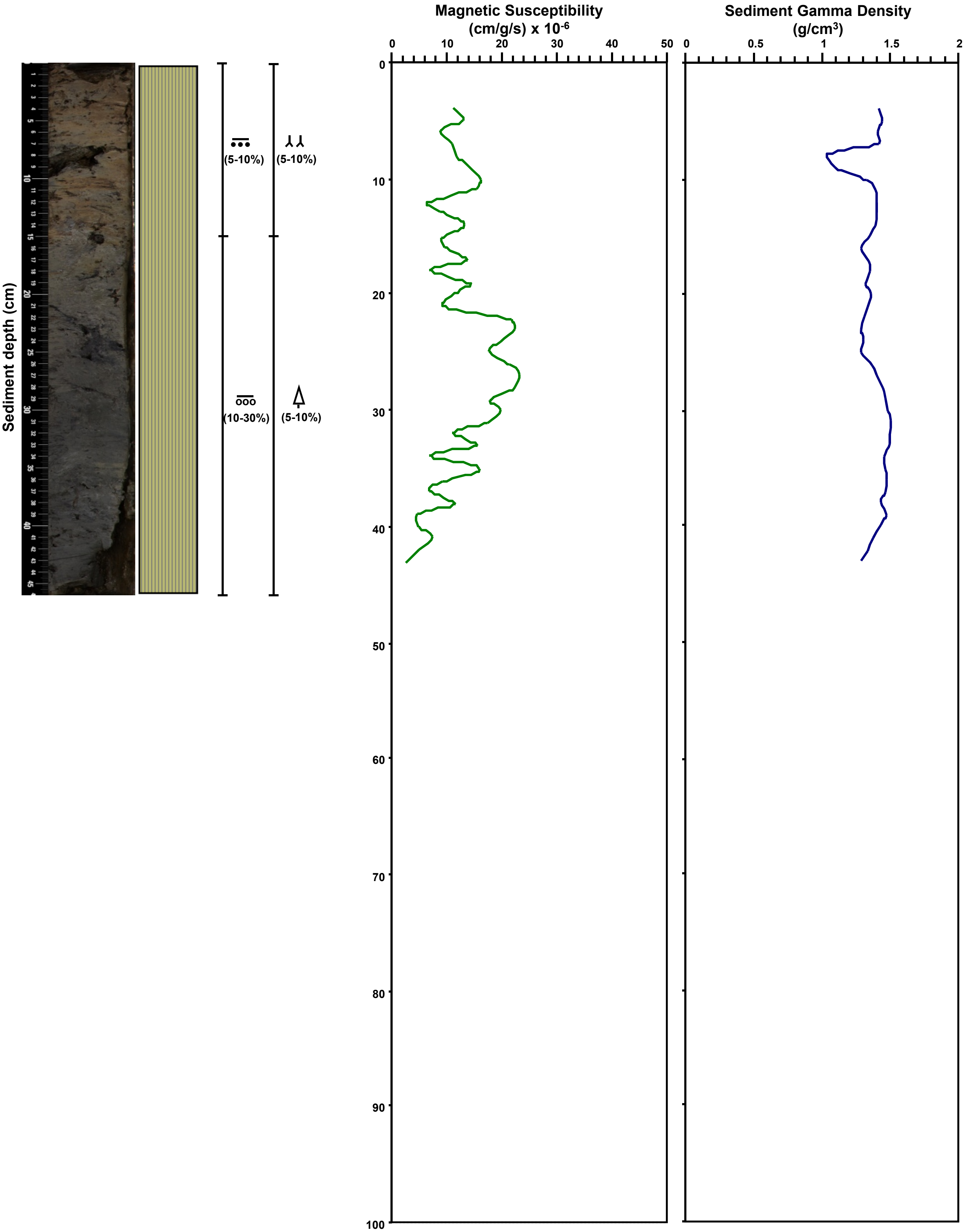
Sediment depth (cm)
(5-10%)
(5-10%)
(10-30%)
(5-10%)
Magnetic Susceptibility
(cm/g/s) x 10^{-6}
0
10
20
30
40
50
Sediment Gamma Density
(g/cm^3)
0
0.5
1
1.5
2
0
10
20
30
40
50
60
70
80
90
100

T3A D2 (45-124 cm)

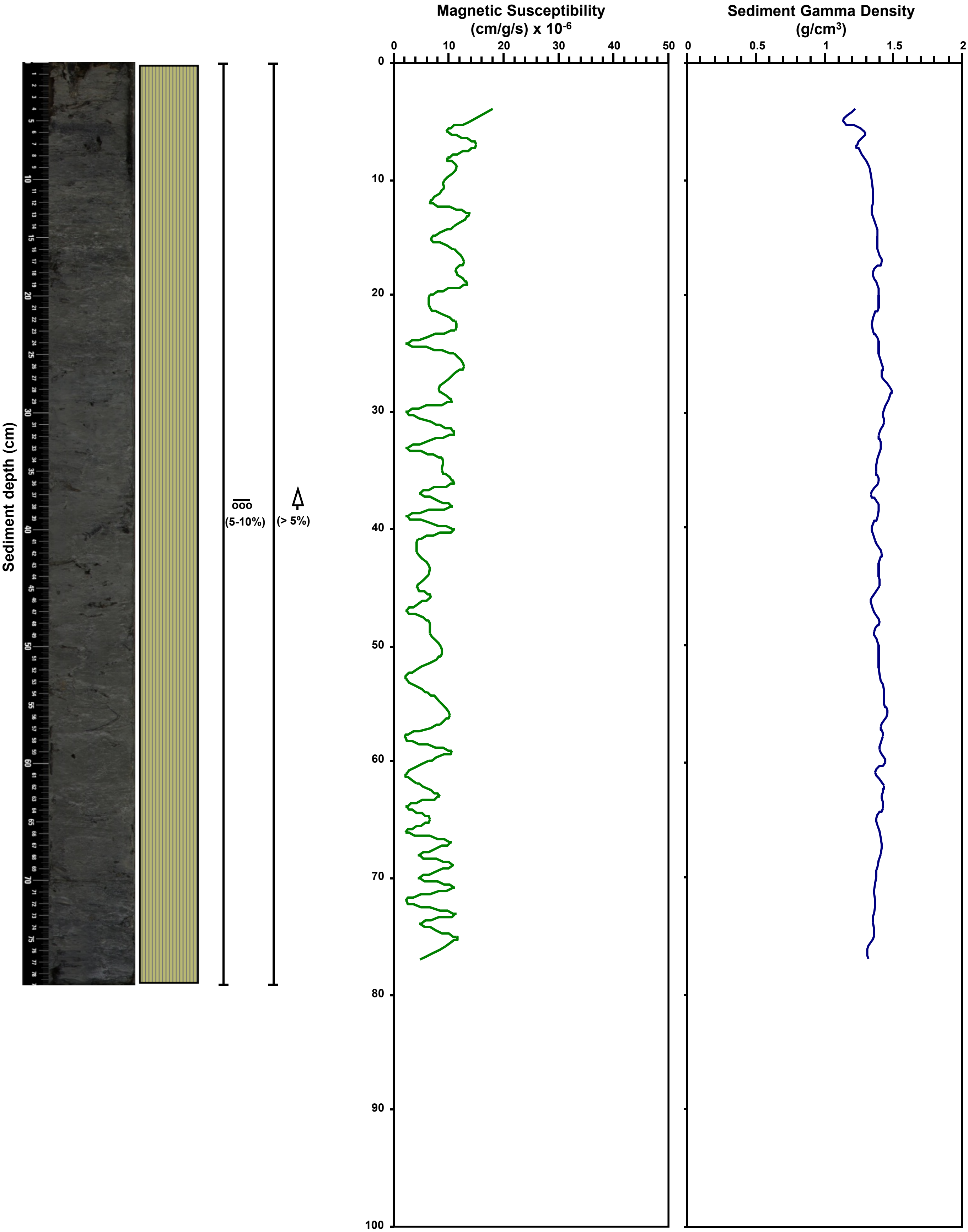

T3A D3 (125-209 cm)

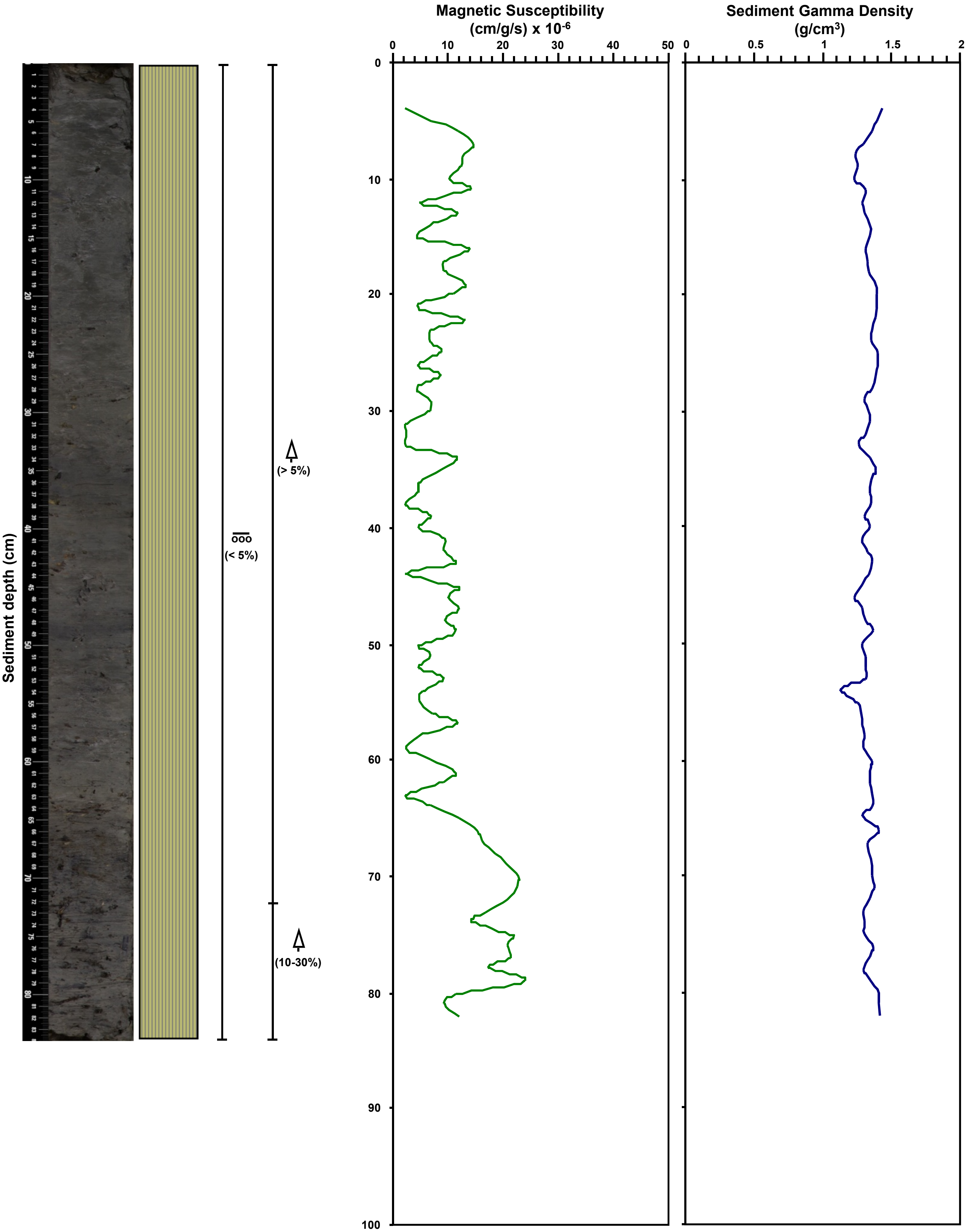

T3B D1 (0-71 cm)

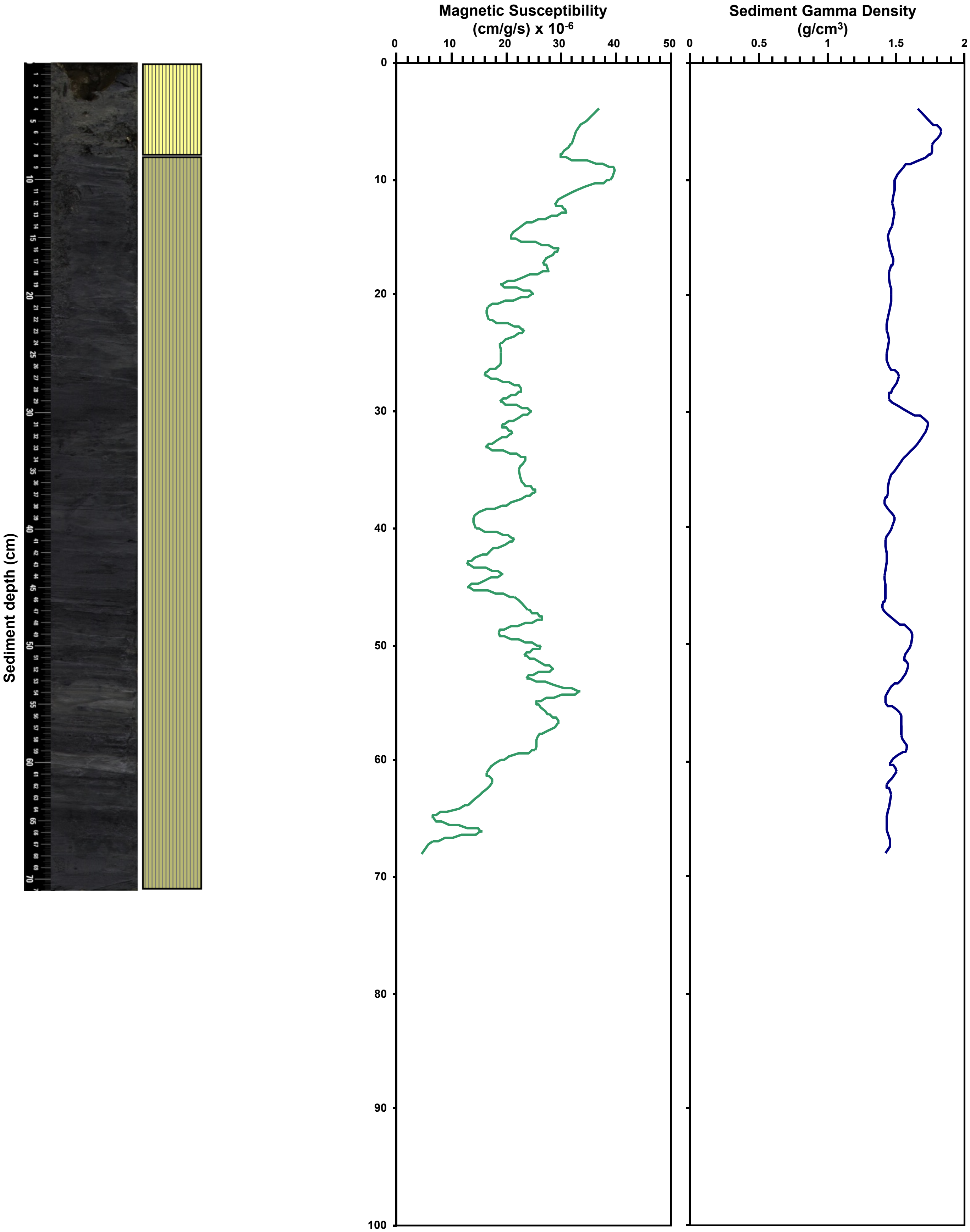
Sediment depth (cm)
Magnetic Susceptibility
(cm/g/s) x 10-6
0
10
20
30
40
50
Sediment Gamma Density
(g/cm3)
0
0.5
1
1.5
2
0
10
20
30
40
50
60
70
80
90
100

T3B D2 (60-147 cm)

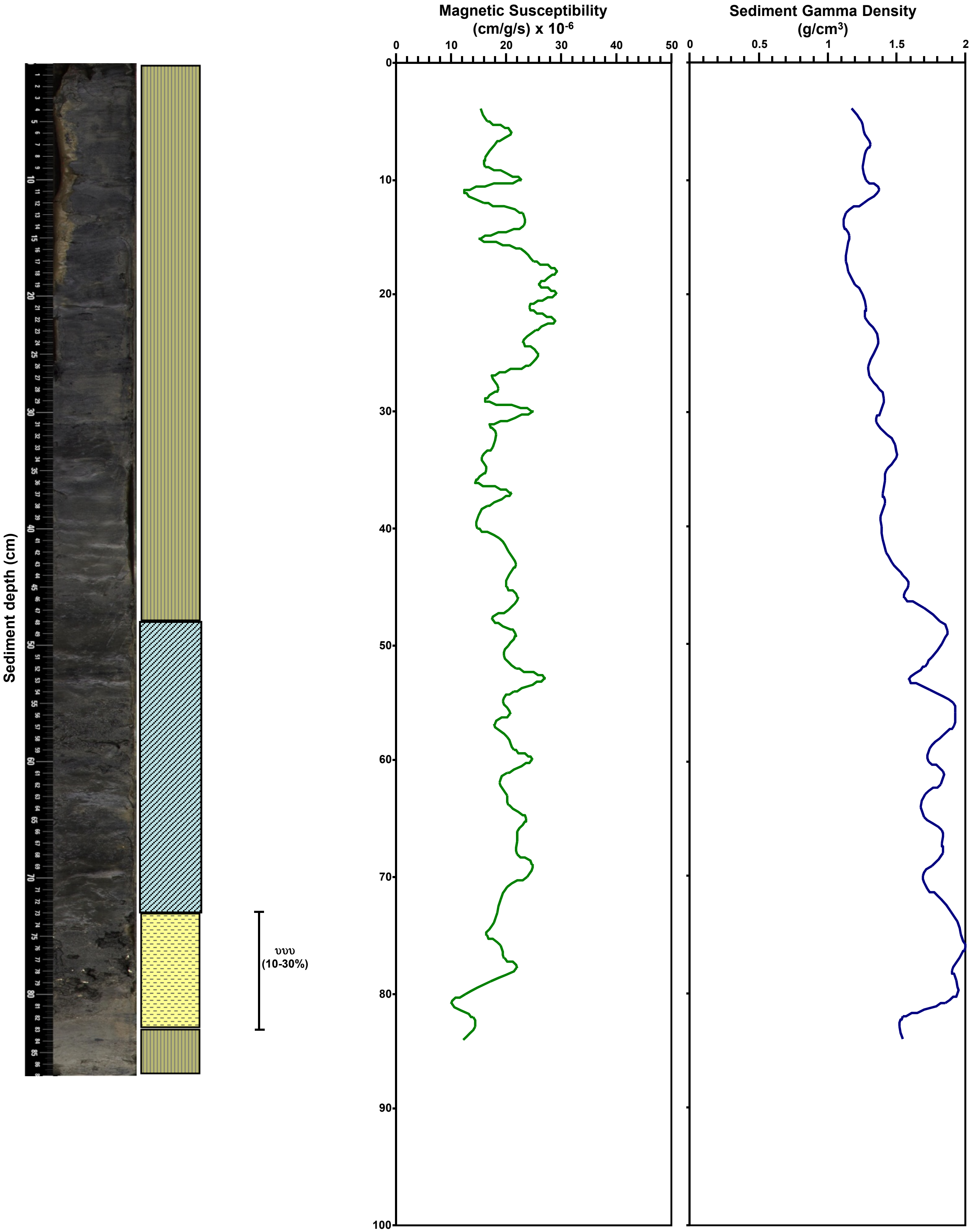

T3B D3 (130-212 cm)

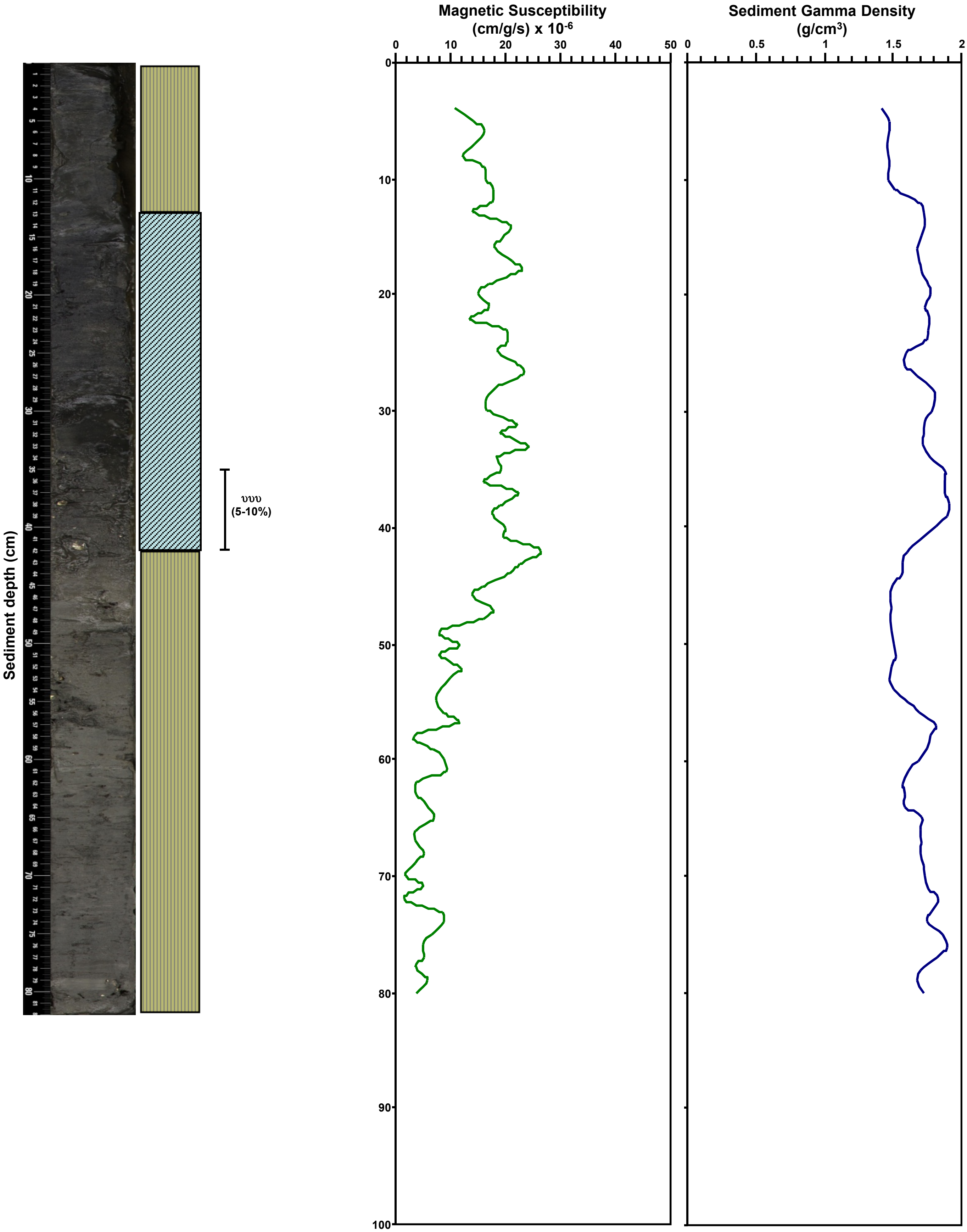

T3C D1 (0-46 cm)

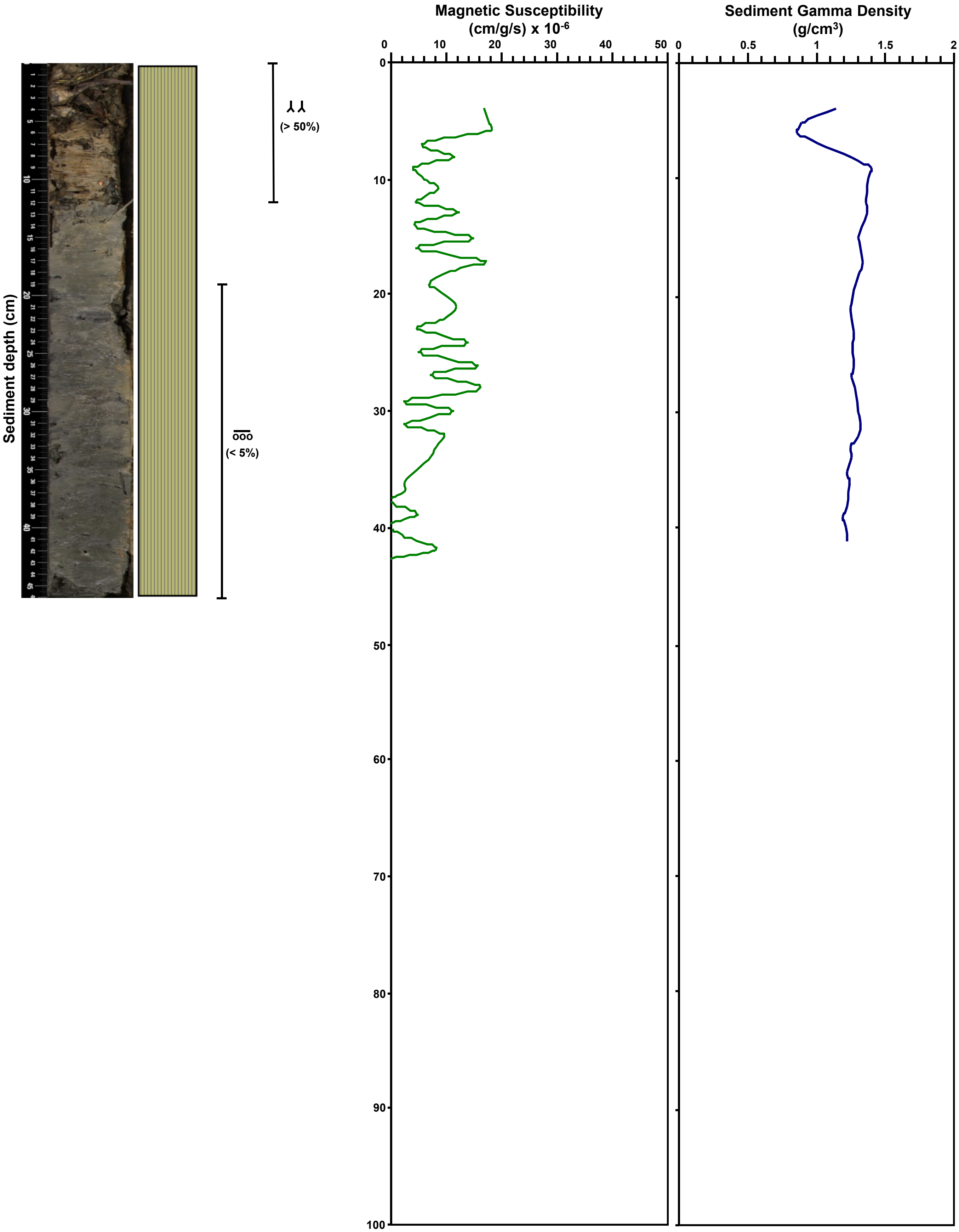
Sediment depth (cm)
(> 50%)
(< 5%)
Magnetic Susceptibility
(cm/g/s) x 10^{-6}
0
10
20
30
40
50
Sediment Gamma Density
(g/cm^3)
0
0.5
1
1.5
2
0
10
20
30
40
50
60
70
80
90
100

T3C D2 (45-127 cm)

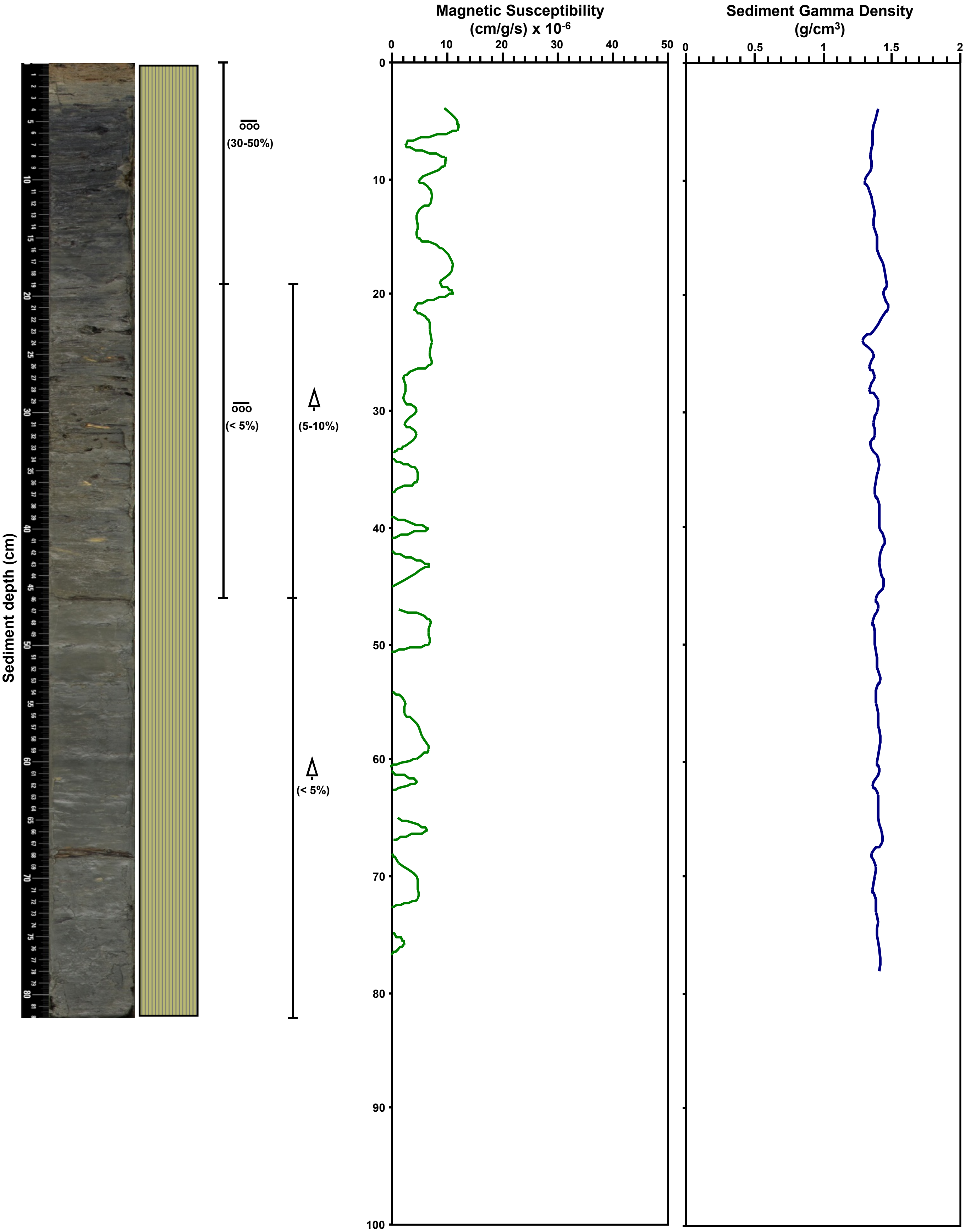

T3C D3 (125-200 cm)

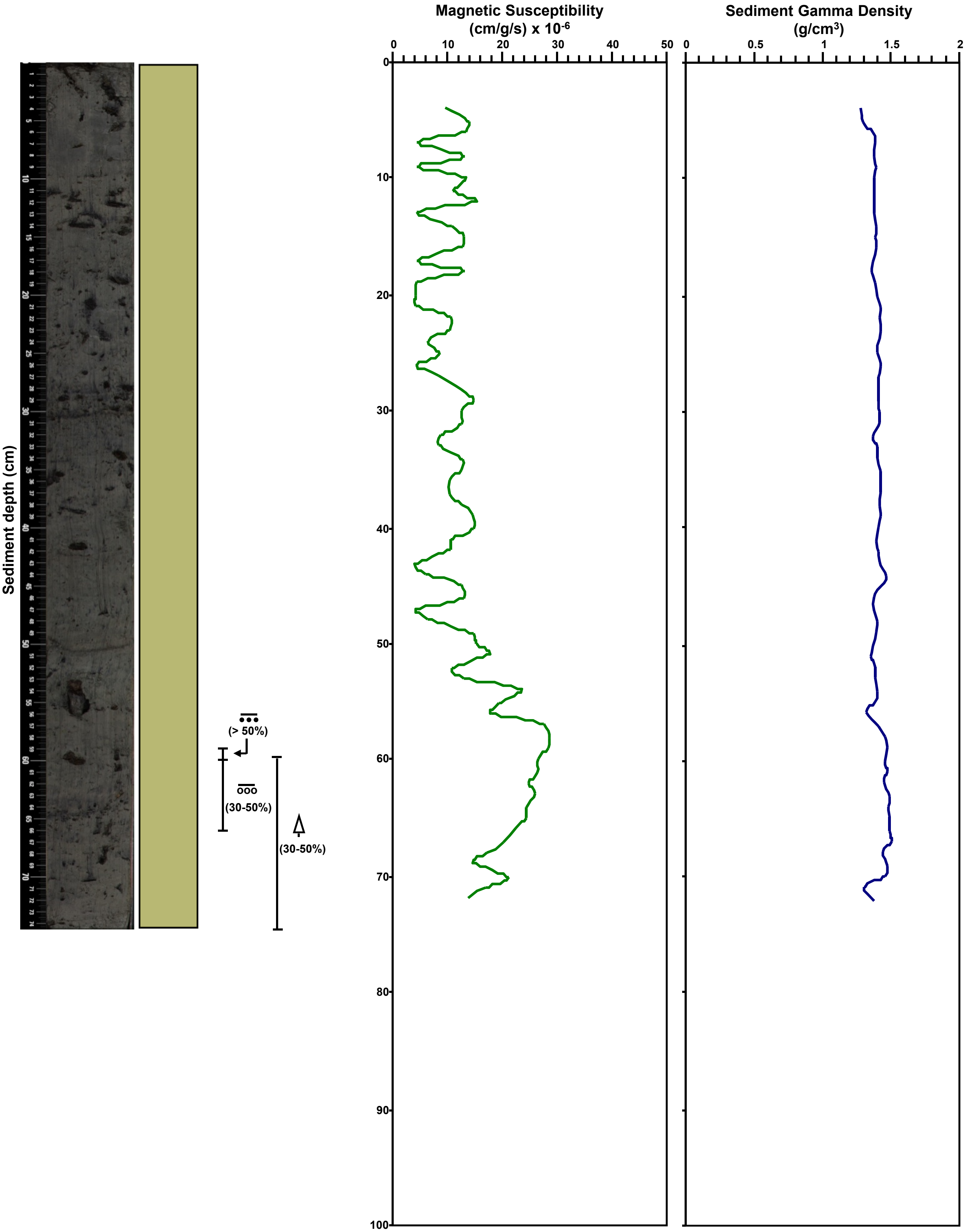

T4A D1 (0-31 cm)

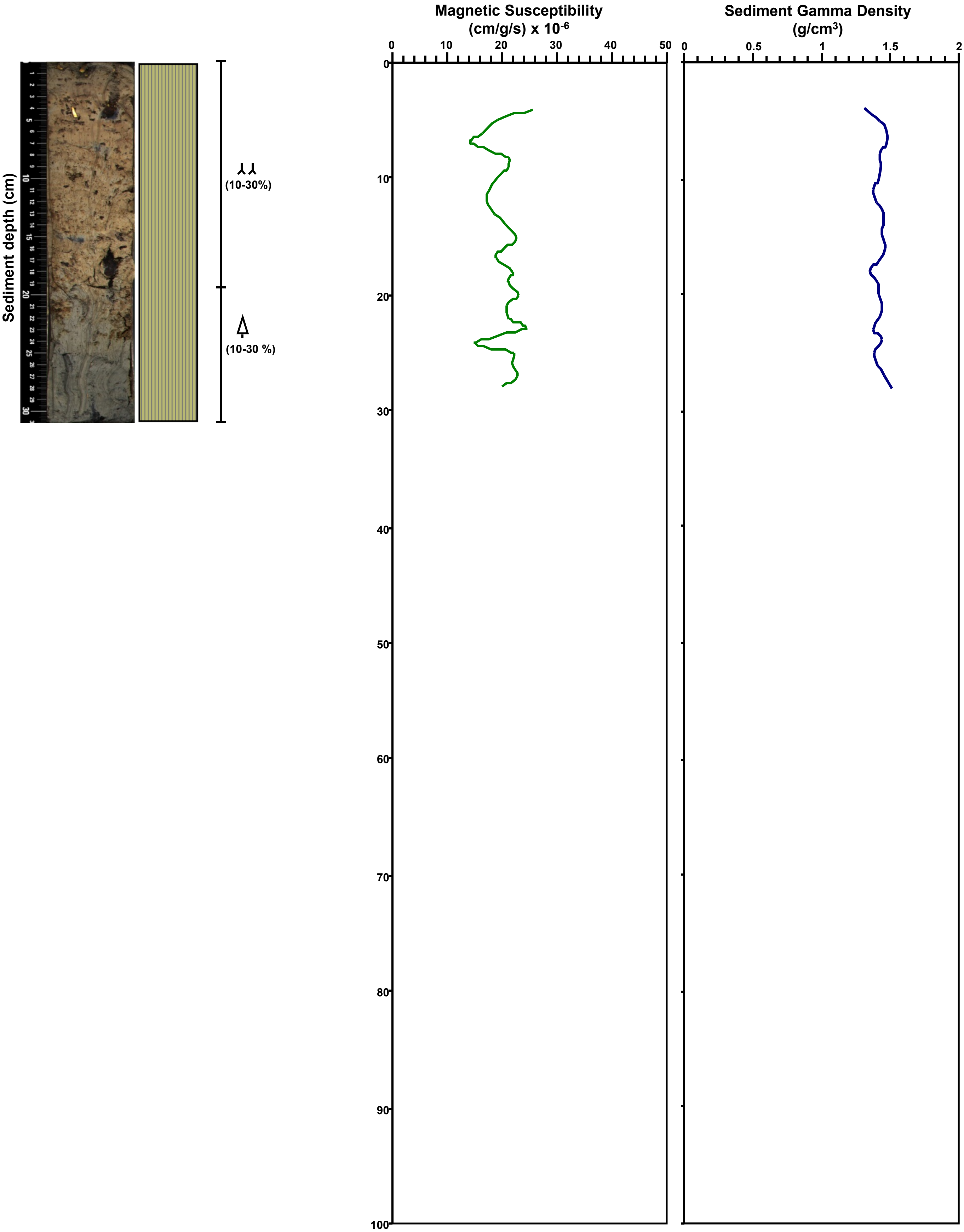
Sediment depth (cm)
(10-30%)
(10-30 %)
Magnetic Susceptibility
(cm/g/s) x 10-6
0
10
20
30
40
50
Sediment Gamma Density
(g/cm3)
0
0.5
1
1.5
2
0
10
20
30
40
50
60
70
80
90
100

T4A D2 (30-100 cm)

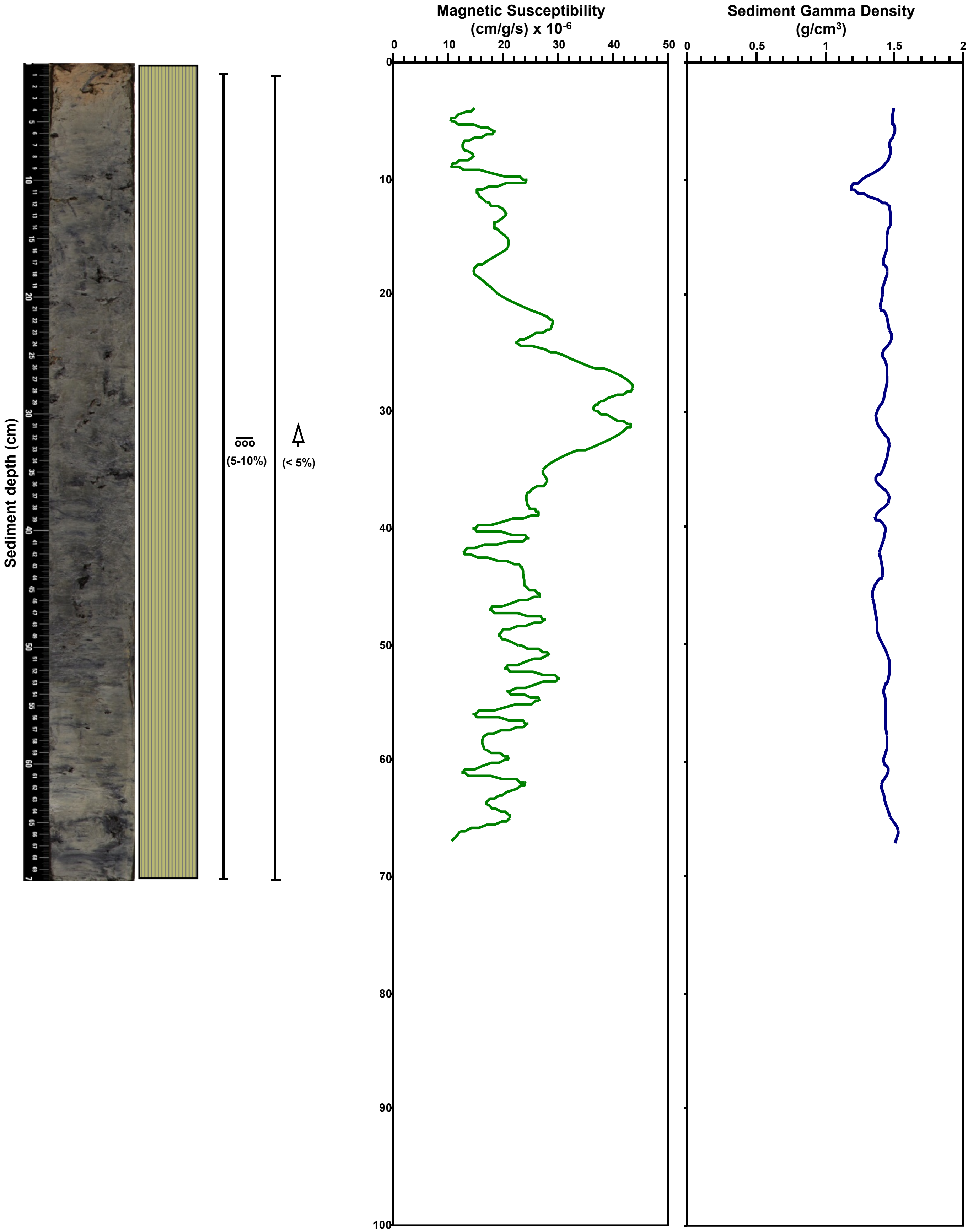

T4A D3 (90-174 cm)

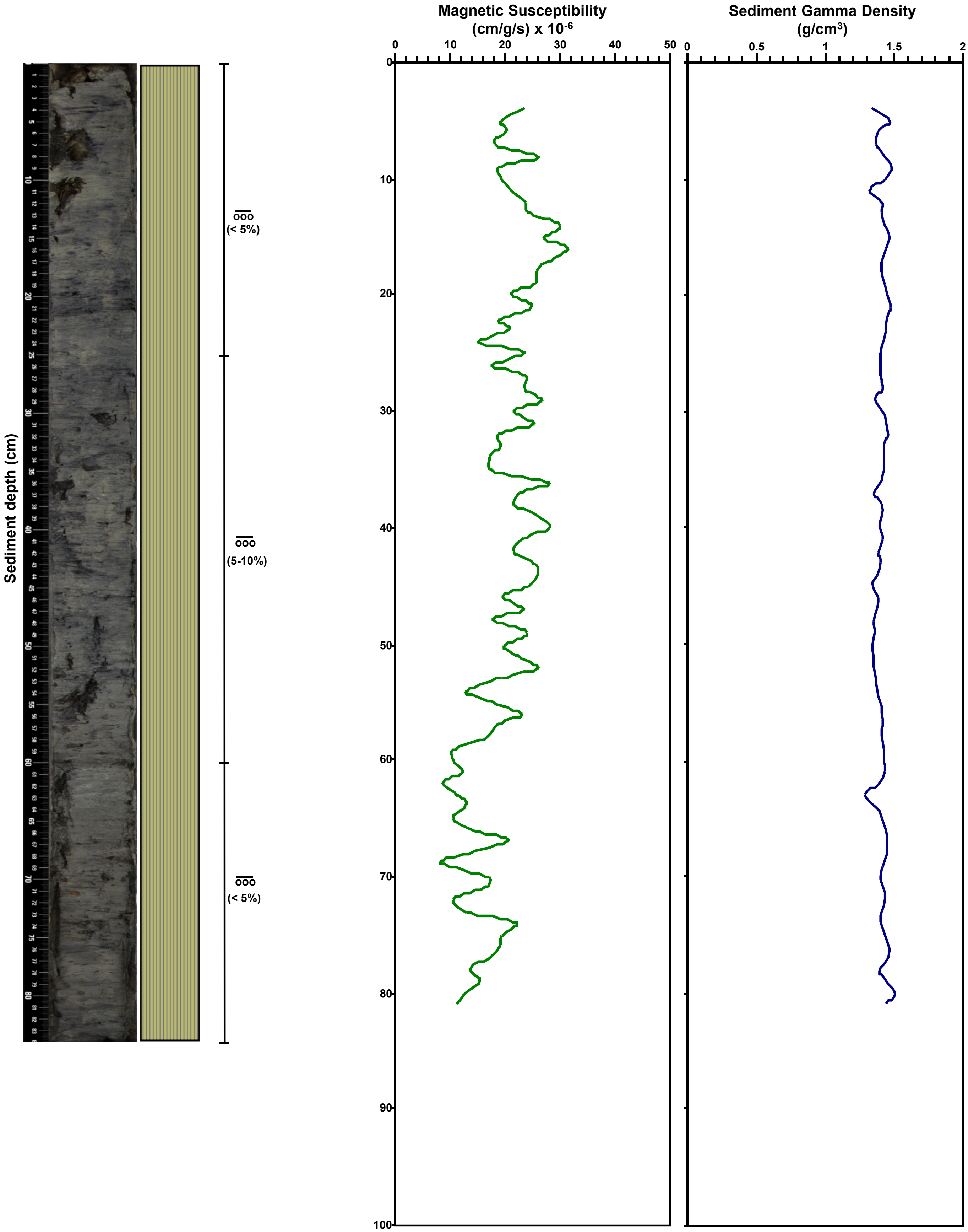

T4A D4 (130-212 cm)

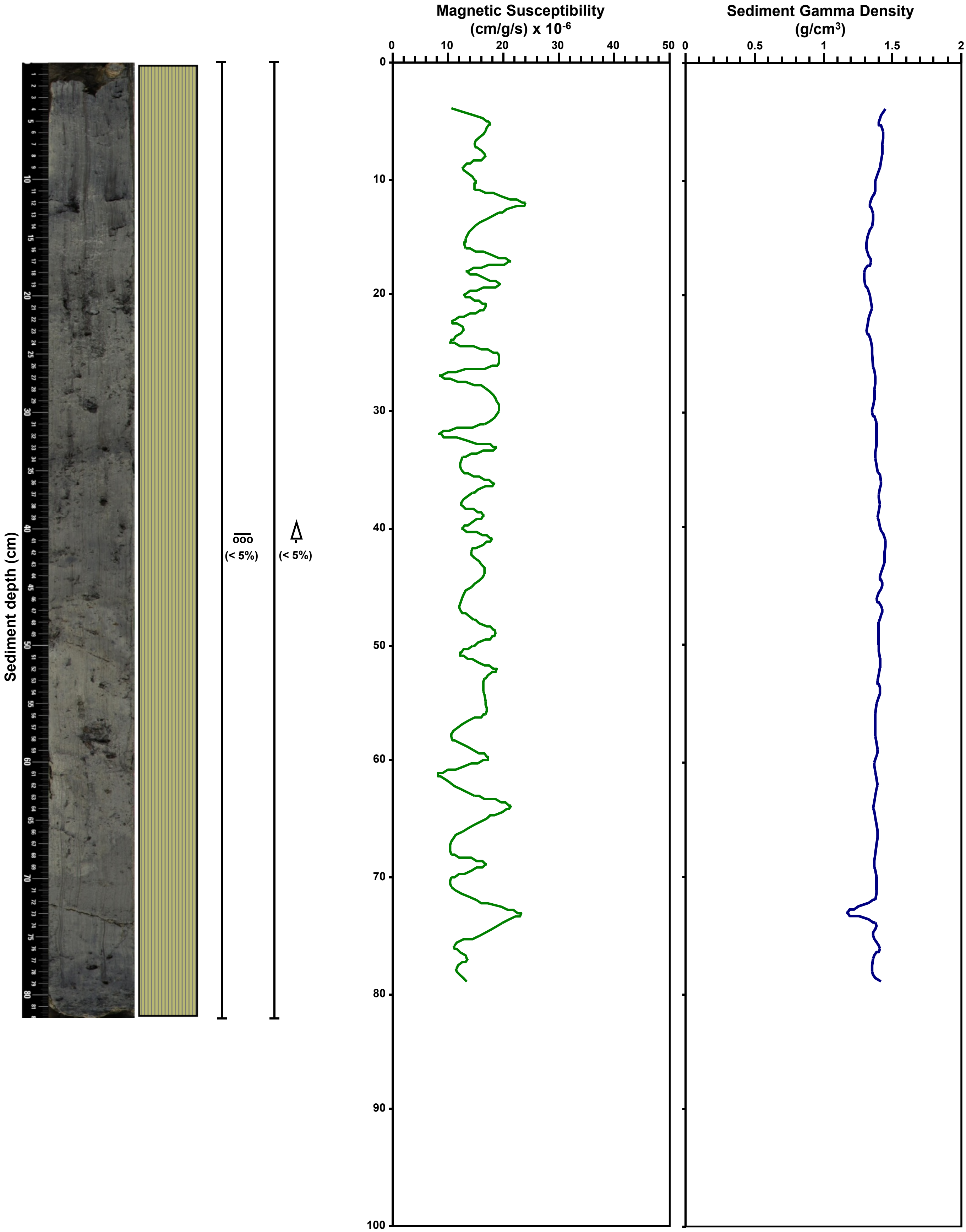

T4B D1 (0-93 cm)

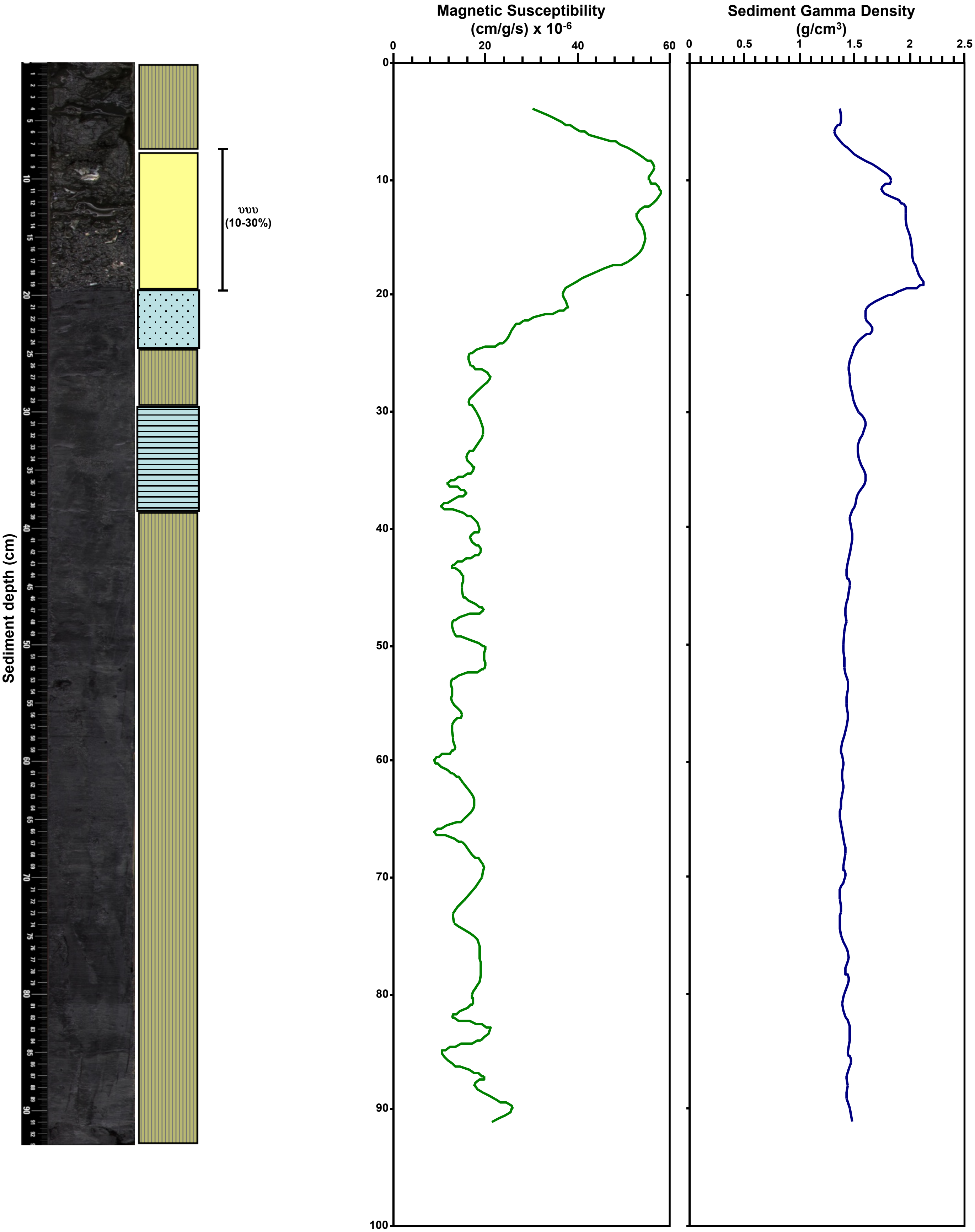
Sediment depth (cm)
υυυ
(10-30%)
Magnetic Susceptibility
(cm/g/s) x 10-6
0
20
40
60
Sediment Gamma Density
(g/cm3)
0
0.5
1
1.5
2
2.5
0
10
20
30
40
50
60
70
80
90
100

T4B D2 (80-157 cm)

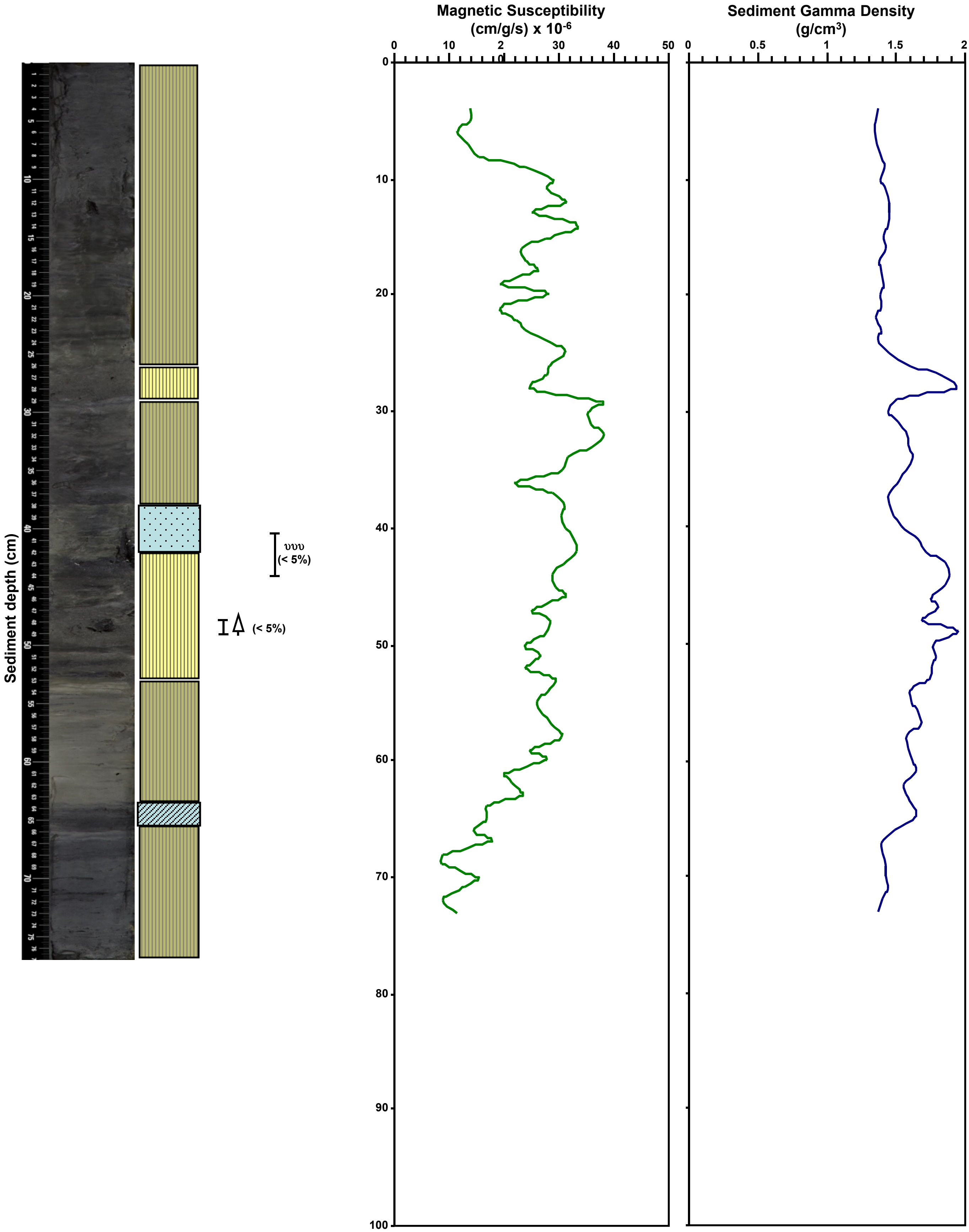

T4B D3 (140-197 cm)

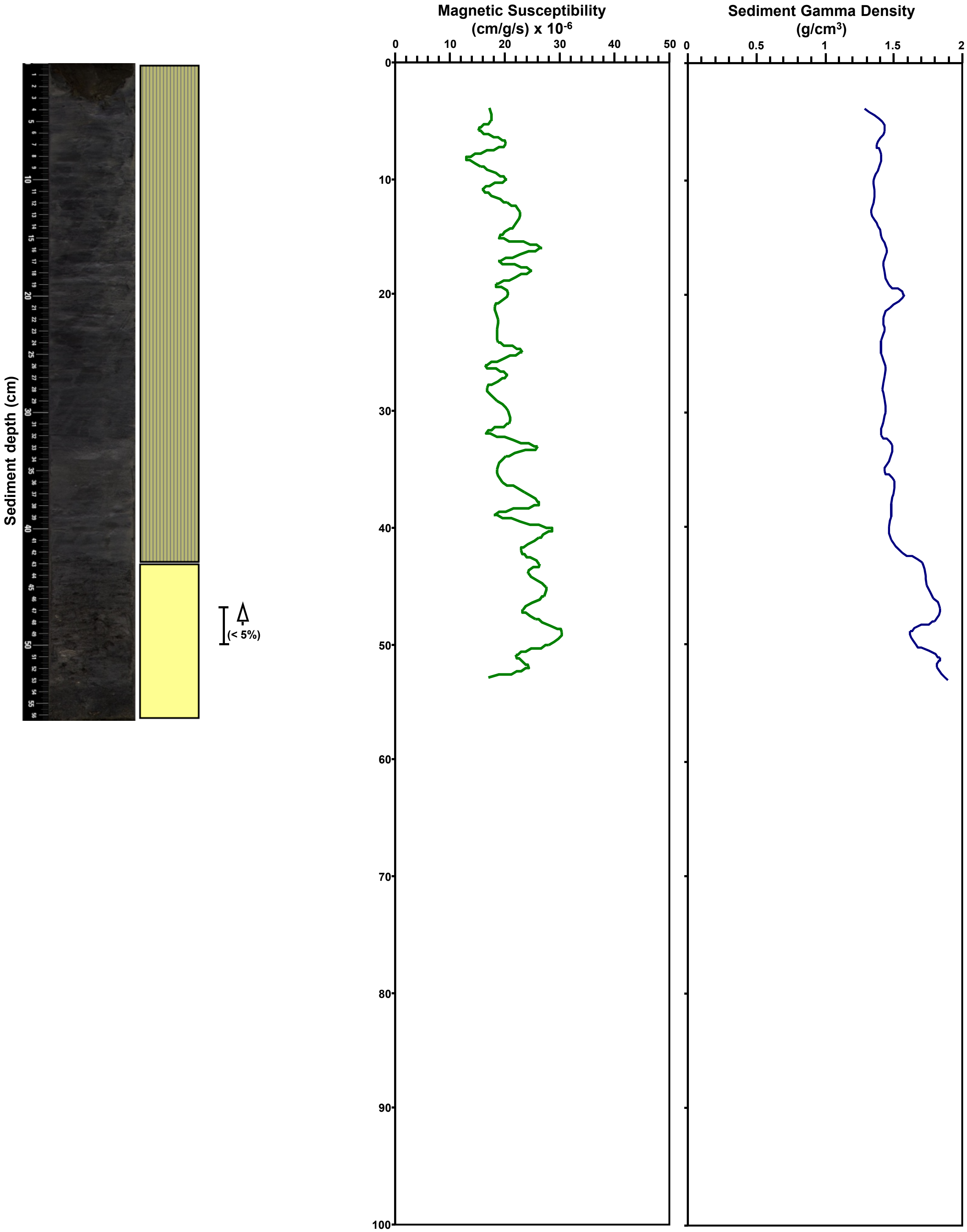

T4C D1 (0-64 cm)

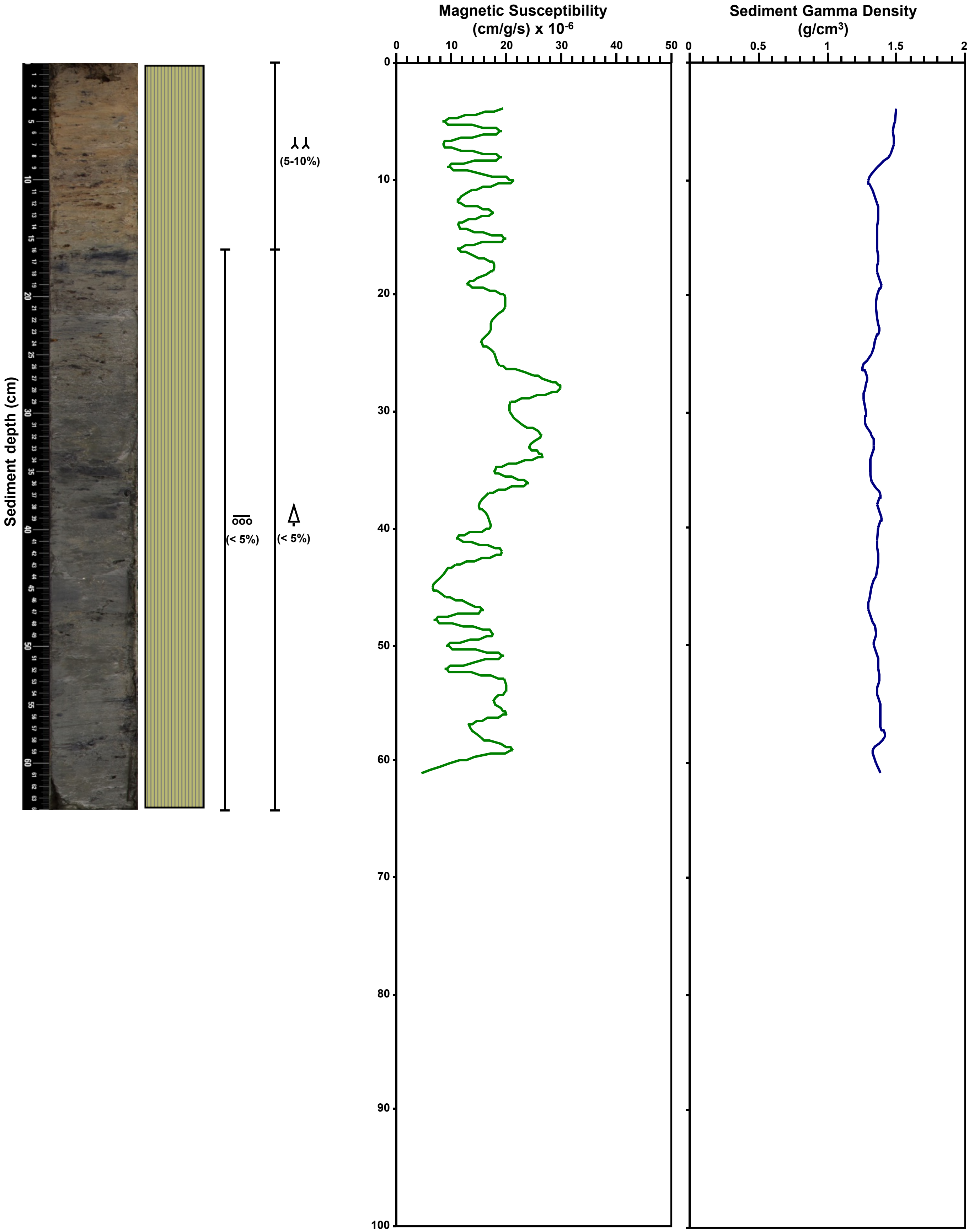
Sediment depth (cm)
(5-10%)
(< 5%)
(< 5%)
Magnetic Susceptibility
(cm/g/s) x 10^{-6}
0
10
20
30
40
50
Sediment Gamma Density
(g/cm^3)
0
0.5
1
1.5
2
0
10
20
30
40
50
60
70
80
90
100

T4C D2 (50-132 cm)

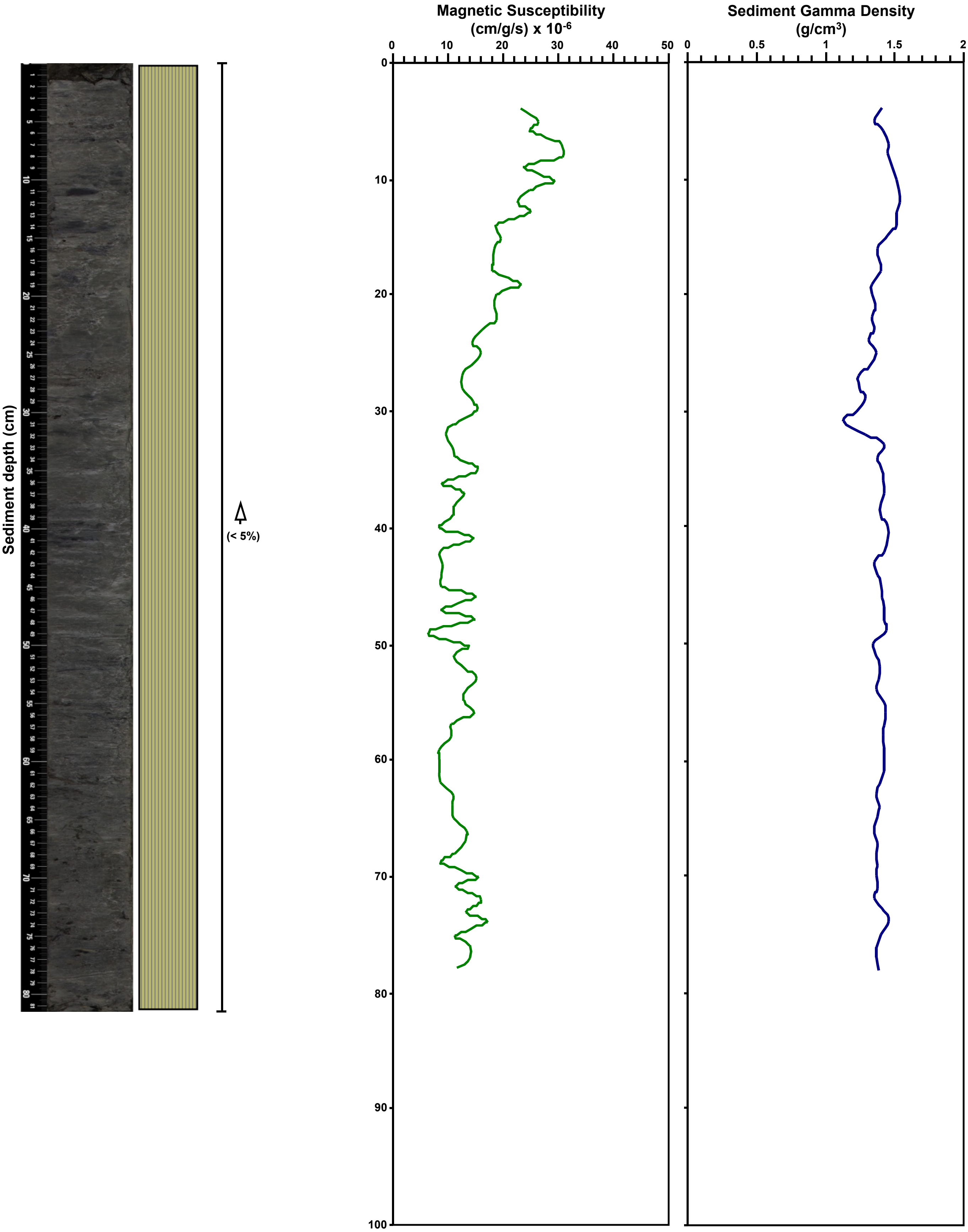

T4C D3 (130-199 cm)

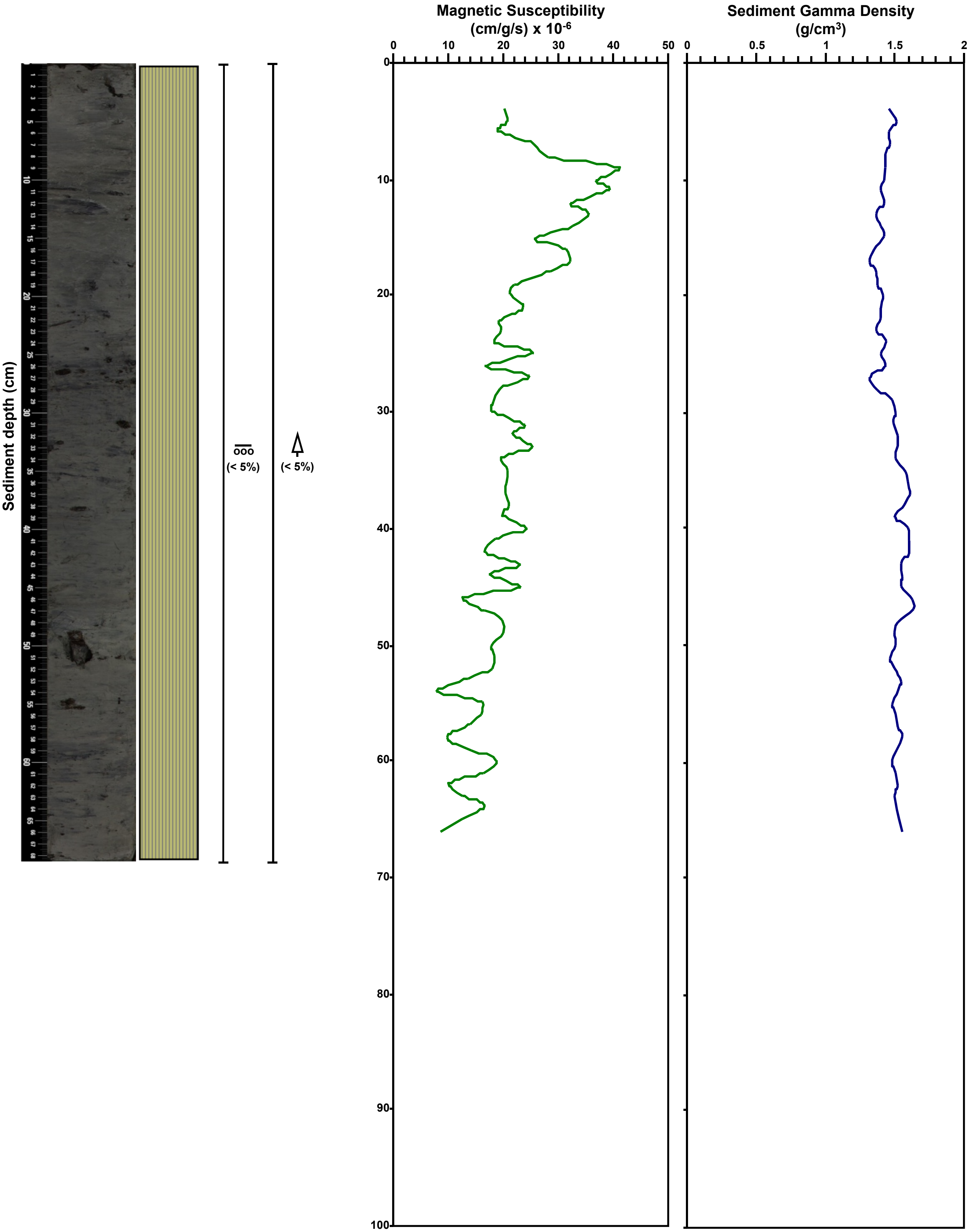

T5A D1 (0-27.3 cm)

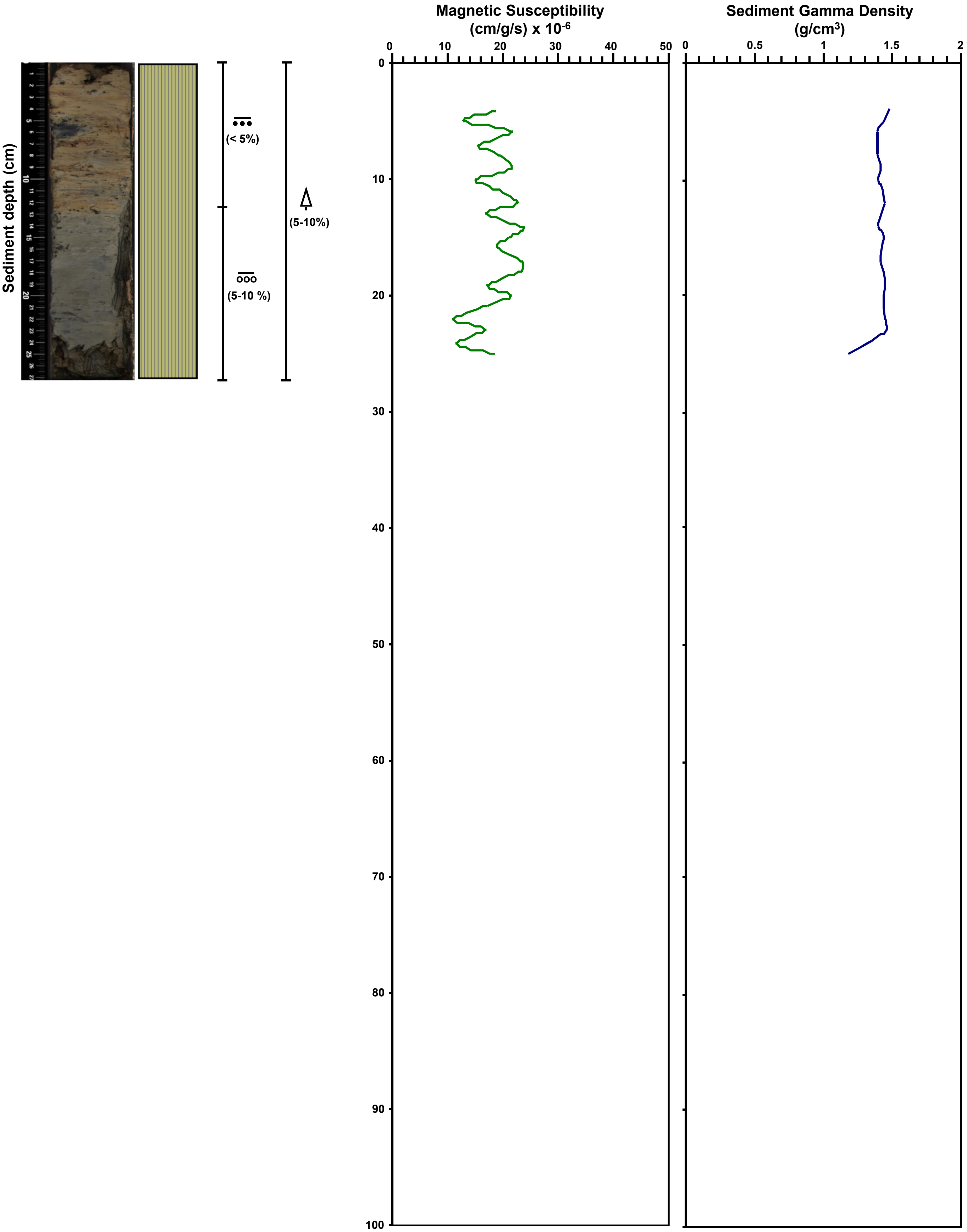

T5A D2 (20-102 cm)

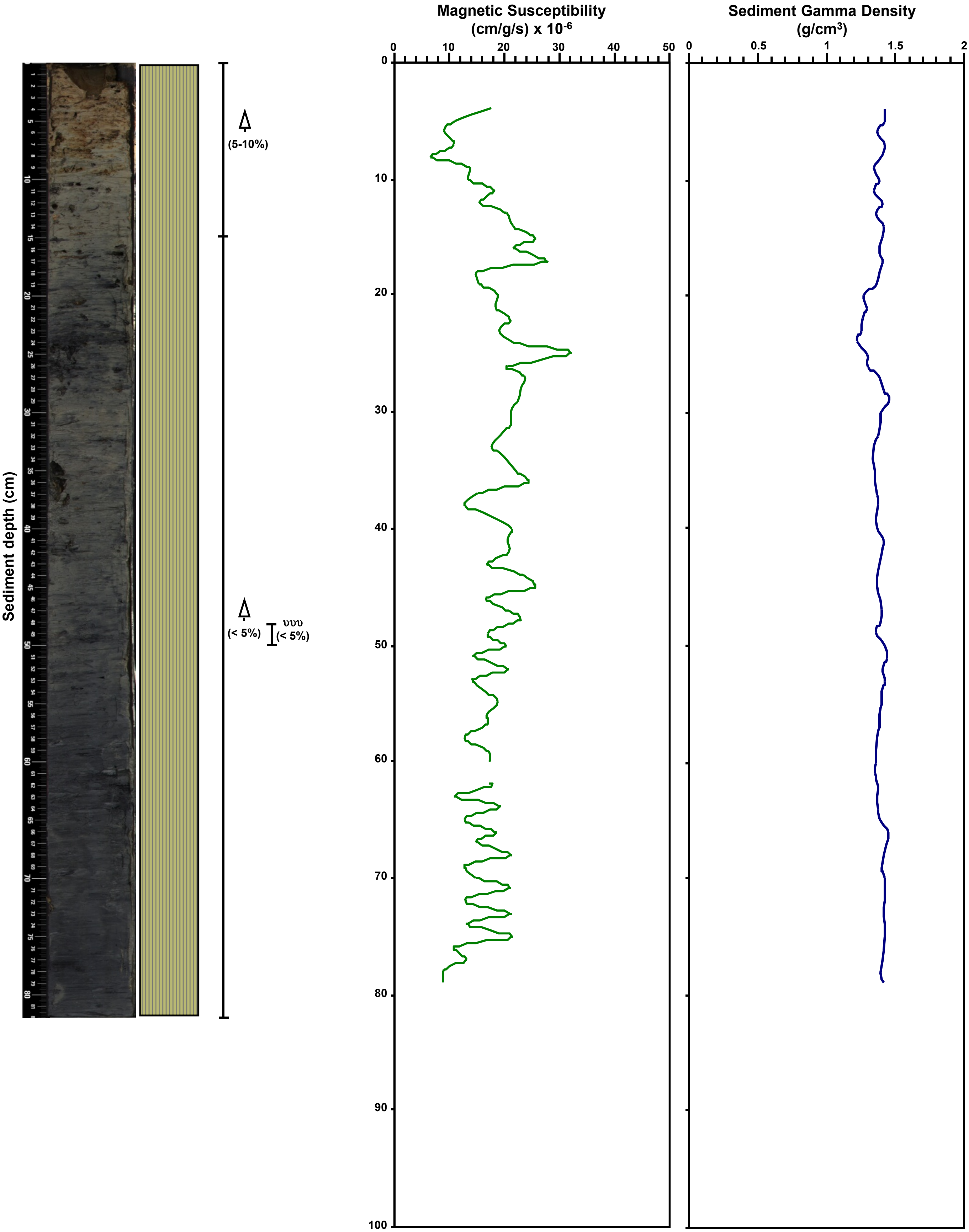

T5A D3 (85-158 cm)

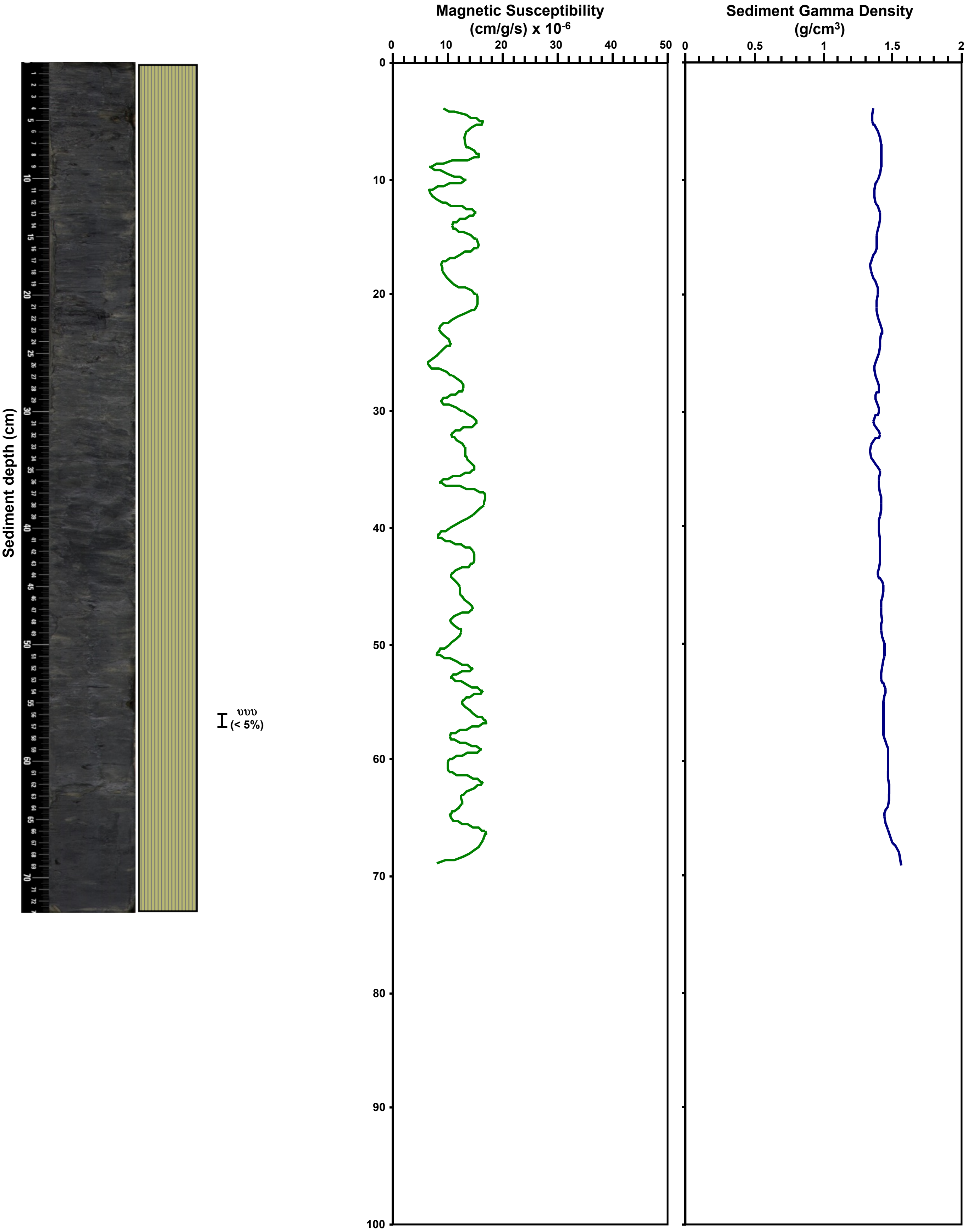

T5A D4 (145-228 cm)

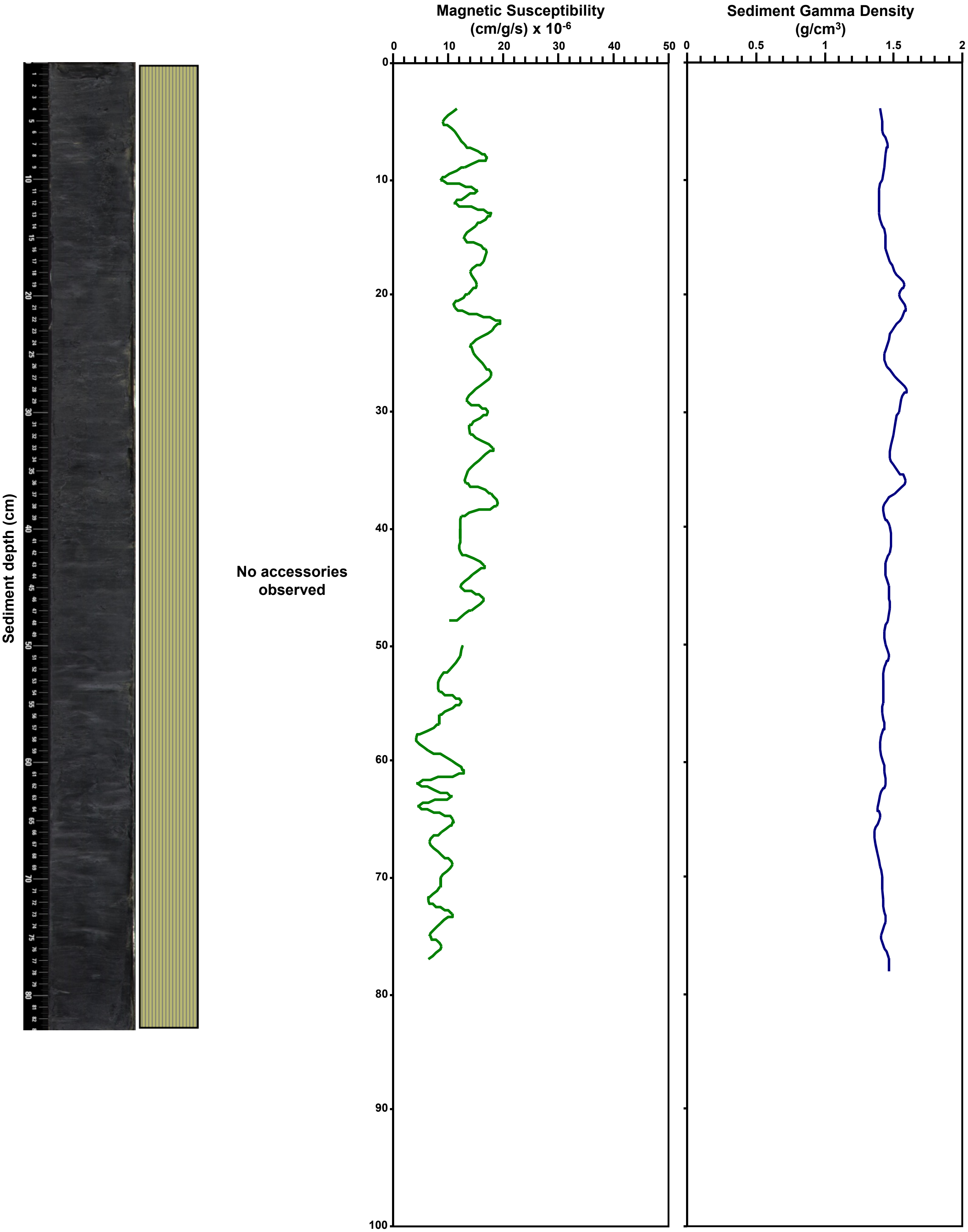

T5B D1 (0-79 cm)

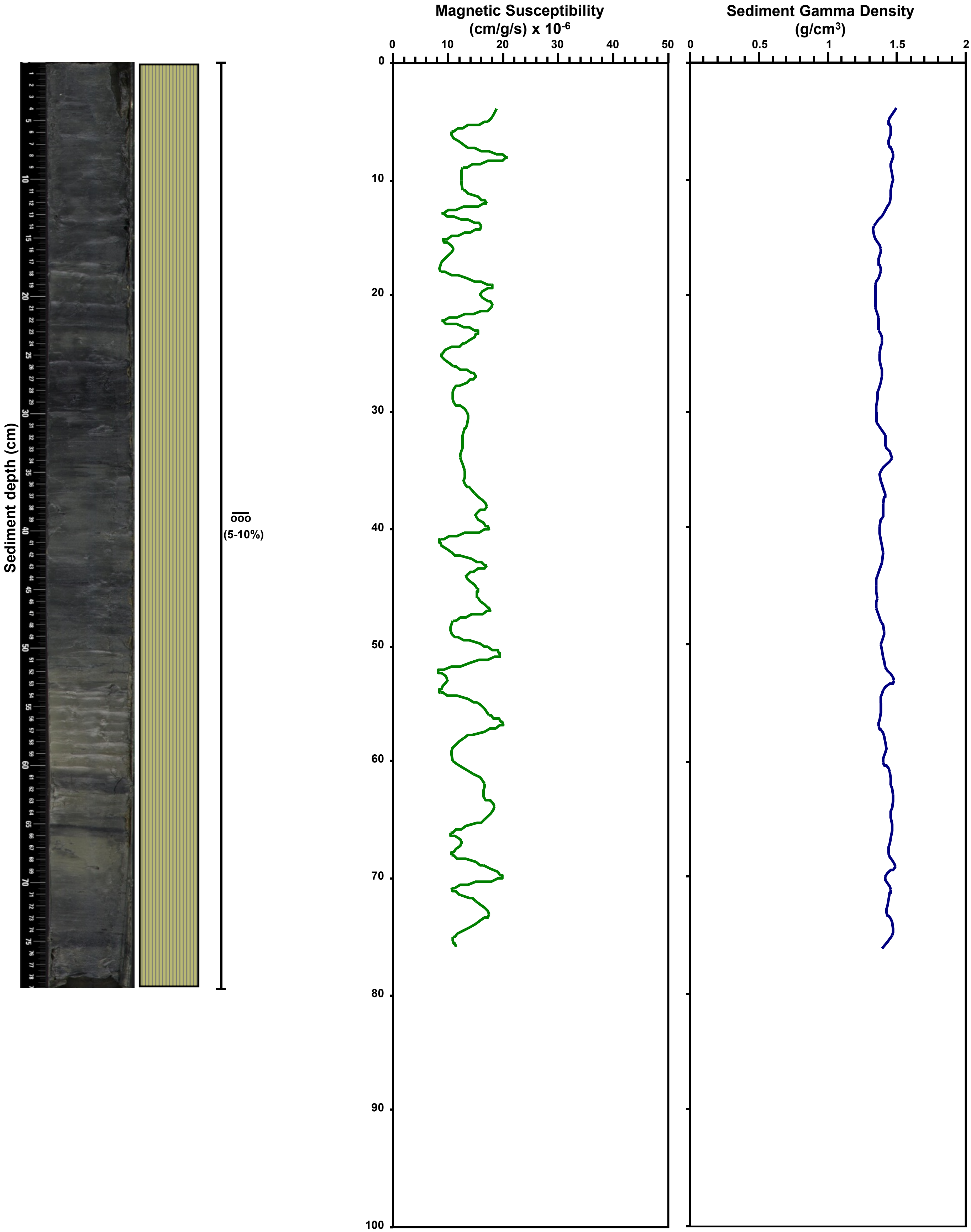
Sediment depth (cm)
ooo
(5-10%)
Magnetic Susceptibility
(cm/g/s) x 10-6
0
10
20
30
40
50
Sediment Gamma Density
(g/cm3)
0
0.5
1
1.5
2
0
10
20
30
40
50
60
70
80
90
100

T5B D2 (70-167 cm)

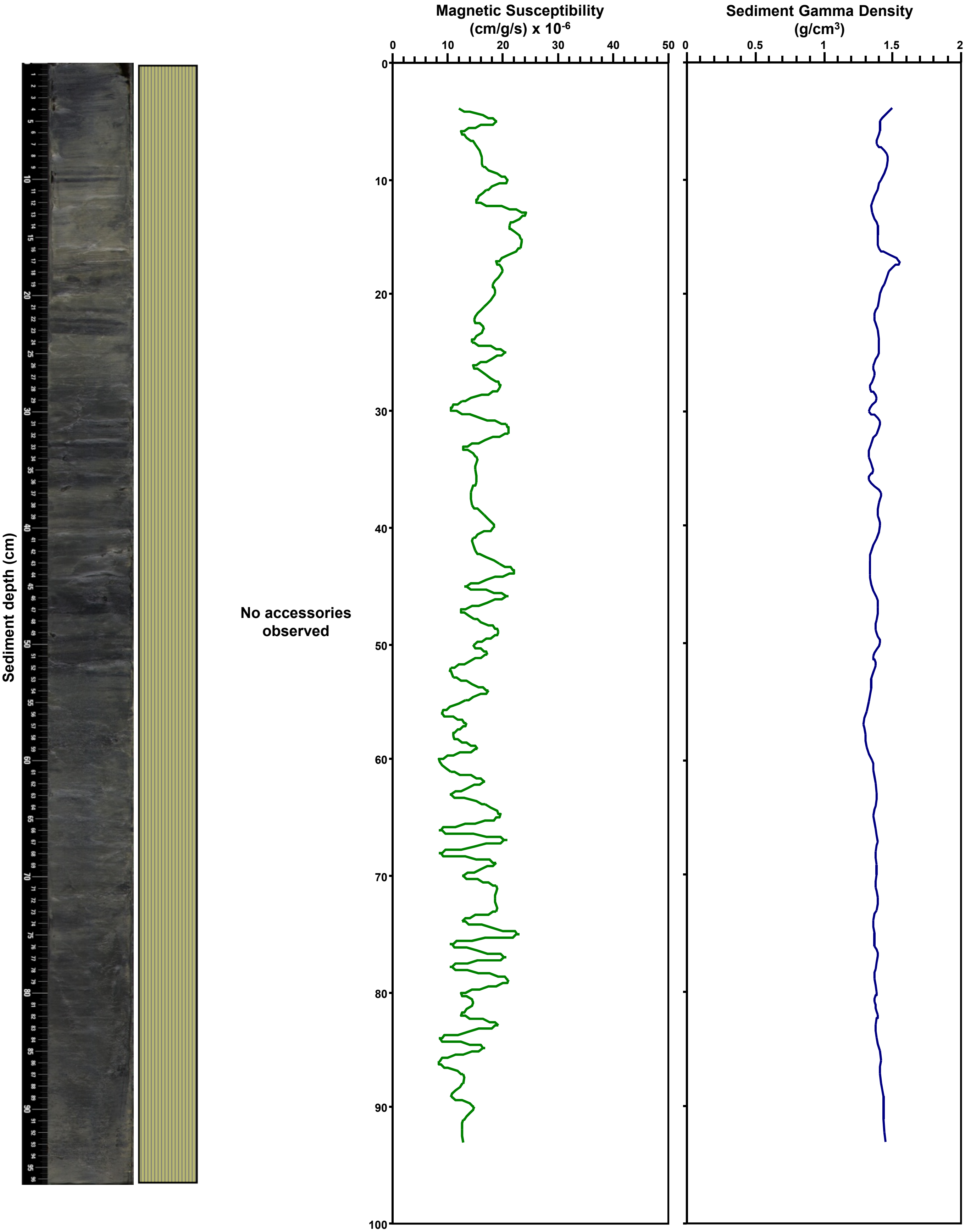

T5B D3 (150-213 cm)

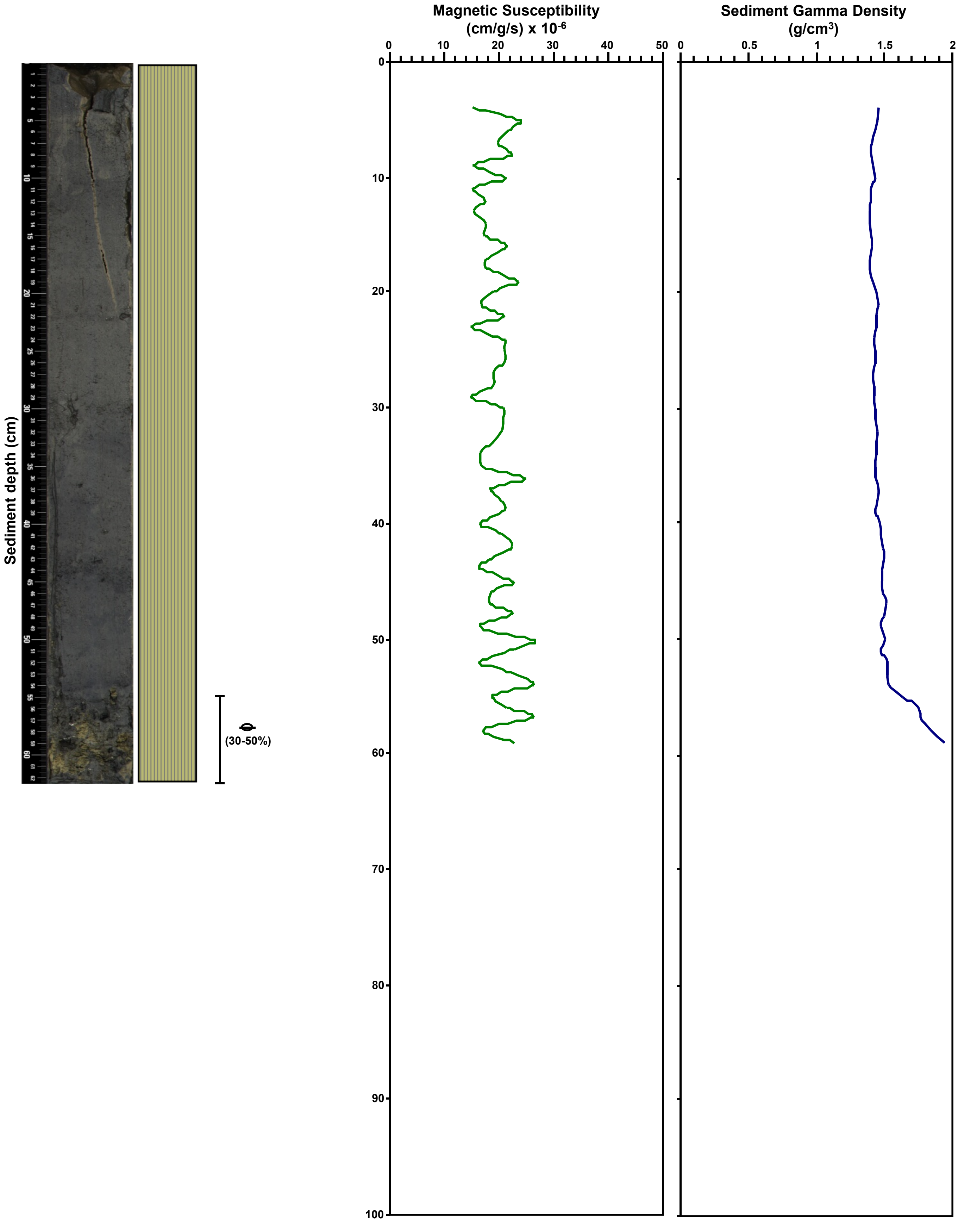

T5C D1 (0-53 cm)

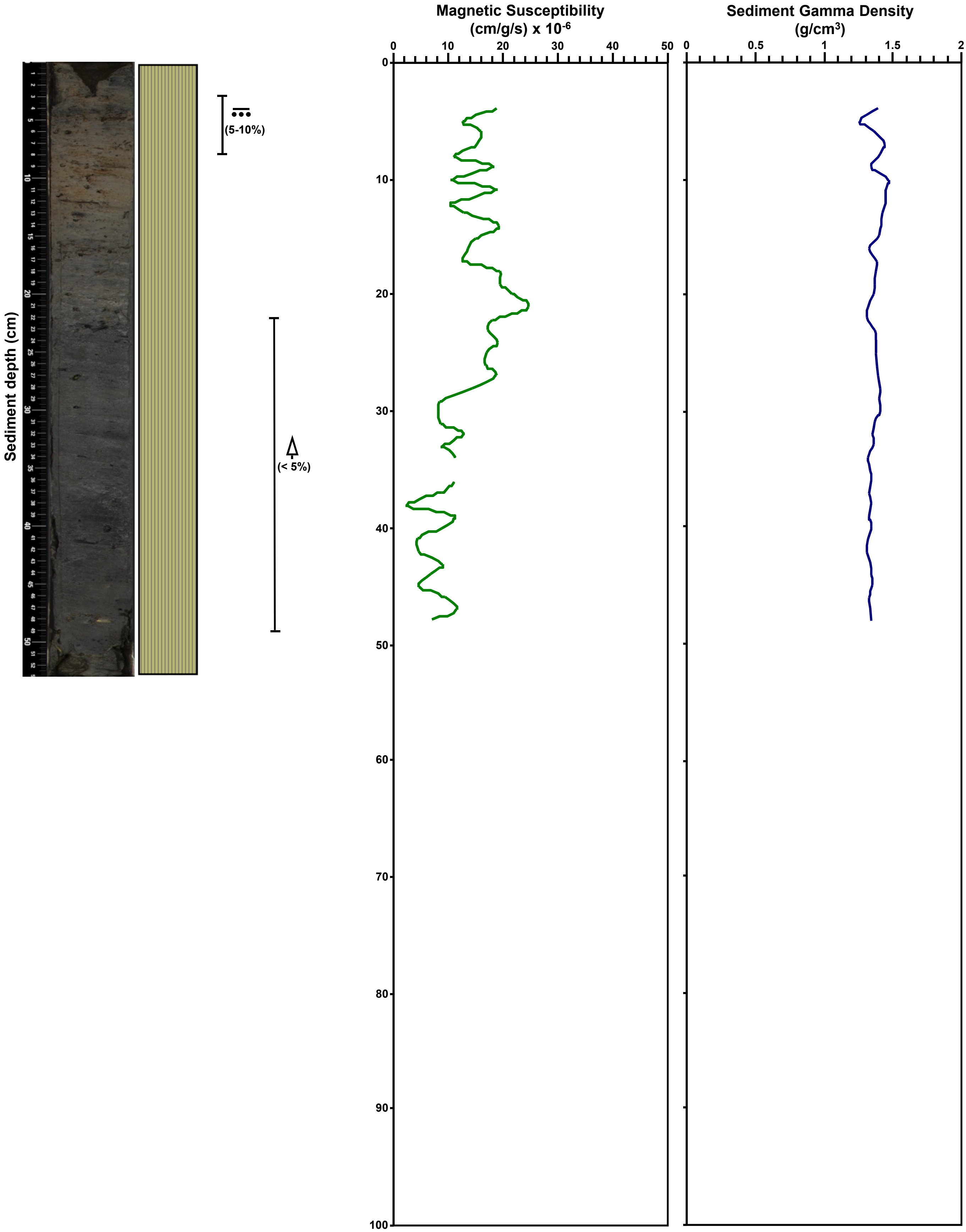
Magnetic Susceptibility
(cm/g/s) x 10-6
0
10
20
30
40
50
Sediment Gamma Density
(g/cm3)
0
0.5
1
1.5
2
Sediment depth (cm)
(5-10%)
(< 5%)
0
10
20
30
40
50
60
70
80
90
100

T5C D2 (50-114 cm)

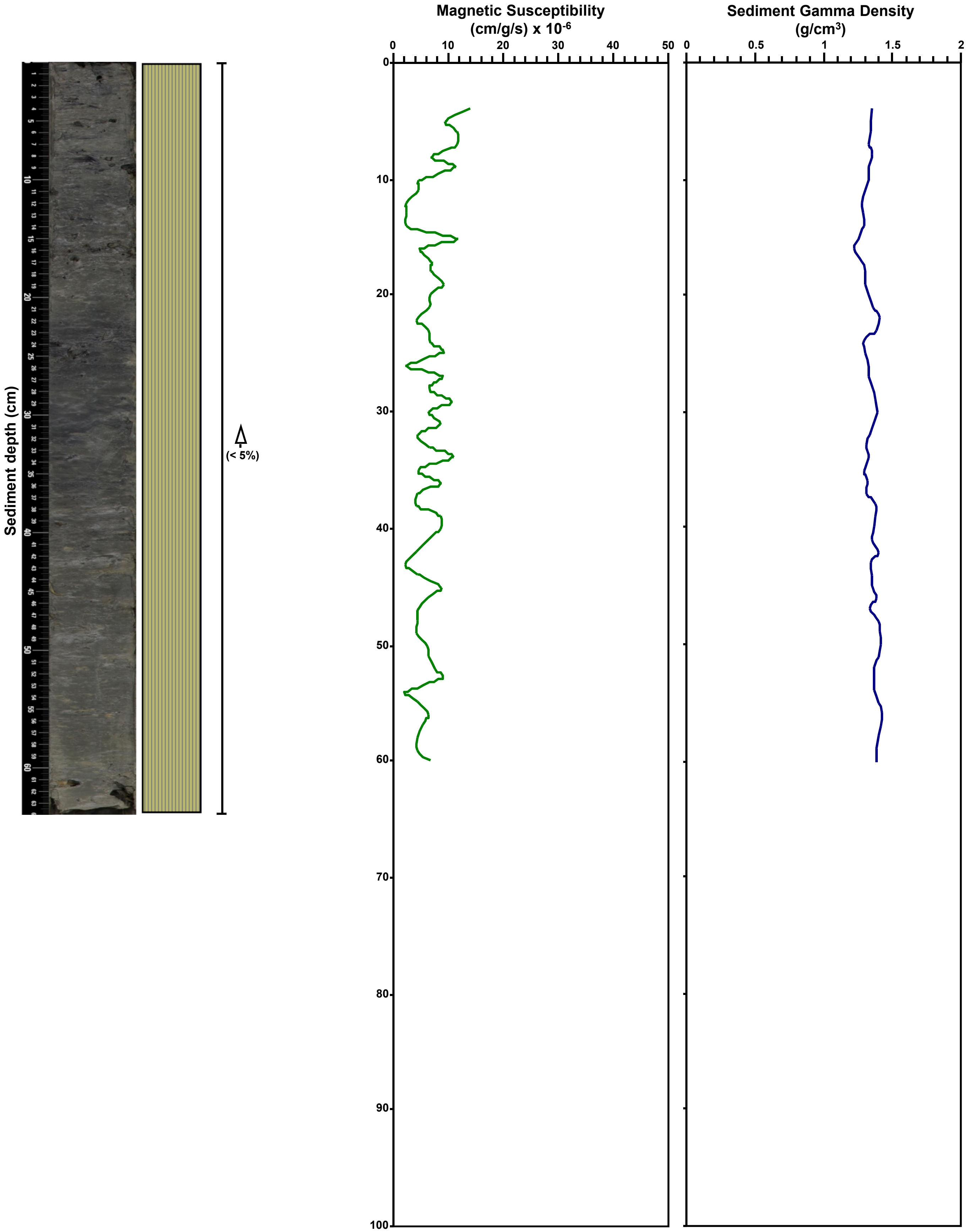

T5C D2’ (72-156 cm)

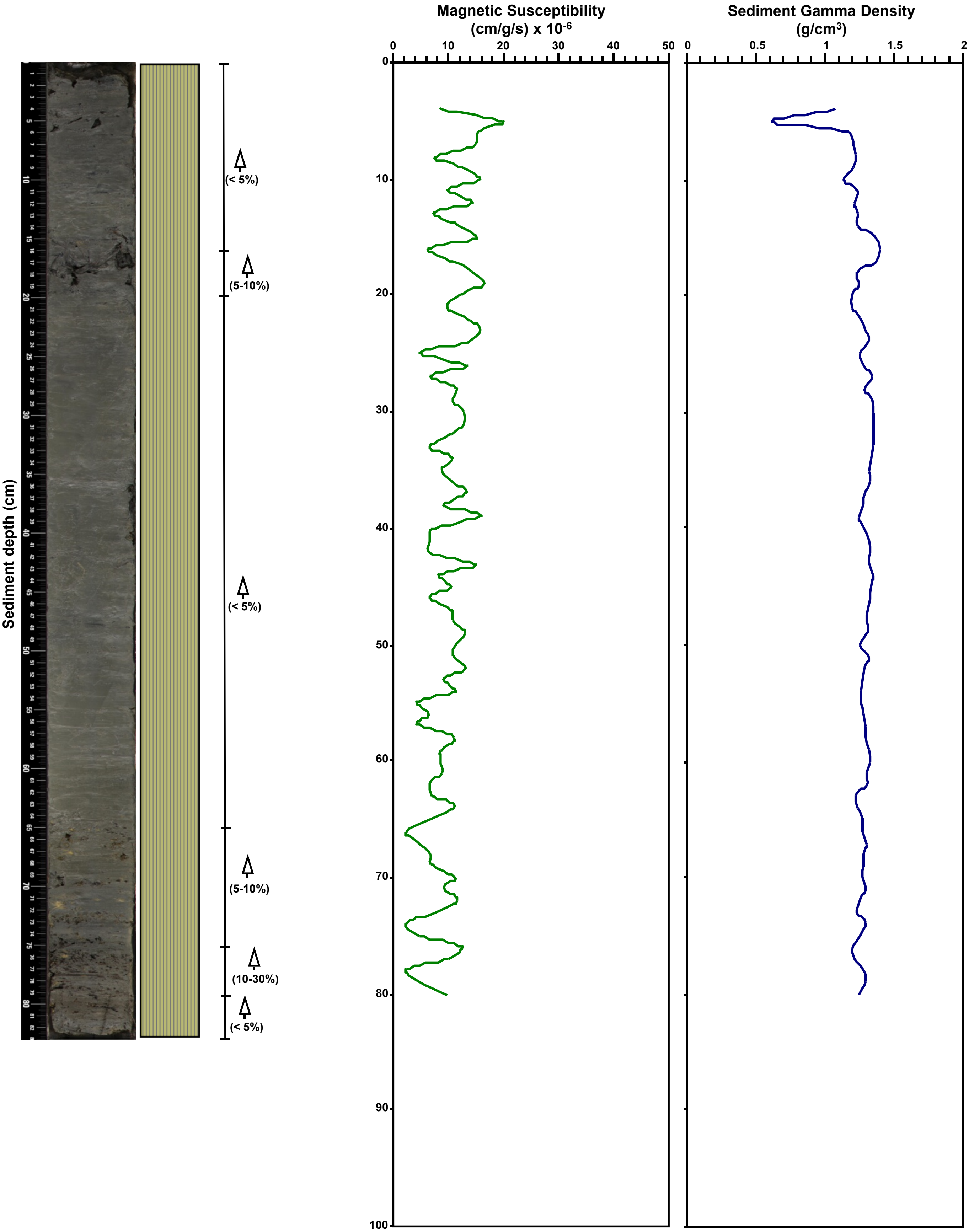

T5C D3 (120-202 cm)